A LIGHTNING MODEL FOR PATTERN RECOGNITION

By

O. GUY MARNEY

Bachelor of Science
Oklahoma State University
Stillwater, Oklahoma
1963

Master of Science
Oklahoma State University
Stillwater, Oklahoma
1965

Submitted to the Faculty of the Graduate College
of the Oklahoma State University
in partial fulfillment of the requirements
for the Degree of
DOCTOR OF PHILOSOPHY
May, 1971

A LIGHTNING MODEL FOR PATTERN RECOGNITION

Thesis Approved:

Arthur M. Breipohl
_____
Thesis Adviser

Harold Fristoe
_____

J. Leroy Folks
_____

James R. McDougal
_____

Durham
_____
Dean of the Graduate College

788654

ii

ACKNOWLEDGEMENTS

I wish to express my most sincere gratitude to my thesis adviser, Professor A. M. Breipohl, for his encouragement and assistance throughout this research, and especially for his promptness in reading the manuscript of this study.

I also wish to thank the other members of my graduate committee, Professor J. R. McDougal, Professor J. L. Folks, and Professor H. T. Fristoe who has served as chairman throughout my graduate study.

In addition, I would like to thank Dixie Jennings for her advice and an excellent job of typing the manuscript.

Finally, I wish to express my appreciation to my wife and sons for their patience and understanding.

TABLE OF CONTENTS

LIST OF TABLES

LIST OF FIGURES

Figure   Page

CHAPTER I

INTRODUCTION

1.1 Statement of the Problem. The premis is that the electromagnetic radiation from a thunderstorm contains a pattern which can be related to meteorological phenomena of the storm. This is the basic pattern recognition problem. However, before a pattern recognition scheme can be effected, the initial problem is to determine what measurements will constitute the patterns to be classified. The specific problem considered here is what measurements are to be selected from the electromagnetic fields generated by thunderstorms for use in future pattern recognition studies designed to identify storm phenomena.

Ignoring very slow changes in the field, lightning discharges may be considered as the major contributor to the electromagnetic field. Also, it has been suggested that the type of discharge changes with the state of development of the storm (11). Thus if the electromagnetic field produced by the model of various types of discharges is observed, parameters in the field waveforms which are related to say storm severity may be selected by varying parameters within the discharge model and observing changes in the field.

1.2 Existing Solutions. Models for portions of the discharge process involved in lightning discharges exist in the literature. A recent text by Uman (19) contains numerous references and serves as an excellent review. Hill (9) has presented a model for computing the

received spectrum resulting from the return stroke portion of a cloud-to-ground discharge. Dennis and Pierce (7) have considered the effect of varying various parameters in the return stroke. Arnold and Pierce (1) have obtained the spectrum of the received field produced by the leader process and by the junction process. Hill (8) has combined the leader process and the return stroke and computed the resulting spectrum.

Each of the above models is valid only for far field conditions. Also the geometry of each model consists of a strictly vertical channel connected with the ground plane. In addition to these limitations the observation point must be located on the ground plane.

In the present project it was desired to consider the radiation at distances as close as 10 Km from the discharges. Also the radiation at altitudes above the ground plane was desired to determine what signal would be received on a horizontal antenna and its relation to the vertical component of signal. The frequency range of interest was 3 to 300 KHz.

Thus the existing models are inadequate for this project. First, far field conditions are not guaranteed at these distances. Second, the field removed from the ground plane was desired in order that a horizontal component of the field would exist. Also it was thought that variation of the channel geometry would be effective in producing significant changes in the received field.

1.3 Present Contribution. A computer model has been developed to compute the Fourier transform of the electromagnetic field received from a general lightning discharge. The discharge is represented by a configuration of oscillating electric dipoles placed end to end, and the

resulting field is assumed to be that due to the superposition of all dipoles in the configuration and their images.

The field resulting from one electric dipole and the procedure for computing the Fourier transform of the field resulting from a configuration of dipoles are discussed in Chapter II. For the present project the time waveforms representing the narrow-band, half-wave linear detected received electromagnetic fields were available for the center frequencies 10, 50, 100, 150, 200, and 250 KHz. The method of approximating these time waveforms is also discussed in this chapter.

The general geometry of the discharges to be modeled, the current waveforms allowed, and the movement of these waveforms through the geometry are discussed in Chapter III. Also the procedures employed by the programs to compute the Fourier transform and the detected waveforms of the resulting fields are discussed.

In Chapter IV computations obtained from the model developed in this work are compared with those obtained from other models in the literature. The comparison includes only the return stroke and the leader process. Incorporation of the streamer process into the model and the results of the narrow-band, half-wave linear detected field calculations are also discussed.

Situations not possible with other models are considered in Chapter V in an attempt to determine how these variations change the received field. Included in this chapter are the results obtained for the observation point located near the discharge and removed from the ground plane and the results for inclined channels.

CHAPTER II

DEVELOPMENT OF THE MODEL

2.1 Introduction. The initial assumption in this work is that
the electromagnetic field generated by a lightning discharge may be ap-
proximated by the superposition of the fields produced by the appropri-
ate configuration of oscillating electric dipoles. Granting this as-
sumption this chapter develops the mathematics required to calculate
the Fourier transform of the field and the narrow-band, half-wave,
linear detected field.

2.2 Field Calculations. The electric dipole may be represented
by a positive time varying charge, Q(t), separated from an equal but
opposite polarity charge -Q(t), by a distance ΔL along the unit vector
(ℓ, m, n) (see Figure 1). Mathematically, the dipole may be expressed
by the polarization vector

$$\vec{P}(t) = Q(t) \ \Delta L \ \vec{a} \qquad , \qquad (2.2.1)$$

where $\vec{a}$ is the unit vector (ℓ, m, n).
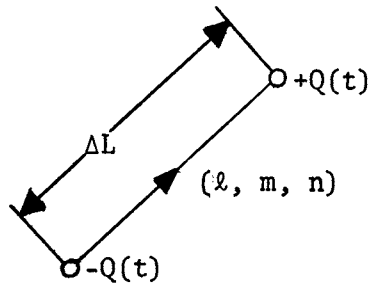
Figure 1. Dipole Representation

The field distribution will be calculated by determining the Hertz vector at the observation point (x, y, z). The Hertz vector resulting from the above polarization vector located at the point (x', y', z') is given by

$$\vec{\Pi}(x, y, z, t) = \frac{1}{4\pi\varepsilon} \int \vec{P}(x', y', z', t - \frac{r}{v}) \frac{1}{r} \, d(x', y', z') \qquad (2.2.2)$$

where r is the distance $[(x - x')^2 + (y - y')^2 + (z - z')^2]^{1/2}$ and v is the propagation velocity of the wave. In these calculations, ΔL will be chosen such that the Hertz vector may be approximated as

$$\vec{\Pi}(x, y, z, t) \doteq \frac{1}{4\pi\varepsilon r} \vec{P}(t - \frac{r}{v}) \qquad , \qquad (2.2.3)$$

or

$$\vec{\Pi}(x, y, z, t) \doteq \frac{1}{4\pi\varepsilon r} Q(t - \frac{r}{v}) \Delta L \, \vec{a} \qquad . \qquad (2.2.4)$$

The field conditions are given in terms of the Hertz vector by the equations

$$\vec{E} = \nabla(\nabla \cdot \vec{\Pi}) - \mu\varepsilon \frac{\partial^2 \vec{\Pi}}{\partial t^2} \qquad , \qquad (2.2.5)$$

and

$$\vec{B} = \mu\varepsilon \ \nabla X \ \frac{\partial \vec{\Pi}}{\partial t} \qquad . \qquad (2.2.6)$$

Assuming the dipole is time harmonic, the above two equations become

$$\vec{E} = \nabla(\nabla \cdot \vec{\Pi}) + \mu\varepsilon\omega^2\vec{\Pi} \qquad (2.2.7)$$

and

$$\vec{B} = j\omega\mu\varepsilon \ \nabla X\vec{\Pi} \qquad . \qquad (2.2.8)$$

In determining the field conditions from the equations for $\vec{E}$ and $\vec{B}$ the calculations are not limited to the far field. Kraus (13) states that the boundary between the near and far fields for a dipole antenna may be taken to be at a radius $R = 2L^2/\lambda$, where L is the length of the antenna and λ is the wavelength of the radiation frequency. If the model were required to represent a cloud to ground discharge one mile in height, a sample R may be calculated using the frequencies of 10 KH and 250 KH, which are the extremes of the narrow band recordings. These frequencies yield R = 0.43 miles for 10 KH and R = 10.7 miles for 250 KH. Thus, at the higher frequencies far field conditions are not guaranteed at distances less than 10 miles, and the calculations must include all components of the field.

To account for the boundary conditions at the earth's surface, image theory is assumed to hold. Under this assumption, the effect of the earth's surface may be represented by the original dipole's image. This consists of a dipole identical to the original dipole located a distance of 2h directly below the original dipole with orientation (-ℓ, -m, n). Here it is assumed that the original dipole was located at a height h above the earth's surface. Reflections between the earth's surface and the ionosphere will be neglected. Thus, the problem of

calculating the radiation from an electric dipole located a height h above the earth's surface will be approximated by calculating the radiation from the original dipole and its image in free space (see Figure 2).
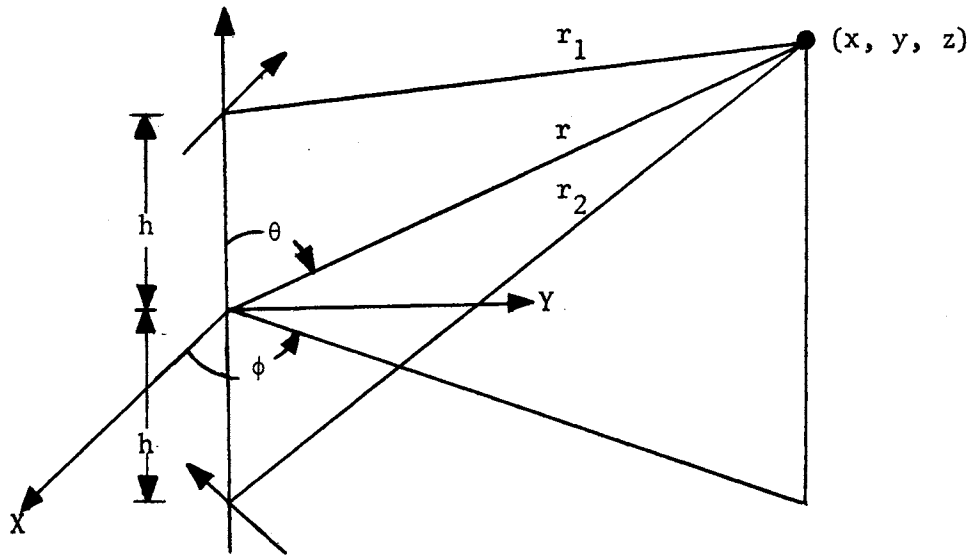
Figure 2. Dipole, Image, and Observation Point

For the present calculation, the dipole will be located at the point (0, 0, h) and its image at (0, 0, -h); the observer is at (x, y, z). The Hertz vector at the observation point is given by

$$(\frac{4\pi\epsilon}{\Delta L}) \vec{\Pi} = \vec{a}_x \, \ell \, \{\frac{Q_1}{r_1} - \frac{Q_2}{r_2}\} + \vec{a}_y \, m \, \{\frac{Q_1}{r_1} - \frac{Q_2}{r_2}\} + \vec{a}_z \, n \, \{\frac{Q_1}{r_1} + \frac{Q_2}{r_2}\} \quad , \quad (2.2.9)$$

where $\vec{a}_x$, $\vec{a}_y$, and $\vec{a}_z$ are unit vectors in the x, y, and z directions, respectively; (ℓ, m, n) and (-ℓ, -m, n) are the direction cosines for the dipole and image, respectively;

$$r_1 = [x^2 + y^2 + (z - h)^2]^{\frac{1}{2}} \qquad ,$$

$$r_2 = [x^2 + y^2 + (z + h)^2]^{\frac{1}{2}} \qquad ,$$

$$Q_1 = Q(t - \frac{r_1}{v}) = Q_0 \exp \{j\omega(t - \frac{r_1}{v})\} \qquad ,$$

and

$$Q_2 = Q(t - \frac{r_2}{v}) = Q_0 \exp \{j\omega(t - \frac{r_2}{v})\} \qquad .$$

Q_1 and Q_2 indicate the time harmonic assumption $Q(t) = Q_0 \exp (j\omega t)$.

The above Hertz vector has been converted to spherical coordinates and the field calculated from the equations for $\vec{E}$ and $\vec{B}$. These results are given in Appendix A in terms of their spherical components E_r, E_θ, E_ϕ, B_r, B_θ, and B_ϕ where $\vec{E} = E_r \vec{a}_r + E_\theta \vec{a}_\theta + E_\phi \vec{a}_\phi$ and $\vec{B} = B_r \vec{a}_r + B_\theta \vec{a}_\theta + B_\phi \vec{a}_\phi$.

Appendix A also presents transformation equations so that the fields produced by various dipoles may be expressed with respect to a common coordinate system.

In this work only $\vec{E}$, the electric intensity vector, will be utilized. The components of $\vec{E}$ may be partitioned according to the following form:

$$E_r = (ER1X + ER2X) + j (ER1Y + ER2Y) \qquad (2.2.10)$$

$$E_\theta = (E\theta1X + E\theta2X) + j (E\theta1Y + E\theta2Y) \qquad (2.2.11)$$

$$E_\phi = (E\phi1X + E\phi2X) + j (E\phi1Y + E\phi2Y) \qquad , \qquad (2.2.12)$$

where the indices 1 and 2 indicate the contribution due to the dipole and the image, respectively; X and Y denote the real and imaginary

parts. With the following substitutions,

$$DRLM = \ell \cos\phi + m \sin\phi$$

$$RMH = r - h \cos\theta$$

$$RPH = r + h \cos\theta$$

$$RNMH = r \, n \cos\theta - h \, n + DRLM \, r \sin\theta$$

$$RNPH = r \, n \cos\theta + h \, n - DRLM \, r \sin\theta \qquad ,$$

the partitioned components of the electric intensity may be written as:

$$ER1X = \frac{\Delta LQ_1}{4\pi\epsilon} \; \frac{\mu\epsilon\omega^2}{r_1} \; [\sin\theta \; DRLM + n \cos\theta]$$

$$+ \frac{1}{r_1^3} \; [- \sin\theta \; DRLM - n \cos\theta - (\frac{\omega}{v})^2 \; RMH \; RNMH] \qquad (2.2.13)$$

$$+ \frac{1}{r_1^5} \; [3 \; RMH \; RNMH] \}$$

$$ER1Y = \frac{\Delta LQ_1}{4\pi\epsilon} \; \{\frac{1}{r_1^2} \; (\frac{\omega}{v}) \; [- \sin\theta \; DRLM - n \cos\theta]$$

$$\qquad\qquad\qquad\qquad\qquad\qquad\qquad\qquad\qquad (2.2.14)$$

$$+ \frac{1}{r_1^4} \; (\frac{\omega}{v}) \; [3 \; RMH \; RNMH] \}$$

$$E\theta1X = \frac{\Delta LQ_1}{4\pi\epsilon} \; \{\frac{\mu\epsilon\omega^2}{r_1} \; [\cos\theta \; DRLM - n \sin\theta]$$

$$+ \frac{1}{r_1^3} \; [- \cos\theta \; DRLM + n \sin\theta - (\frac{\omega}{v})^2 \; h \sin\theta \; RNMH] \qquad (2.2.15)$$

$$+ \frac{1}{r_1^5} \; [3 \; h \sin \; RNMH] \}$$

$$E\theta 1Y = \frac{\Delta LQ_1}{4\pi\epsilon} \left\{ \frac{1}{r_1^2} \left(\frac{\omega}{v}\right) [- \cos\theta \ DRLM + n \ \sin\theta] \right.$$

$$\left. + \frac{1}{r_1^4} \left(\frac{\omega}{v}\right) [3 \ h \ \sin\theta \ RNMH] \right\} \qquad (2.2.16)$$

$$E\phi 1X = \frac{\Delta LQ_1}{4\pi\epsilon} \left\{ \left[- \frac{\mu\epsilon\omega^2}{r_1} + \frac{1}{r_1^3}\right] [\ell \ \sin\phi - m \ \cos\phi] \right\} \qquad (2.2.17)$$

$$E\phi 1Y = \frac{\Delta LQ_1}{4\pi\epsilon} \left\{ \frac{1}{r_1^2} \left(\frac{\omega}{v}\right) [\ell \ \sin\phi - m \ \cos\phi] \right\} \qquad (2.2.18)$$

$$ER2X = \frac{\Delta LQ_2}{4\pi\epsilon} \left\{ \frac{\mu\epsilon\omega^2}{r_2} [- \sin\theta \ DRLM + n \ \cos\theta] \right.$$

$$+ \frac{1}{r_2^3} [\sin\theta \ DRLM - n \ \cos\theta - \left(\frac{\omega}{v}\right)^2 RPH \ RNPH] \qquad (2.2.19)$$

$$\left. + \frac{1}{r_2^5} [3 \ RPH \ RNPH] \right\}$$

$$ER2Y = \frac{\Delta LQ_2}{4\pi\epsilon} \left\{ \frac{1}{r_2^2} \left(\frac{\omega}{v}\right) [\sin\theta \ DRLM - n \ \cos\theta] \right.$$

$$\left. + \frac{1}{r_2^4} \left(\frac{\omega}{v}\right) [3 \ RPH \ RNPH] \right\} \qquad (2.2.20)$$

$$E\theta 2X = \frac{\Delta LQ_2}{4\pi\epsilon} \left\{ \frac{\mu\epsilon\omega^2}{r_2} [- \cos\theta \ DRLM - n \ \sin\theta] \right.$$

$$+ \frac{1}{r_2^3} [\cos\theta \ DRLM + n \ \sin\theta + \left(\frac{\omega}{v}\right)^2 h \ \sin\theta \ RNPH] \qquad (2.2.21)$$

$$\left. + \frac{1}{r_2^5} [- 3 \ h \ \sin\theta \ RNPH] \right\}$$

$$E\theta 2Y = \frac{\Delta LQ_2}{4\pi\epsilon} \left\{ \frac{1}{r_2^2} \left(\frac{\omega}{v}\right) [\cos\theta \ DRLM + n \ \sin\theta] \right.$$

$$\left. + \frac{1}{r_2^4} \left(\frac{\omega}{v}\right) [-3 \ h \ \sin\theta \ RNPH] \right\} \qquad (2.2.22)$$

$$E\phi 2X = \frac{\Delta LQ_2}{4\pi\varepsilon} \left\{ \left[\frac{\mu\varepsilon\omega^2}{r_2} - \frac{1}{r_2^3} \right] [\ell \sin - m \cos\phi] \right\} \qquad (2.2.23)$$

$$E\phi 2Y = \frac{\Delta LQ_2}{4\pi\varepsilon} \left\{ \frac{1}{r_2^2} \left(\frac{\omega}{v} \right) (-\ell \sin\phi + m \cos\phi) \right\} \qquad . \qquad (2.2.24)$$

Throughout this section notation such as Q_1 or ER1X has been used for compactness without any explicit mention of the variables involved. Before proceeding to the next section the variables of the functions of Equations 2.2.13 through 2.2.24 should be considered.

ER1X will be used as an example for this set of equations. First note, from Equation 2.2.13, $ER1X/Q_1$ is a function of frequency (ω), the dipole orientation parameters (ℓ, m, n), the dipole length (ΔL), and the variables relating the dipole position to that of the observation point. Thus for a specified dipole length, orientation, and position $ER1X/Q_1$ may be considered as a function of frequency $H_{r1x}(\omega)$. That is, $ER1X = Q_1 H_{r1x}(\omega)$.

Also recall that $Q_1 = Q(t - r_1/v)$. For the time harmonic assumption, which was introduced to obtain ER1X, $Q(t) = Q_0 \exp(j\omega t)$ or $Q_1 = Q_0 \exp\{j\omega(t - r_1/v)\}$. Thus

$$ER1X = Q_0 \left\{ \exp j\omega(t - \frac{r_1}{v}) \right\} H_{r1x}(\omega) \qquad .$$

For fixed frequency $\omega = \omega_0$, ER1X is a function of time and may be written as

$$ER1X(t) = Q(t) \left\{ \exp(- j\omega_0 \frac{r_1}{v}) \right\} H_{r1x}(\omega_0) \qquad (2.2.25)$$

or

$$ER1X(t) = Q(t - \frac{r_1}{v}) H_{r1x}(\omega) \qquad . \qquad (2.2.26)$$

In the following section it will be illustrated that $H_{r1x}(\omega)$ may be considered a system function for an input of $Q(t - r_1/v)$. Similarly, $\exp(-j\omega \, r_1/v) \, H_{r1x}(\omega)$ may be considered as a system function for an input of $Q(t)$; however, $H_{r1x}(\omega)$ was chosen for notational convenience.

2.3 <u>Fourier Transform of $\vec{E}$</u>. Consider a system characterized by the system function $H(\omega)$. An input $f(t)$ produces an output response $g(t)$ given by (14).

$$g(t) = \frac{1}{2\pi} \int_{-\infty}^{\infty} G(\omega) \, e^{j\omega t} d\omega \qquad , \qquad (2.3.1)$$

where

$$G(\omega) = H(\omega) \, F(\omega) \qquad . \qquad (2.3.2)$$

$F(\omega)$ and $G(\omega)$ are the Fourier transforms of $f(t)$ and $g(t)$, respectively. If the input $f(t)$ is time harmonic with angular frequency ω_0, that is

$$f(t) = Q_0 \, e^{j\omega_0 t} \qquad ,$$

the $F(\omega)$ becomes

$$F(\omega) = 2\pi \, Q_0 \, \delta(\omega - \omega_0) \qquad ,$$

and

$$g(t) = \int_{-\infty}^{\infty} H(\omega) \, Q_0 \, e^{j\omega t} \, \delta(\omega - \omega_0) \, d\omega$$

$$\qquad (2.3.3)$$

$$= H(\omega_0) \, f(t) \qquad .$$

This is exactly the procedure used to obtain the components of $\vec{E}$. That is the Hertz vector, and thus the magnitude of the dipole moment, was assumed time harmonic and the output time response was derived. Thus

according to Equation 2.3.3 if the Q_i terms are deleted each of the expressions ER1X through Eϕ2Y may be considered as system functions of the form $H(\omega)$ relating the retarded dipole charge to the corresponding component of the electric intensity. These system functions will be denoted by $H_{r1x}(\omega),\ldots,H_{\phi 2y}(\omega)$.

The Fourier transform of the components of the electric intensity due to an electric dipole with specified length, orientation, and position with respect to the observation point may be calculated from equations of the form 2.3.2. Let $G_{r1}(\omega)$, $G_{\theta 1}(\omega)$, and $G_{\phi 1}(\omega)$ be the spherical components resulting from the original dipole.

$$G_{r1}(\omega) = \{H_{r1x}(\omega) + jH_{r1y}(\omega)\} \, F_1(\omega) \qquad (2.3.4)$$

$$G_{\theta 1}(\omega) = \{H_{\theta 1x}(\omega) + jH_{\theta 1y}(\omega)\} \, F_1(\omega) \qquad (2.3.5)$$

$$G_{\phi 1}(\omega) = \{H_{\phi 1x}(\omega) + jH_{\phi 1y}(\omega)\} \, F_1(\omega) \qquad (2.3.6)$$

where $F_1(\omega)$ is the Fourier transform of the retarded charge

$$Q_1 = Q(t - \frac{r_1}{v})\qquad .$$

The contributions due to the image are obtained similarly by replacing 1 with 2 in the above expressions. $F_2(\omega)$ is the transform of $Q_2 = Q(t - r_2/v)$.

Let the subscripts ki denote the ith dipole for k = 1 and its image for k = 2. Assuming superposition is valid, the field components produced by a configuration of n dipoles and the associated images are

$$G_r(\omega) = \sum_{i=1}^{n} \sum_{k=1}^{2} G_{rki}(\omega) = \sum_{i=1}^{n} \sum_{k=1}^{2} H_{rki}(\omega) \, F_{ki}(\omega) \qquad (2.3.7)$$

$$G_\theta(\omega) = \sum_{i=1}^{n} \sum_{k=1}^{2} G_{\theta k i}(\omega) = \sum_{i=1}^{n} \sum_{k=1}^{2} H_{\theta k i}(\omega) \, F_{k i}(\omega) \qquad (2.3.8)$$

$$G_\phi(\omega) = \sum_{i=1}^{n} \sum_{k=1}^{2} G_{\phi k i}(\omega) = \sum_{i=1}^{n} \sum_{k=1}^{2} H_{\phi k i}(\omega) \, F_{k i}(\omega) \qquad (2.3.9)$$

where

$$H_{rki}(\omega) = H_{rkix}(\omega) + jH_{rkiy}(\omega)$$

$$H_{\theta k i}(\omega) = H_{\theta k i x}(\omega) + jH_{\theta k i y}(\omega)$$

$$H_{\phi k i}(\omega) = H_{\phi k i x}(\omega) + jH_{\phi k i y}(\omega) \qquad .$$

Equations 2.3.7 through 2.3.9 may be expressed in the vector form

$$\vec{G}(\omega) = \sum_{i=1}^{n} \sum_{k=1}^{2} \vec{H}_{ki}(\omega) \, F_{ki}(\omega) \qquad , \qquad (2.3.10)$$

for

$$\vec{H}_{ki}(\omega) = \vec{a}_r \, H_{rki}(\omega) + \vec{a}_\theta \, H_{\theta k i}(\omega) + \vec{a}_\phi \, H_{\phi k i}(\omega) \qquad .$$

Equation 2.3.10 summarizes the procedure, in this work, to calculate the Fourier transform of the electric intensity produced by a configuration of n dipoles and the associated images. This procedure is illustrated in Figure 3.

One additional note should be made. If the transform of f(t) is F(ω), the transform of f(t - τ) is F(ω) exp (-jωτ). Thus

$$F_{1i}(\omega) = F_i(\omega) \exp\left(-j\omega \frac{r_{1i}}{v}\right)$$

and

$$F_{2i}(\omega) = F_i(\omega) \exp\left(-j\omega \frac{r_{2i}}{v}\right) \qquad ,$$

where $F_i(\omega)$ is the transform of $Q_i(t)$, the charge for the ith dipole

and image. This indicates the equivalence of Equations 2.2.25 and
2.2.26.
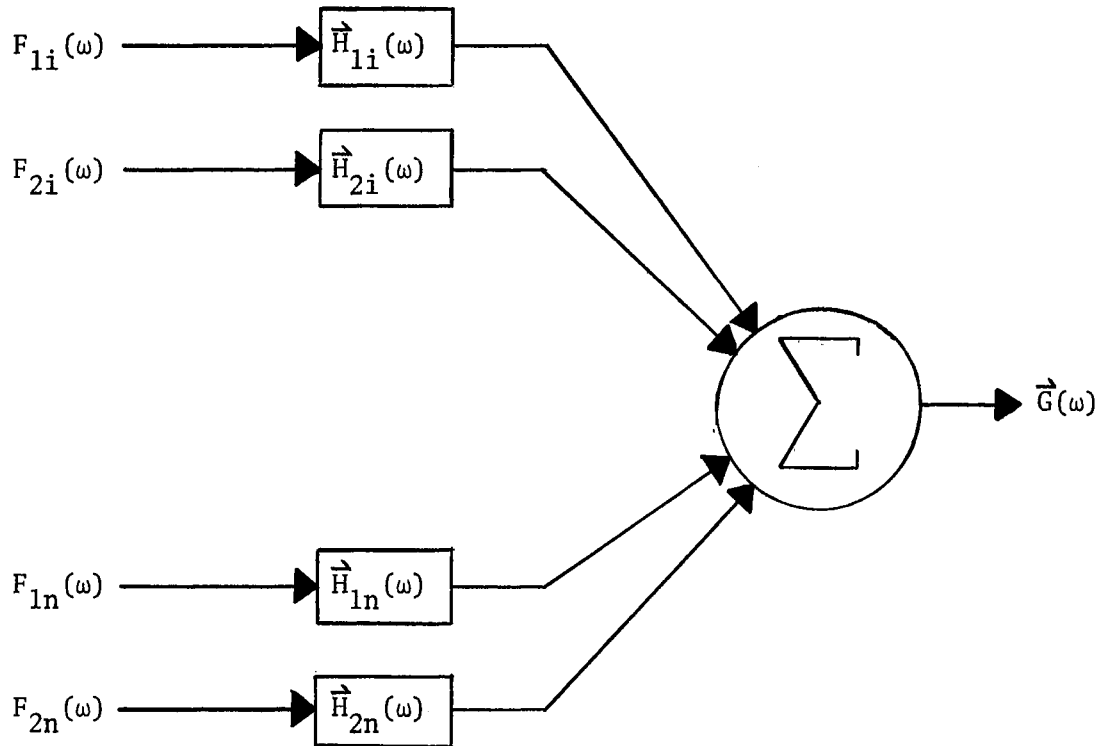
Figure 3. The Relation of $F(\omega)$, $\vec{H}(\omega)$, and $\vec{G}(\omega)$

2.4 The Detected Field. The procedure for determination of the
narrow-band, half-wave linear detected field is developed in this sec-
tion. The development is presented in scalar form.

Consider the system of Figure 4. $G(\omega)$ denotes a scalar component
of $\vec{G}(\omega)$ discussed in the previous section; $H_\beta(\omega)$ is the system function
of a band-pass filter with bandwidth β about a center frequency ω_c;
$H_D(\omega)$ represents a half-wave linear detector; $H_L(\omega)$ represents a low-
pass filter. $X(\omega)$, $Y(\omega)$, and $Z(\omega)$ are the corresponding outputs with

inverse transforms $x(t)$, $y(t)$, and $z(t)$, respectively.

$$G(\omega) \longrightarrow \boxed{H_\beta(\omega)} \xrightarrow{X(\omega)} \boxed{H_D(\omega)} \xrightarrow{Y(\omega)} \boxed{H_L(\omega)} \longrightarrow Z(\omega)$$
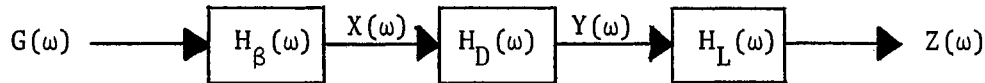
Figure 4. Detection System

$H_\beta(\omega)$ is assumed to be nonzero only in the frequency interval $\omega_c - \beta/2 \leq |\omega| \leq \omega_c + \beta/2$. Thus $X(\omega)$ is easily obtained from

$$X(\omega) = H_\beta(\omega) \, G(\omega) \qquad , \omega_c - \beta/2 \leq |\omega| \leq \omega_c + \beta/2$$

$$\hspace{10cm} (2.4.1)$$

$$= 0 \qquad , \text{otherwise} \qquad .$$

Since the half-wave linear detector is a nonlinear device, it is necessary to transform $X(\omega)$ into $x(t)$ and proceed with the development in the time domain. Thus $H_D(\omega)$ is avoided.

An inverse Fourier transform algorithm (4) may be used to compute $x(t)$ from $X(\omega)$. Bendat and Piersol (3) indicate the number of discrete samples of $X(\omega)$ required to describe $x(t)$ is 2BT, where B is the highest frequency present in $X(\omega)$ and the time function is assumed to exist from 0 to T seconds. The band-limited, time-limited assumption is not theoretically possible but may be closely approximated.

The maximum B required for this work is 250.5 KH; a maximum T of 1 second should be sufficient to represent most discharges. Thus $2BT = .5001 \times 10^6$ samples are required. The Fourier transform algorithm, in addition to other storage requirements, requires a matrix to

store the 2BT samples of $X(\omega)$. Since $X(\omega)$ is complex, on the order of 10^6 samples must be stored for the 2BT requirement alone. This number is prohibitive and must be reduced.

The 2BT requirement was deduced from the requirement that $X(\omega)$ be sampled at Nyquist co-interval points $2\pi/T$ apart on the frequency scale from $-2\pi B$ to $2\pi B$. Thus the number of samples required was given by

$$n = \frac{4\pi B}{\frac{2\pi}{T}} = 2BT \qquad .$$

In an attempt to use the fact that $X(\omega)$ represents a real bandpass time signal to reduce the 2BT requirement, a very fortunate situation arises. In general $x(t)$ is

$$x(t) = \frac{1}{2\pi} \int_{-\infty}^{\infty} X(\omega) \exp(j\omega t) \, d\omega \qquad . \qquad (2.4.2)$$

Since $x(t)$ is real and $X(\omega)$ is nonzero only for $\omega_c - \beta/2 \leq |\omega| \leq \omega_c + \beta/2$, (14),

$$x(t) = \text{Re} \{\frac{1}{\pi} \int_{\omega_c - \frac{\beta}{2}}^{\omega_c + \frac{\beta}{2}} X(\omega) \exp(j\omega t) \, d\omega\} \qquad . \qquad (2.4.3)$$

Making the change of variables $\eta = \omega - \omega_c + \beta/2$,

$$x(t) = \text{Re} \{\exp[j(\omega_c - \frac{\beta}{2})t] \frac{1}{\pi} \int_0^{\beta} X(\eta + \omega_c - \frac{\beta}{2}) \exp(j\eta t) \, d\eta\} \qquad . \qquad (2.4.4)$$

The integral in Equation 2.4.4 is the inverse transform of $X(\omega)$ shifted from the interval $[\omega_c - \beta/2, \omega_c + \beta/2]$ to the interval $[0, \beta]$. That is $X(\eta + \omega_c - \beta/2)$ is required from 0 to β on the frequency scale. Sampling $X(\eta + \omega_c - \beta/2)$ at Nyquist co-interval points $2\pi/T$ apart requires $\beta T/2\pi$ samples, where $\beta/2\pi \leq 1$ KHz for applications of this work. Thus

the inverse transform indicated in Equation 2.4.4 can be effected by
the Fourier transform algorithm.

In general this inverse will be a complex function of time
$f_1(t) + jf_2(t)$.

$$f_1(t) + jf_2(t) = \frac{1}{\pi} \int_0^\beta X(\eta + \omega_c - \frac{\beta}{2}) \exp(j\eta t) \, d\eta \quad . \quad (2.4.5)$$

Equation 2.4.4 may now be written as

$$x(t) = f_1(t) \cos(\omega_c - \frac{\beta}{2})t - f_2(t) \sin(\omega_c - \frac{\beta}{2})t \quad . \quad (2.4.6)$$

Consider the function $v(t) \cos(\omega t + \phi(t))$ which may be exapnded into

$v(t) \cos(\omega t + \phi(t)) = v(t) \cos \phi(t) \cos \omega t - v(t) \sin \phi(t) \sin \omega t$.
Thus $x(t)$ may be presented in the form

$$x(t) = v(t) \cos[\omega_c t + \phi(t)] \quad , \quad (2.4.7)$$

where

$$v(t) = \{f_1^2(t) + f_2^2(t)\}^{\frac{1}{2}}$$

$$\phi(t) = -\frac{\beta t}{2} + \tan^{-1} \frac{f_2(t)}{f_1(t)} \quad .$$

Davenport and Root (6) have derived the response of a half-wave
linear detector followed by an ideal low-pass filter for a narrow-band
input of the form $x(t) = v(t) \cos[\omega_c t + \phi(t)]$ to be

$$z(t) = \frac{a \, v(t)}{\pi} \quad , \quad (2.4.8)$$

where a is the scale factor of $y(t) = a \, x(t)$, $x(t) \geq 0$. Thus

$$z(t) = \frac{a}{\pi} \{f_1^2(t) + f_2^2(t)\}^{\frac{1}{2}} \quad . \quad (2.4.9)$$

Equation 2.4.9 is the major results of this section. That is, if the ideal approximation to $H_L(\omega)$ is acceptable, the narrow-band, half-wave linear detected field may be obtained by multiplying $G(\omega)$ by $H_\beta(\omega)$ over the frequency interval $\omega_c - \beta/2 \leq \omega \leq \omega_c + \beta/2$ to obtain $X(\omega)$, taking the inverse transform of $X(\omega + \omega_c - \beta/2)$ over the frequency interval $0 \leq \omega \leq \beta$ to obtain $f_1(t) + jf_2(t)$, and introducing these functions into Equation 2.4.9 to obtain $z(t)$.

If the ideal approximation to $H_L(\omega)$ is not acceptable, $z(t)$ of Equation 2.4.9 may be transformed, multiplied by the $H_L(\omega)$ desired, and the resulting product transformed to obtain a time function $z(t)$ which does not involve the ideal low-pass filter assumption.

CHAPTER III

GENERAL DISCHARGE AND IMPLEMENTATION

3.1 Introduction. In Chapter II the field equations were developed for one oscillating electric dipole and its image in free space. These equations were interpreted as system functions relating the dipole charge to the components of the electric field. The procedure for obtaining $\vec{G}(\omega)$, the Fourier transform of the received field due to a configuration of n dipoles, from these system functions was outlined. With $\vec{G}(\omega)$ available it was shown mathematically how z(t), the narrow-band half-wave linear detected field, could be obtained.

Fortran IV programs have been developed to compute $\vec{G}(\omega)$ and z(t). This chapter will discuss the general form of discharge modeled, what inputs are required for the programs to construct the discharge geometry, and how the current waveforms are to be specified. With this information the procedure used by the programs to calculate $\vec{G}(\omega)$ and z(t) will be discussed.

3.2 General Form of Discharge. The general geometry of the discharge model, illustrated in Figure 5, consists of L_0 straight segments connecting the points (X_0, Y_0, Z_0) and (X_b, Y_b, Z_b) with N_b branching segments extending outward from (X_b, Y_b, Z_b). Each of these segments, $L = 1,...,L_0 + N_b$, consists of N(L) oscillating electric dipoles of length $\Delta L(L)$ placed end to end through the length of the segment. The direction cosines for each dipole within a segment is $(\ell(L), m(L), n(L))$

corresponding to the orientation of that segment.
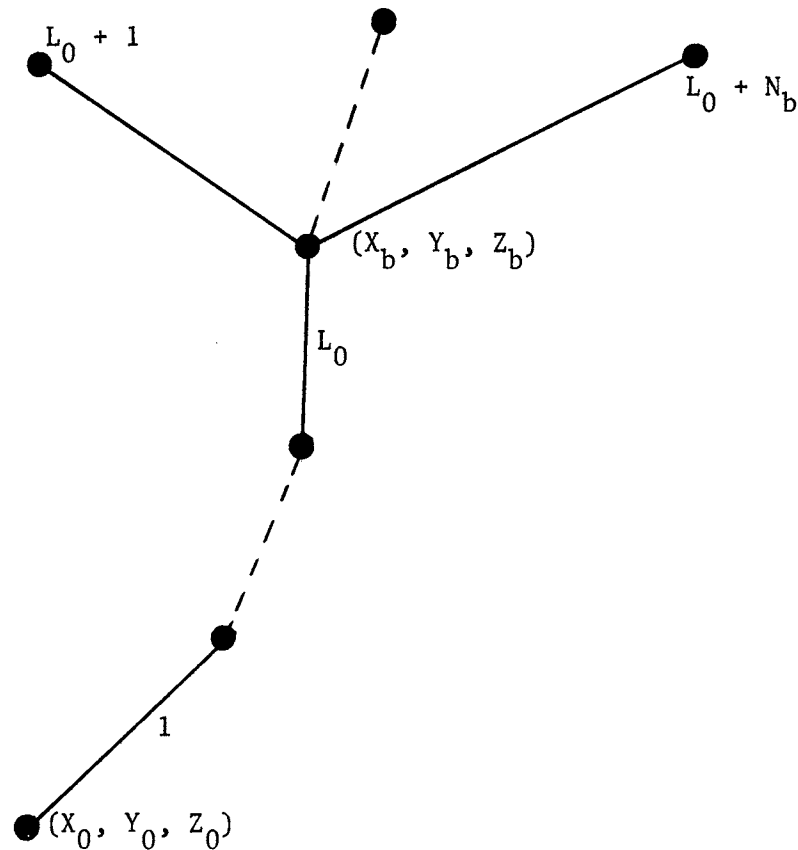
Figure 5. General Discharge Geometry

If the point (X_0, Y_0, Z_0) is specified to be a point on the earth's surface, $Z_0 = 0$, one may consider the segments from $(X_0, Y_0, 0)$ to (X_b, Y_b, Z_b) to approximate the main channel of a cloud-to-ground discharge and the branching segments to represent streamers feeding the main channel. Also intracloud discharges may be modeled by allowing (X_0, Y_0, Z_0) to be above the earth's surface. However, this requires knowledge of the current waveforms existing in such discharges. Since

these waveforms are not available at present (19) for intracloud discharges, the discussion will be limited to cloud-to-ground discharges where the processes involved are better understood.

Three separate currents are allowed in the model. At time T_{OL} a time-varying current $I_L(t)$ is allowed to progress down the main channel from (X_b, Y_b, Z_b) to (X_0, Y_0, Z_0) with a velocity $V_L(t)$. At a later time T_{OR} a return current $I_R(t)$ is allowed to move up the channel from (X_0, Y_0, Z_0) to (X_b, Y_b, Z_b) with a velocity $V_R(t)$. Still later in time, T_{OS}, a third current $I_S(t)$ moves from (X_b, Y_b, Z_b) towards the branch tips with a velocity $V_S(t)$. These three currents are to approximate the stepped or dart leader, the return stroke, and the streamer process, respectively. Any one of these may be deleted from the model by specifying the corresponding current to be zero. The only requirement on the current waveforms is that analytical expressions for the Fourier transforms of the waveforms be available.

3.3 <u>Specification of Geometry and Velocities</u>. In constructing a particular discharge the two programs require the specification of two points in space: (X_0, Y_0, Z_0), the tip of the main channel, and (X_a, Y_a, Z_a), the position where the field is to be determined. Z equal to zero corresponds to the earth's surface. With the number of segments in the main channel, L_0, and the number of branches, N_b, decided the geometry of the discharge is then established by specifying the direction cosines, $(\ell(L), m(L), n(L))$, and the length, determined by the product $N(L)\Delta L(L)$, of each segment. $N(L)$ is the number of dipoles in the Lth segment, and $\Delta L(L)$ is the length common to all dipoles within that segment.

The velocities determining the propagation of the current waveforms

through the geometry are assumed to have the exponential forms

$$V_L(t) = V_{LO} \exp[-G_L(t - T_{OL})]U(t - T_{OL}) \qquad ,$$

$$V_R(t) = V_{RO} \exp[-G_R(t - T_{OR})]U(t - T_{OR}) \qquad ,$$

$$V_S(t) = V_{SO} \exp[-G_S(t - T_{OS})]U(t - T_{OS}) \qquad ,$$

where U is the unit step function. These velocities are specified through the parameters V_{LO}, G_L and T_{OL} for the leader current, V_{RO}, G_R and T_{OR} for the return current and V_{SO}, G_S and T_{OS} for the streamer current.

A word of caution about choosing values for V_0 and G in the above expressions is in order. The maximum distance attainable by a velocity of the above exponential form is V_0/G. Thus V_{LO}/G_L and V_{RO}/G_R must be chosen larger than the length of the main channel, and V_{SO}/G_S must be larger than the longest branching segment.

The value of zero is allowable for G to obtain a constant velocity in any of the above expressions. Also if a current is to be excluded from the model, computation time will be saved by specifying the corresponding velocity to be zero.

A time delay term is built into the leader velocity which allows the current to pause for DELAY seconds before each dipole that is a multiple of a specified integer, NDSP, before proceeding through the next dipole with the velocity existing before the delay. The length of the delay is selected from a normal distribution by specifying the desired mean and standard deviation. Also an odd integer IX must be specified to initialize the random selection.

The input data required by both programs are identical. The

variables discussed above are listed below with associated format and the order in which they are required by the programs.

X_0, Y_0, Z_0, L_0, N_b (3E14.5, 1X, I3, 1X, I1)

$N(L)$, $\ell(L)$, $m(L)$, $n(L)$, $L(L)$ (I3,4E14.5), for $L = 1,\ldots,L_0 + N_b$

X_a, Y_a, Z_a (3E14.5)

V_{SO}, G_S, V_{LO}, G_L, V_{RO}, G_R (4E14.5/2E14.5)

T_{OS}, T_{OL}, T_{OR}, IX   (3E14.5, I9)   .

3.4 Specification of Current Waveforms. The procedure used to calculate $\vec{G}(\omega)$, the Fourier transform of the received field due to a configuration of n dipoles, is summarized by Equation 2.3.10.

$$\vec{G}(\omega) = \sum_{i=1}^{n} \sum_{k=1}^{2} \vec{H}_{ki}(\omega) \, F_{ki}(\omega) \qquad . \qquad (2.3.10)$$

The subscripts ki denote the ith dipole for k = 1 and its image for k = 2. $\vec{H}_{ki}(\omega)$ represents the system functions derived in Chapter II. $F_{ki}(\omega)$ denotes the Fourier transform of the retarded dipole charge $Q_{ki}(t - r_{ki}/v)$. It was shown in Section 2.3 that

$$F_{1i}(\omega) = F_i(\omega) \, \exp\left(-j\omega \frac{r_{1i}}{v}\right) \qquad , \qquad (3.4.1)$$

and

$$F_{2i}(\omega) = F_i(\omega) \, \exp\left(-j\omega \frac{r_{2i}}{v}\right) \qquad , \qquad (3.4.2)$$

where $F_i(\omega)$ is the transform of $Q_i(t)$. This results from an equal charge assumed on the dipole and its image. Thus to obtain the $F_{ki}(\omega)$ required by Equation 2.3.10 it is necessary to determine $F_i(\omega)$, the

transform of the charge waveform on each dipole in the configuration.

Up to now only currents have been specified in the segments. However if a length is to be approximated by an electric dipole, the equation of continuity requires the following relation for the dipole charge and the current flowing through that length.

$$\frac{\partial Q_i(t)}{\partial t} = I_i(t) \qquad ,$$

or

$$Q_i(t) = \int_{-\infty}^{t} I_i(t')\, dt' \qquad .$$

$F_i(\omega)$ is given by (14)

$$F_i(\omega) = I_i(\omega)\left[\pi\delta(\omega) + \frac{1}{j\omega}\right] \qquad ,$$

where $\delta(\omega)$ is the delta function, and $I_i(\omega)$ is the transform

$$I_i(\omega) = \int_{-\infty}^{\infty} I_i(t)\, \exp(-j\omega t)\, dt \qquad .$$

In this work the d.c. terms, $\omega = 0$, will not be considered. With this understanding $F_i(\omega)$ may be expressed by

$$F_i(\omega) = \frac{1}{j\omega} \int_{-\infty}^{\infty} I_i(t)\, \exp(-j\omega t)\, dt \qquad . \qquad (3.4.3)$$

Before expressions for $F_i(\omega)$ can be obtained from the integral 3.4.3 it is necessary to discuss the times involved. The convention adopted in this work is that a dipole in the configuration is considered "on" and conducting with the current flowing through that segment only when the corresponding velocity has progressed through the length approximated by that dipole. These times are calculated within the programs from the velocity expressions and stored in columns six and seven

of a matrix $D(i, j)$.

Let dipoles in the main channel have i subscripts from 1 to N_n and those in the branches have i subscripts from $N_n + 1$ to N_d, where N_n denotes the number of dipoles in the main channel and N_d is the total number of dipoles in the configuration. With this notation $D(i, 6)$ for $i = 1,\ldots,N_n$ is the time the ith dipole is considered conducting with the leader current $I_i(t)$; $D(i, 7)$ for $i = 1,\ldots,N_n$ is the time the ith dipole is considered conducting with the return current $I_R(t)$; and $D(i, 6)$ for $i = N_n + 1,\ldots,N_d$ is the similar time for the streamer current $I_S(t)$.

The "off" times or the times at which the currents are assumed to cease flowing in the length approximated by the ith dipole are denoted as $T_{1,i}$, $T_{2,i}$ and $T_{3,i}$ for the leader, return and streamer currents, respectively. A large degree of flexibility is allowed in selecting these "off" times. For example a reasonable choice for $T_{1,i}$ would be $T_{1,i} = D(i, 7)$. That is, the leader current is assumed to stop flowing and be replaced by the return current when the return velocity reaches that length represented by the dipole. A value of $D(N_n, 6)$ plus some time delay could be chosen for $T_{2,i}$. Thus the return current is assumed to cease flowing some time delay after the return velocity reaches the top of the main channel. The only point to be made here is that the "off" times are denoted by the parameters $T_{1,i}$, $T_{2,i}$ and $T_{3,i}$ and are to be selected in conjunction with the current waveforms.

Thus with the six parameters for the conducting times the current waveforms for each dipole in the configuration can be expressed in one of two forms. For dipoles in the main channel the current corresponding to the ith dipole is

$$I_i(t) = I_L(t)\{U[t - D(i, 6)] - U[t - T_{1,i}]\}$$

$$(3.4.4)$$

$$+ I_R(t)\{U[t - D(i, 7)] - U[t - T_{2,i}]\}, \quad 1 \leq i \leq N_n \quad .$$

The current corresponding to dipoles in the branching segments is

$$I_i(t) = I_S(t)\{U[t - D(i, 6)] - U[t - T_{3,i}]\}, \quad N_n + 1 \leq i \leq N_d . \quad (3.4.5)$$

Substituting the above current equations into Equation 3.4.3 yields

$$F_i(\omega) = \frac{1}{j\omega} \{\int_{D(i, 6)}^{T_{1,i}} I_L(t) \exp(-j\omega t) \, dt$$

$$(3.4.6)$$

$$+ \int_{D(i, 7)}^{T_{2,i}} I_R(t) \exp(-j\omega t) \, dt\}, \quad 1 \leq i \leq N_n$$

for dipoles in the main channel and

$$F_i(\omega) = \frac{1}{j\omega} \int_{D(i, 6)}^{T_{3,i}} I_S(t) \exp(-j\omega t) \, dt, \quad N_n + 1 \leq i \leq N_d \quad (3.4.7)$$

for dipoles in the branching segments.

In summary to obtain the expressions for $F_{ki}(\omega)$ required by Equation 2.3.10 it is necessary to decide on the current waveforms to be used and the associated "off" times for these currents. These "off" times may be constants, functions of $D(i, 6)$ or $D(i, 7)$, or even infinity if the time delays of the current waveforms are chosen properly. With the above specified only two analytical expressions for $F_i(\omega)$ are required for all elements in the configuration. These are obtained from Equation 3.4.6 for elements in the main channel and Equation 3.4.7 for elements in the branching segments. For elements in the main channel the programs require an analytical expression derived from the

integral 3.4.6 of the form

$$F_i(\omega) = F_i[\omega, D(i, 6), D(i, 7), T_{1,i}, T_{2,i}], \quad 1 \leq i \leq N_n$$

that is a function of angular frequency and the four time parameters.

To represent elements in the branches an analytical expression of the

form

$$F_i(\omega) = F_i[\omega, D(i, 6), T_{3,i}], \quad N_n + 1 \leq i \leq N_d$$

derived from the integral 3.4.7 is required. With these two analytical

expressions the programs substitute the proper parameters for the dipole

under consideration to obtain $F_i(\omega)$, utilize Equations 3.4.1 and 3.4.2

to obtain $F_{ki}(\omega)$, and introduce the $F_{ki}(\omega)$ into the summation 2.3.10.

3.5 $\vec{G}(\omega)$ Program. This section is not intended as a detailed dis-

cussion of a computer program. It is included to given an understanding

of the actual procedure employed in calculating the Fourier transform

of the radiated field. With this discussion and the corresponding For-

tran program listed in Appendix B one should be able to assess the pro-

cedure used in the computations.

The indicies on the dipoles are as follows. The index i = 1 cor-

responds to the dipole touching the point (X_0, Y_0, Z_0). The index in-

creases to i = N_n for the dipole in the main channel touching the

branching point. The dipole with index i = N_n + 1 touches the branching

point and is in the first branch specified by the input data. The last

dipole, i = N_d, is the dipole in the last specified branch furthest

removed from the branching point.

With the input data discussed in Section 3.3 the program first

calculates the center of each dipole in the configuration. The

rectangular coordinates of these centers are stored in $D(i, 1)$, $D(i, 2)$ and $D(i, 3)$, $i = 1,\ldots,N_d$. These values are used to calculate r_{1i} and r_{2i}, the distance from the observation point to the dipole center and image center, respectively. These values are stored in $D(i, 4)$ and $D(i, 5)$, $i = 1,\ldots,N_d$.

Next the program calculates the "on" times for the streamer, leader, and return currents. Before discussing the particulars associated with each current, the general procedure will be discussed. The general velocity expression for the three currents is

$$V(t) = V_0 \exp[-G(t - T_0)]U(t - T_0) \quad .$$

Let T_n, the "on" time for the nth dipole, be expressed by the time the velocity moves through the segments represented by the first $n - 1$ dipoles plus the time required to travel the length, d_n, corresponding to the nth dipole. That is

$$T_n = T_{n-1} + \Delta T_n \quad ,$$

where

$$T_{n-1} = T_0 + \sum_{j=1}^{n-1} \Delta T_j \quad .$$

The expressions for ΔT_n are determined from the above relations and the integral expression

$$d_n = \int_{T_{n-1}}^{T_n} V(t) \, dt \quad .$$

For zero values of G this results in

$$\Delta T_n = \frac{d_n}{V_0} \quad .$$

For G not equal to zero the expression is

$$\Delta T_n = \frac{1}{G} \ln\{\frac{V_{00}}{V_{00} - G d_n}\} \qquad ,$$

where

$$V_{00} = V_0 \exp[-G(T_{n-1} - T_0)] \qquad .$$

With the above expression for ΔT_n the program calculates the stream-er current "on" times for dipoles in the branches starting each branch at the common time T_{0S}. These values are stored in $D(i, 6)$, $i = N_n + 1$, ...,N_d. Specifying N_b, the number of branches, equal to zero will omit these calculations.

If V_{L0} is specified nonzero, the times at which dipoles in the main channel are considered conducting with the leader current are com-puted. Calculations start at time T_{0L} with the N_n^{th} dipole and progress down the main channel. These computed values are stored in the first N_n rows of $D(i, 6)$.

For a nonzero value of V_{R0} the "on" times for the return current are computed beginning with the first dipole at time T_{0R} and progress up the main channel. These values are retained in $D(i, 7)$, $i = 1,...,$ N_n.

$\vec{G}(\omega)$ is calculated at the discrete frequencies 1 through 10 KHz in 1 KHz steps, 15 through 100 KHz in 5 KHz steps and 110 through 250 KHz in 10 KHz steps. These values were chosen to give good representation on semi-log plots from 1 to 250 KHz with only forty-three frequencies required. Denoting these frequencies by f_j, the calculation of the first value of $\vec{G}(\omega)$ is begun by setting $\omega_j = 2\pi f_j$. Utilizing $D(i, 1)$ through $D(i, 5)$ the system functions contained in Equations 2.2.13

through 2.2.24 are evaluated for the first dipole and its image.

As mentioned in Chapter II, these system functions were derived with respect to a spherical coordinate system with origin directly beneath the dipole center on the earth's surface, [D(i, 1), D(i, 2), 0]. In order to sum the contributions from all dipoles in the configuration a common set of coordinates is required. The point $(X_0, Y_0, 0)$ is chosen as origin for this reference coordinate system. The system functions evaluated above are then transformed to the spherical components of the common coordinate system.

These system functions could be used to compute $\vec{G}(\omega)$ in the form $G_r \vec{A}_r + G_\theta \vec{A}_\theta + G_\phi \vec{A}_\phi$. However in this work only the horizontal and vertical components are retained. The convention adopted is to let the horizontal component correspond to the ϕ - component and the vertical consist of the r - and θ - components projected on the vertical axis. With this notation the system functions for the horizontal and vertical components are calculated.

The analytical expressions for $F_i(\omega)$ which contain D(i, 6) and D(i, 7) as parameters are evaluated at ω_j for the dipole under consideration. $F_{1i}(\omega_j)$ and $F_{2i}(\omega_j)$ are obtained by multiplying $F_i(\omega_j)$ by $\exp[-j\omega_j \, D(i, 4)/v]$ and $\exp[-j\omega_j \, D(i, 5)/v]$, respectively. $F_{1i}(\omega_j)$ and $F_{2i}(\omega_j)$ are multiplied by the appropriate system functions to obtain the contribution from this dipole to the horizontal and vertical components of $\vec{G}(\omega_j)$.

The program then returns to the point the first dipole was selected, selects the next dipole, and performs the same calculations leading to the contribution from that dipole and image. This procedure is repeated until the contributions from all dipoles have been summed to

obtain the horizontal and vertical components of $\vec{G}(\omega_j)$. The magnitude and phase of the horizontal and vertical components of $\vec{G}(\omega_j)$ and the frequency f_j are printed out. The program then selects the next frequency and repeats the above procedure for the remaining frequencies.

3.6 z(t) Program. This program was developed to calculate the horizontal and vertical components of the narrow-band, half-wave linear detected fields for 1 KHz bandwidths about each of the six center frequencies 10, 50, 150, 200 and 250 KHz. The procedure employed is summarized by Equations 2.4.1, 2.4.5 and 2.4.9.

$$X(\omega) = H_\beta(\omega) \; G(\omega) \qquad , \; \omega_c - \beta/2 \leq |\omega| \leq \omega_c + \beta/2$$

$$\hspace{10cm} (2.4.1)$$

$$= 0 \qquad\qquad , \text{ otherwise}$$

$$f_1(t) + jf_2(t) = \frac{1}{\pi} \int_0^\beta X(\eta + \omega_c - \frac{\beta}{2}) \exp(j\eta t) \, d\eta \qquad (2.4.5)$$

$$z(t) = \frac{1}{\pi} \{f_1^2(t) + f_2^2(t)\}^{\frac{1}{2}} \qquad\qquad . \quad (2.4.9)$$

That is, to compute z(t), a narrow-band, half-wave linear detected component of the field, it is necessary to multiply the component of $\vec{G}(\omega)$ by the system function of the desired band-pass filter and compute the magnitude of the inverse transform of that product shifted on the frequency axis.

This program is essentially an extension of the $\vec{G}(\omega)$ program. The horizontal and vertical components of $\vec{G}(\omega)$, $G_h(\omega)$ and $G_v(\omega)$, are computed in exactly the same manner as in the previous program. The only difference is in the values chosen for the sample frequencies ω_j. Rather than calculating $\vec{G}(\omega)$ for frequencies across the band from 1 to 250 KHz,

the frequencies are chosen only in the 1 KHz bands about the six center frequencies.

The first center frequency, f_c, is selected and $G_h(\omega_j)$ and $G_v(\omega_j)$ are computed for $f_j = f_c - 500$ Hz with a spacing of $1000/256$ Hz. This spacing allows 256 samples over the band considered and permits a time representation of $z(t)$ for $0 \leq t < .256$ seconds in accordance with the Fourier transform algorithm.

As $G_h(\omega_j)$ and $G_v(\omega_j)$ are calculated, $X_h(\omega_j)$ and $X_v(\omega_j)$ are formed by multiplying by the assumed $H_\beta(\omega_j)$, which for simplicity was chosen to be unity over the 1 KHz band and zero elsewhere. The real and imaginary parts of $X_h(\omega_j)$ and $X_v(\omega_j)$ are stored in the four rows of the matrix $XK(k, j)$, $k = 1,\ldots,4$ and $j = 1,\ldots,256$.

If $f(t)$ is a time function with Fourier transform $F(\omega)$ for $-b \leq \omega \leq b$ and zero elsewhere, then $f(t)$ is given by the inversion integral

$$f(t) = \frac{1}{2\pi} \int_{-b}^{b} F(\omega) \exp (j\omega t)\, d\omega \qquad .$$

The algorithm's approximation to this integral requires samples of $F(\omega)$ in the following order. For N even, the first $N/2$ equally spaced samples represent $F(\omega)$ for $0 \leq \omega \leq b$; the remaining $N/2$ samples represent $F(\omega)$ for $-b \leq \omega \leq 0$. Equation 2.4.5 can then be modified to this form by allowing the first 256 samples to be the calculated samples of $X(\omega_j)$, $f_c - 500$ Hz $\leq f_j < f_c + 500$ Hz, and the remaining 256 samples to be zero.

These samples are accepted by the algorithm in the array names DATA (1,J) and DATA (2,J) representing the real and imaginary parts of $F(\omega)$. These arrays are transformed in place, within the accuracy of the algorithm, to give the real and imaginary parts of $f(t)$. The

procedure used by the program is then to define the arrays as

$$\text{DATA } (1,J) = XK (1,j) \qquad , j = J = 1,\ldots,256$$

$$= 0 \qquad , \qquad J = 257,\ldots,2560$$

and

$$\text{DATA } (2,j) = XK (2,j) \qquad , j = J = 1,\ldots,256$$

$$= 0 \qquad , \qquad J = 257,\ldots,2560 \qquad .$$

The additional padding with zeros is introduced to obtain better time resolution. The algorithm's subroutine is then called and the magnitude $(2/\pi T) |\text{DATA } (1,J) + j \text{ DATA } (2,J)|$ calculated for $J = 1,\ldots,2560$. The factor 2 is required because of the difference in the inversion integral defining $f(t)$ and Equation 2.4.5. The factor $1/T$, $T = .256$ seconds, is required by the algorithm. With the $1/\pi$ factor these values represent $z(t_J)$ for the horizontal component at sample values $t_J = (J - 1)(10^{-4})$ seconds. These values of $z(t_J)$ and t_J are printed out for $J = 1,\ldots,$ 512 corresponding to $0 \leq t \leq 51.1$ msec.

The vertical component is calculated by redefining the array DATA as

$$\text{DATA } (1,J) = XK (3,j) \qquad , j = J = 1,\ldots,256$$

$$= 0 \qquad , \qquad J = 257,\ldots,2560$$

and

$$\text{DATA } (2,J) = XK (4,j) \qquad , j = J = 1,\ldots,256$$

$$= 0 \qquad , \qquad J = 257,\ldots,2560 \qquad .$$

The same procedure is followed to compute the vertical component of $z(t_J)$. After these values are printed, the program returns to select the next center frequency and repeats the procedure beginning with calculation of $G_h(\omega_j)$ and $G_v(\omega_j)$ about the new center frequency.

CHAPTER IV

MODEL COMPARISON

4.1 Introduction. In this chapter the procedure described in

Chapter III is employed to calculate the magnitude of the Fourier trans-

form of the received field due to a return stroke, a stepped leader

process, and a combination stepped leader and return stroke. These

spectra are compared with those obtained from other models existing in

the literature.

The incorporation of streamer processes into the model is consid-

ered, and the results of the narrow-band, half-wave linear detected

field calculations are discussed.

4.2 Return Stroke. It is assumed (9,19) prior to the return

stroke, $t < T_{OR}$, the leader process has deposited a uniform distribution

of negative charge along the channel length between the cloud and the

ground. The original source of this negative charge was the lower por-

tion of the cloud. The function of the return stroke is to transport

or partially transport this distributed negative charge to ground. This

distribution is symbolized with five electric dipoles in Figure 6, where

the Q_L terms denote the static charge on the dipoles due to the pre-

ceding leader process, and the $q_i(t)$ denote the time varying charge re-

sulting from the return stroke current. Specifying the $q_i(t)$ terms to

be zero for $t < T_{OR}$, $i = 1,2,\ldots,5$, Figure 6 indicates a net static

charge $-Q_L$ per unit length down the channel with the lower portion of

the cloud reflecting the absence of this distributed charge.

Cloud

5th Dipole

$+5Q_L + q_5(t)$ $\}$ $+5Q_L + q_5(t)$

$-5Q_L - q_5(t)$
$+4Q_L + q_4(t)$ $\}$ $-Q_L + [q_4(t) - q_5(t)]$

$-4Q_L - q_4(t)$
$+3Q_L + q_3(t)$ $\}$ $-Q_L + [q_3(t) - q_4(t)]$

$-3Q_L - q_3(t)$
$+2Q_L + q_2(t)$ $\}$ $-Q_L + [q_2(t) - q_3(t)]$

1st Dipole

$-2Q_L - q_2(t)$
$+1Q_L + q_1(t)$ $\}$ $-Q_L + [q_1(t) - q_2(t)]$

$-1Q_L - q_1(t)$ $\}$ $-Q_L + [0 - q_1(t)]$

Ground
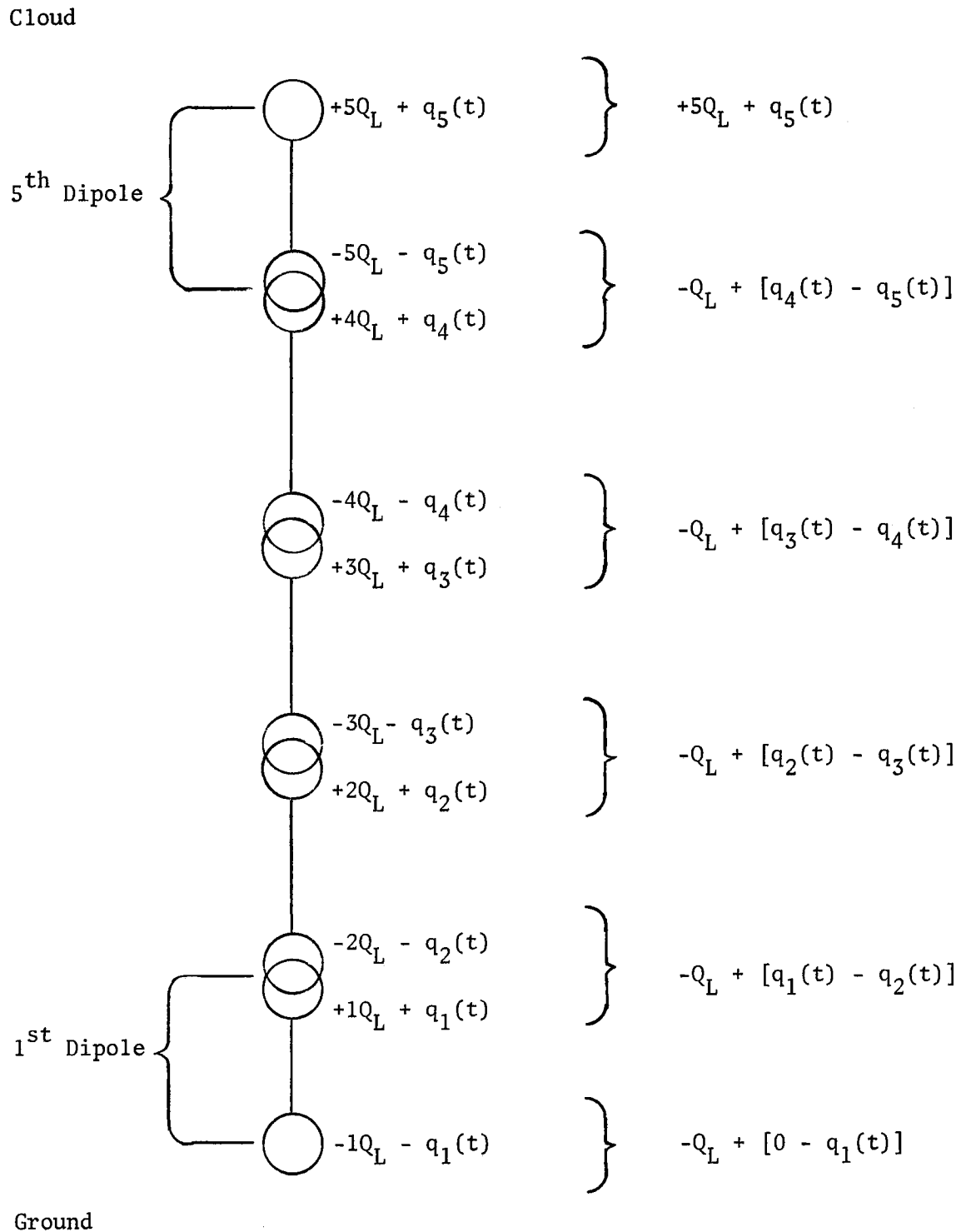
Figure 6. Dipole Approximation of Channel

In the notation of the preceding chapter, at time $t = T_{OR}$ a positive current $I_R(t)$ is assumed to progress up the channel from the first dipole to the fifth. $D(i, 7)$ denotes the time the ith dipole is considered conducting with $I_R(t)$, and $T_{2,i}$ is the "off" time. The charge on the ith dipole is

$$Q_i(t) = i \; Q_L + q_i(t) \qquad , \qquad (4.2.1)$$

where

$$q_i(t) = \int_{-\infty}^{t} I_R(t)\{U[t' - D(i, 7)] - U[t' - T_{2,i}]\} \; dt' \; . \quad (4.2.2)$$

Note for a current progressing up the channel

$$T_{OR} < D(1, 7) < D(2, 7) < \cdots < D(5, 7) \qquad .$$

Assuming $T_{2,i}$ infinite for all i and recalling that $I_R(t) \geq 0$ yields

$$q_i(t) \geq q_2(t) \geq \cdots \geq q_5(t) \qquad .$$

That is, each of the quantitites $[q_i(t) - q_{i+1}(t)]$ is greater than or equal to zero, and the effect of the return stroke modeled with a series of dipoles in this fashion reduces the negative charge distributed along the channel by the leader process and transports this charge to ground as required.

The widely accepted model of Bruce and Golde (5) for the current of a return stroke at the ground is

$$i(t) = I_0[\exp (- \alpha t) - \exp (- \beta t)] \qquad , \qquad (4.2.3)$$

where typical values for the first return stroke of a discharge are $I_0 = 3 \times 10^4$ amp., $\alpha = 2 \times 10^4$ sec^{-1}, and $\beta = 2 \times 10^5$ sec^{-1}. The

accompanying expression for the velocity determining the upward movement of the current is

$$V(t) = V_0 \exp(-\gamma t) \quad , \qquad (4.2.4)$$

with typical values for a first return stroke of $V_0 = 8 \times 10^7$ m/sec and $\gamma = 3 \times 10^4$ sec^{-1}. V_0 and γ correspond to V_{RO} and G_R, respectively, in the expression

$$V_R(t) = V_{RO} \exp[-G_R(t - T_{OR})]U(t - T_{OR})$$

used to calculate the values of $D(i, 7)$.

The Bruce and Golde current model is incorporated into the dipole model of the return stroke as

$$I_R(t) = I_0\{\exp[-\alpha(t - T_{OR})] - \exp[-\beta(t - T_{OR})]\}U(t - T_{OR}) \quad . \quad (4.2.5)$$

The Fourier transform of $Q_i(t)$ given in Equation 4.2.1 denoted by $F_i(\omega)$ is

$$F_i(\omega) = i\, Q_L 2\pi\delta(\omega) + I_i(\omega)[\pi\delta(\omega) + \frac{1}{j\omega}] \quad , \qquad (4.2.6)$$

where $I_i(\omega)$ is the transform of

$$I_R(t)\{U[t - D(i, 7)] - U[t - T_{2,i}]\} \quad .$$

If all $T_{2,i}$ are equal, the above expression requires continuity of current in all dipoles with index less than or equal to i for values of time greater than or equal to $D(i, 7)$.

Ignoring the d.c. terms and allowing $T_{2,i}$ to be infinite, $F_i(\omega)$ required by the programs is

$$F_i(\omega) = \frac{1}{j\omega} I_i(\omega) \quad ,$$

or

$$F_i(\omega) = \exp[-j\omega D(i, 7)] \frac{I_0}{j\omega} \left[\frac{\exp\{\alpha[T_{OR}-D(i, 7)]\}}{\alpha + j\omega} - \frac{\exp\{\beta[T_{OR}-D(i, 7)]\}}{\beta + j\omega} \right] .$$

(4.2.7)

Using the typical values for a first return stroke,

$I_0 = 3 \times 10^4$ amp $\qquad \alpha = 2 \times 10^4 \ sec^{-1} \qquad \beta = 2 \times 10^5 \ sec^{-1}$

$V_{RO} = 8 \times 10^7$ m/sec $\qquad G_R = 3 \times 10^4 \ sec^{-1} \qquad T_{OR} = 0$ sec ,

Equation 4.2.7 was introduced into the $\vec{G}(\omega)$ program, and the vertical component of the field was computed for a vertical discharge extending from the earth's surface to a height of 1 Km. These results are shown in Figures 7 through 11 for the observation point located 100 Km from the channel on the ground plane. In this chapter and the next only the Fourier spectrum, that is the amplitude of the Fourier transform, will be presented.

In Figure 7 the 1 Km channel length is approximated by one thousand dipoles with 1 M lengths; in Figure 8 one hundred dipoles with 10 M lengths are used for the approximations; Figure 9 results from ten dipoles with lengths of 100 M; Figure 10 results from five dipoles with lengths of 200 M; Figure 11 results from two dipoles 500 M long.

The point to be made from a comparison of these curves is that the accuracy of the model is not improved at the expense of utilizing dipoles shorter than 10 M to approximate the discharge length for the frequency range considered.

Hill (9) indicates the spectrum for a first return stroke should be a smooth curve with a maximum of fifty to sixty μvolt sec/M occurring approximately at 5 KHz. It was noted that the procedure employed by
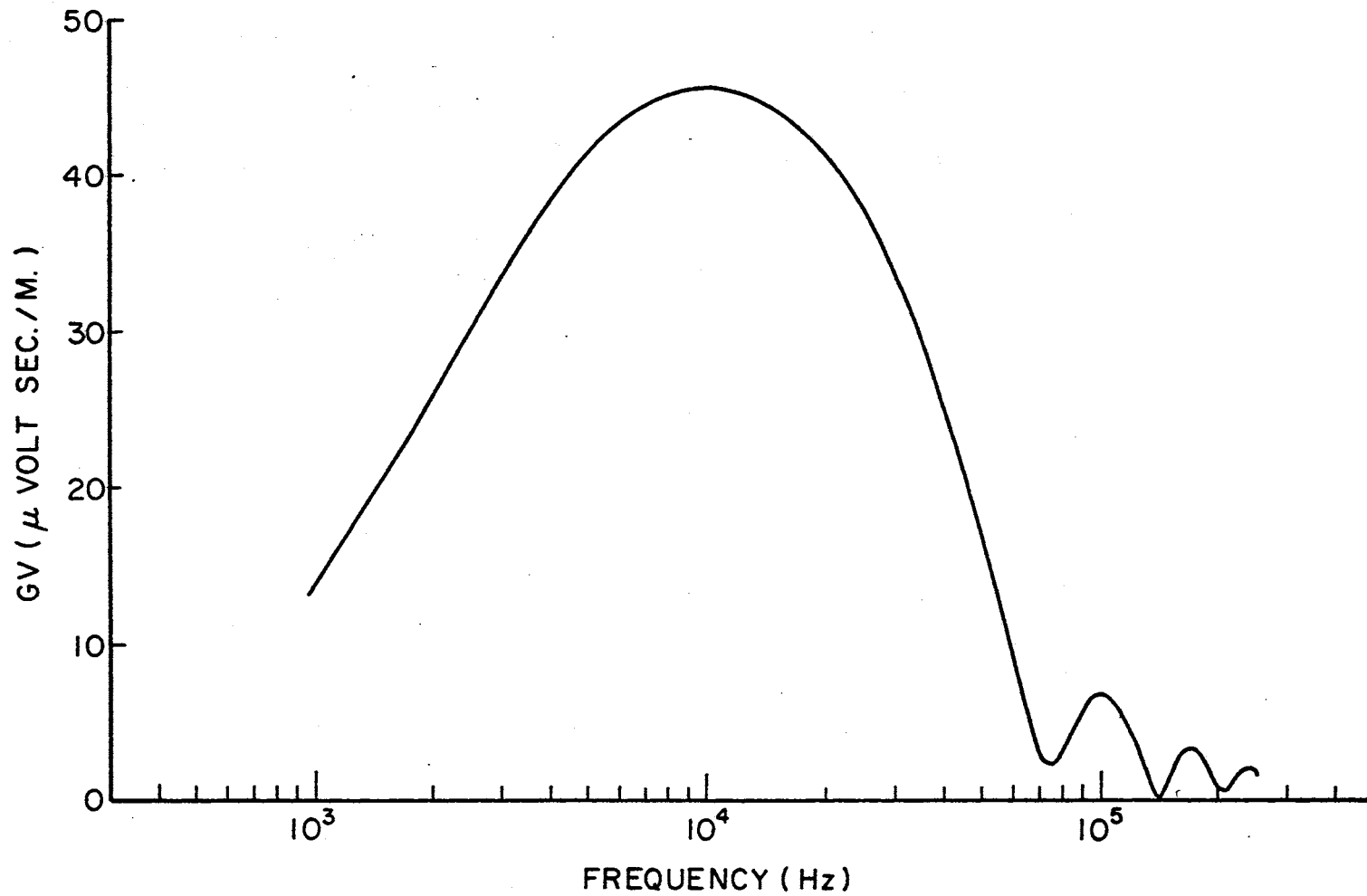
Figure 7. 1 Km Vertical Return Stroke With 1 M Dipoltes
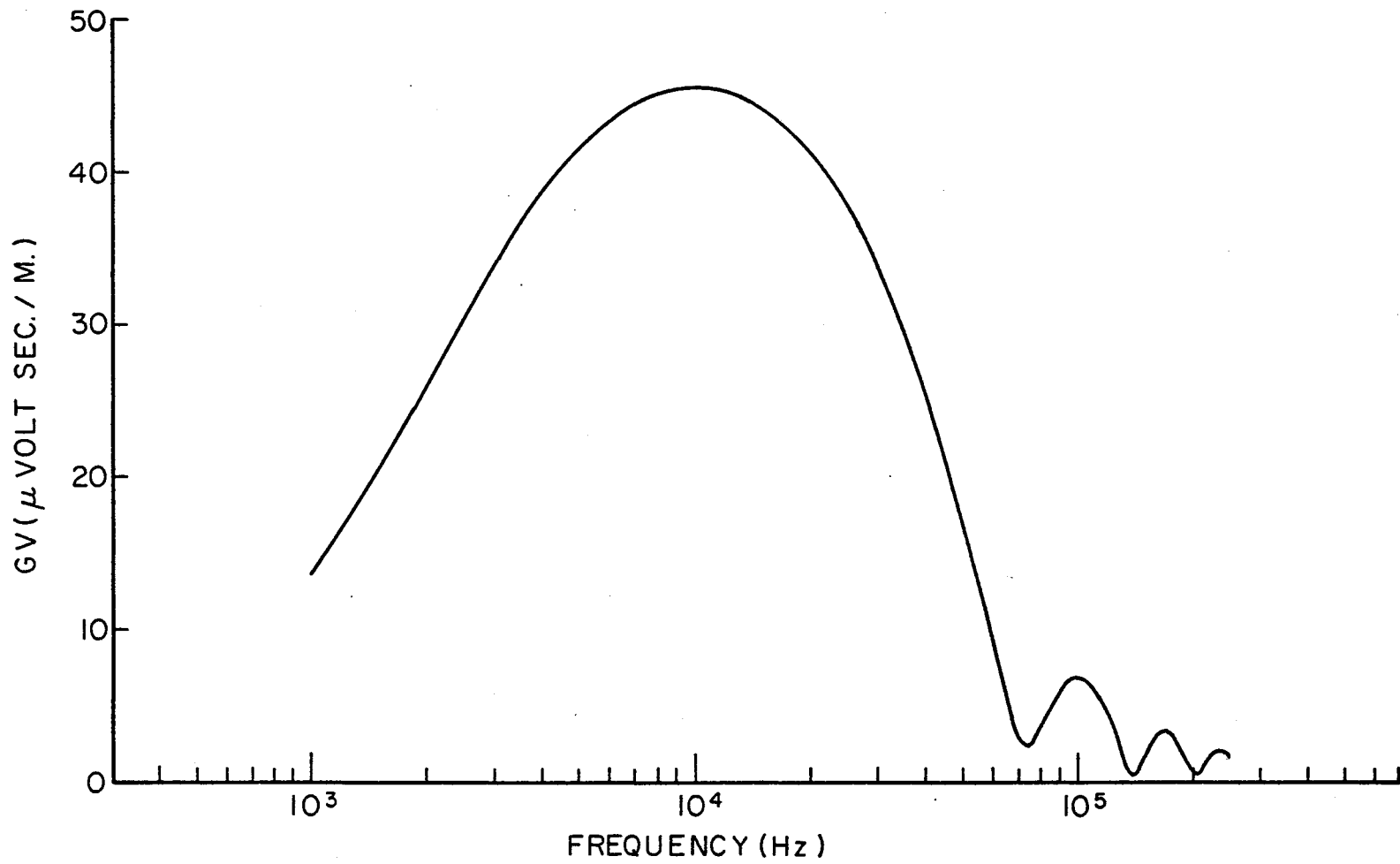
Figure 8. 1 Km Vertical Return Stroke With 10 M Dipoles
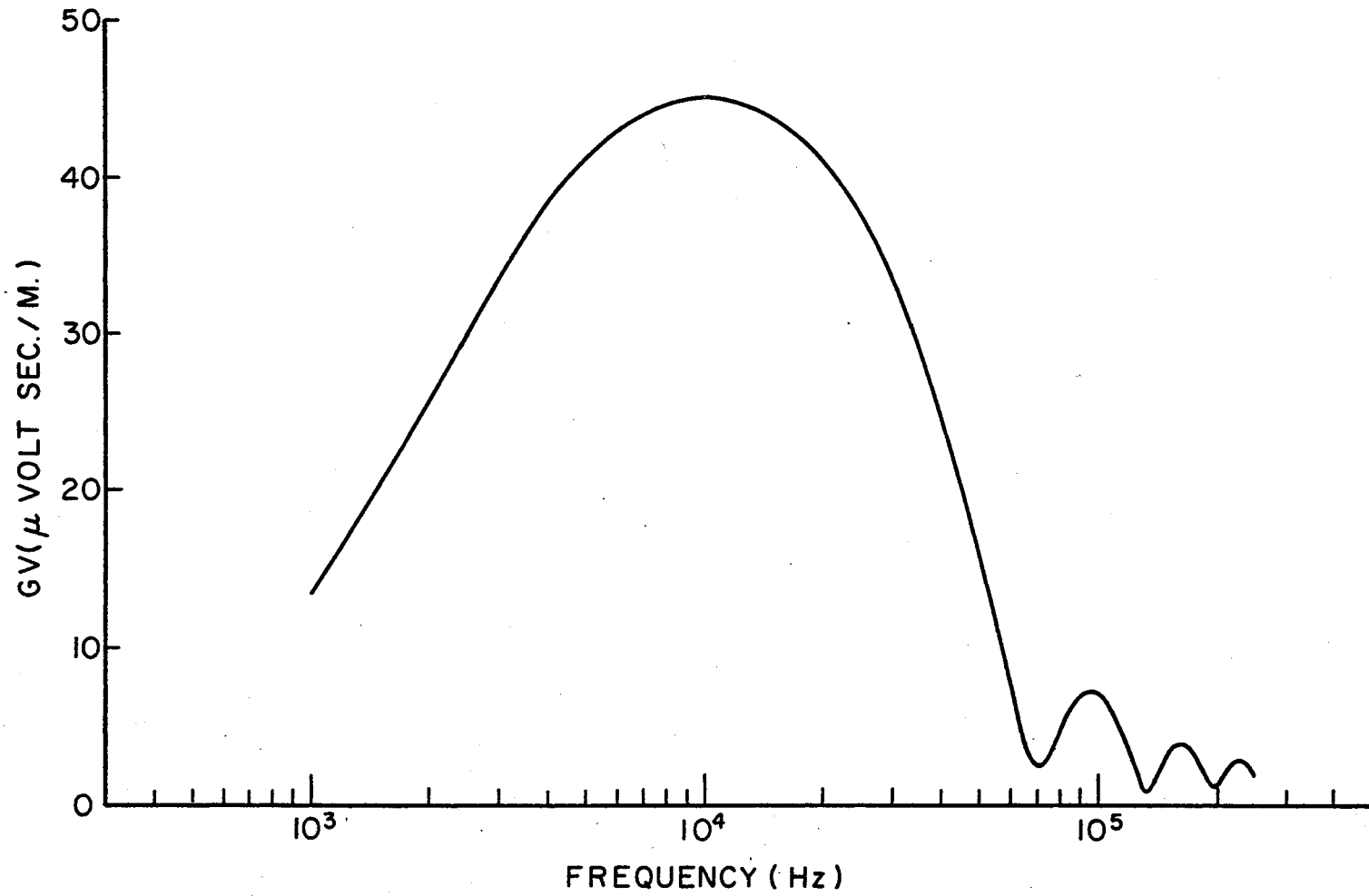
Figure 9. 1 Km Vertical Return Stroke With 100 M Dipoles
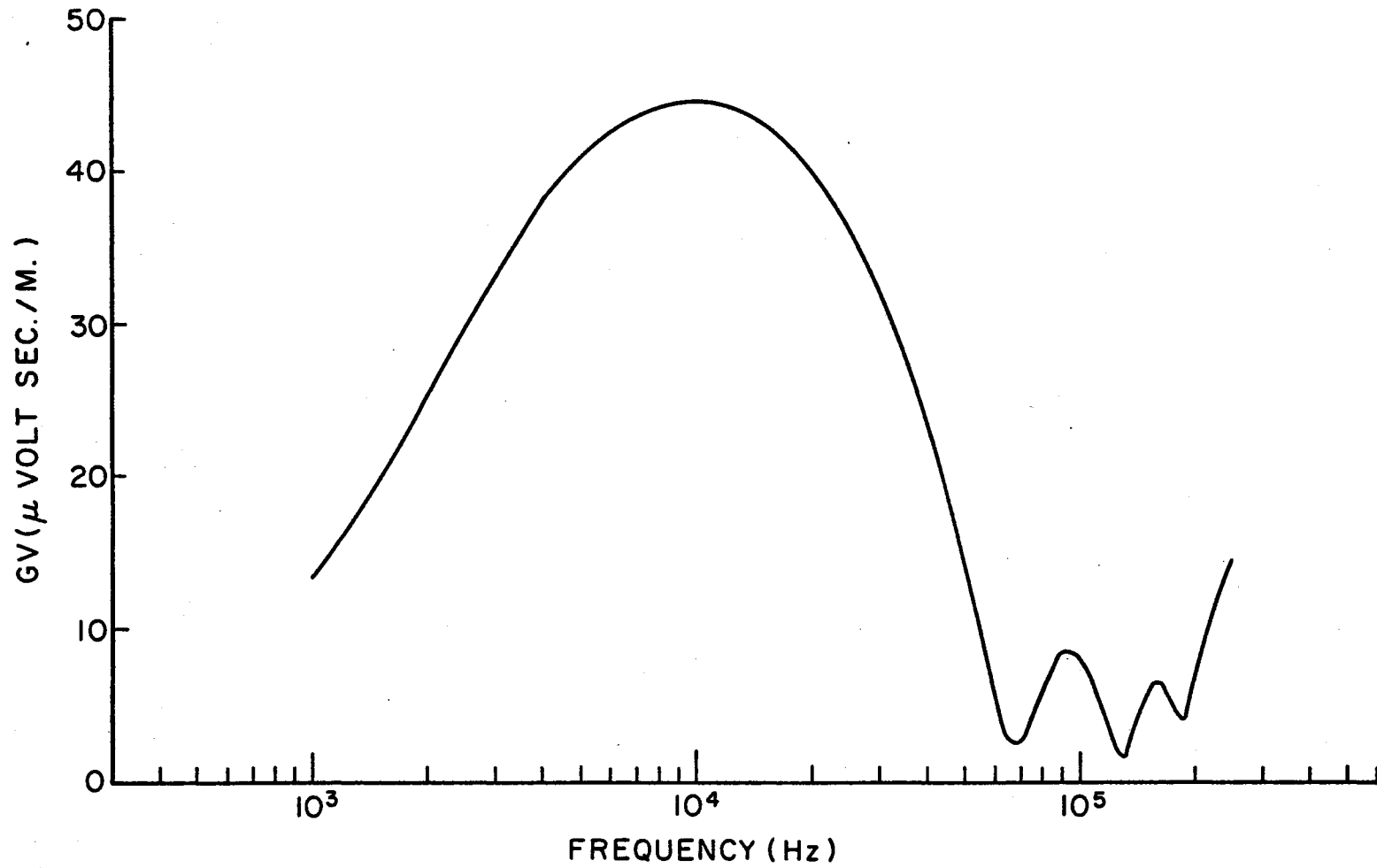
Figure 10. 1 Km Vertical Return Stroke With 200 M Dipoles
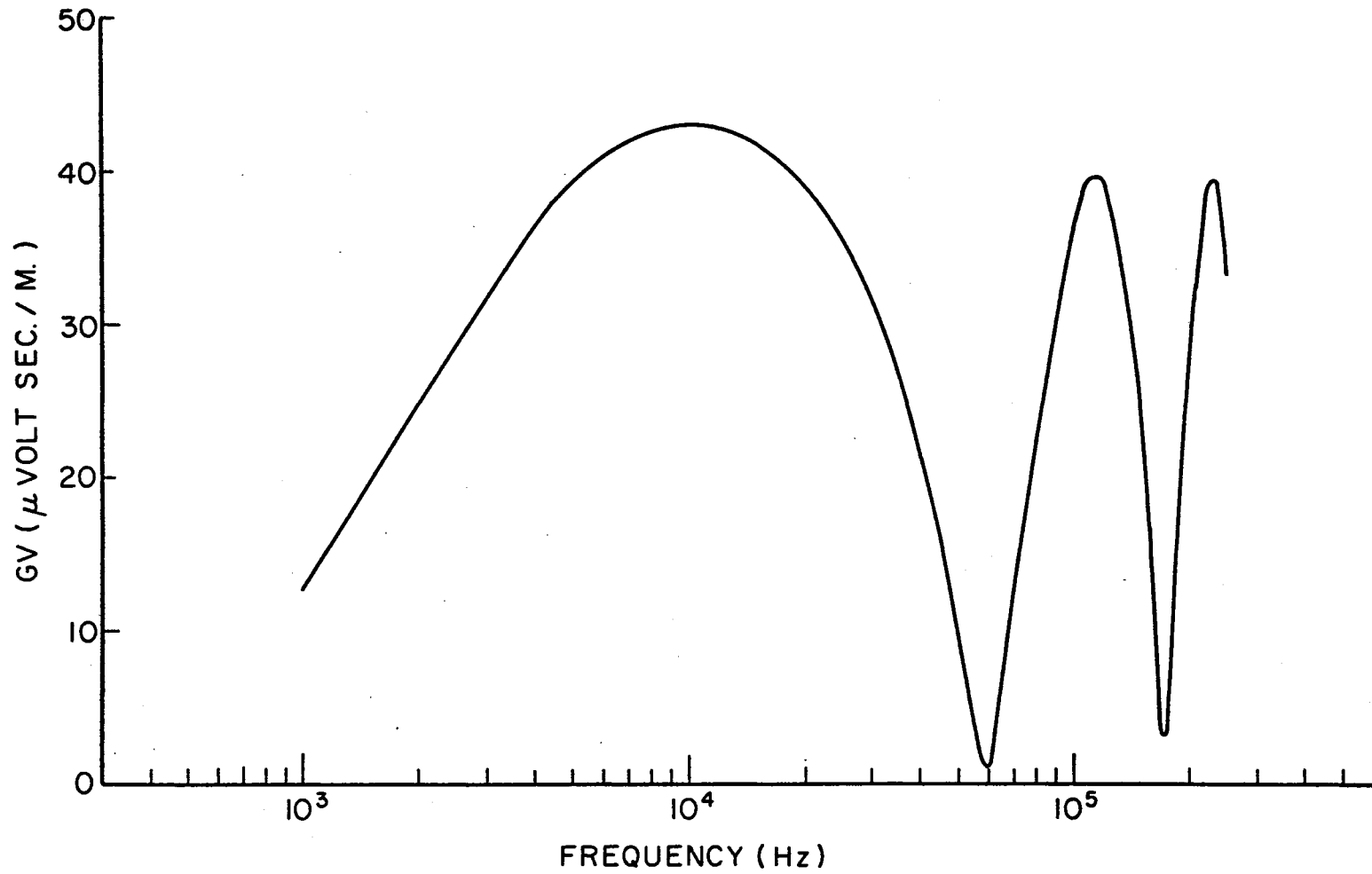
Figure 11. 1 Km Vertical Return Stroke With 500 M Dipoles

Hill in computing the transform of the field allowed the channel length
to extend to the length permitted by the velocity expression $V_R(t)$ in
an infinite amount of time. For the values of V_{RO} and G_R assumed here
the maximum channel length achieved is determined by V_{RO}/G_R = 2 2/3 Km.

Figure 12 was obtained from an identical set of parameters as dis-
cussed previously, with the number of 10 M dipoles changed from one
hundred to two hundred sixty-six to approximate the 2 2/3 Km channel
length. This graph is very similar to that given by Hill's model in
magnitude and position of the maximum value for the same current and
velocity parameters.

It is concluded that the minor peaks which occur in the first five
graphs of this chapter are a result of terminating the channel length
before the current has decayed sufficiently. That is, for a channel
length of 1 Km the time required for the return stroke current to prog-
ress through this length is 15.7 μsec. One may think of the return
current waveform time decay as being governed by α. This represents an
effective time constant of 50 μsec. Thus 15.7 μsec is less than one-
third of the decay time constant, and the return stroke current is of
appreciable magnitude at this time.

The shifting of the maximum values from 10 KHz to 5 KHz as the
channel height was increased from 1 Km to 2 2/3 Km is a very interesting
situation which will be discussed in the next chapter.

4.3 Stepped Leader. Although the programs developed in this work
are capable of implementing a variety of models for the stepped or dart
leader processes, only one model which is readily adaptable to the pro-
grams will be discussed.

First, it is assumed at time T_{OL} a leader pulse with current
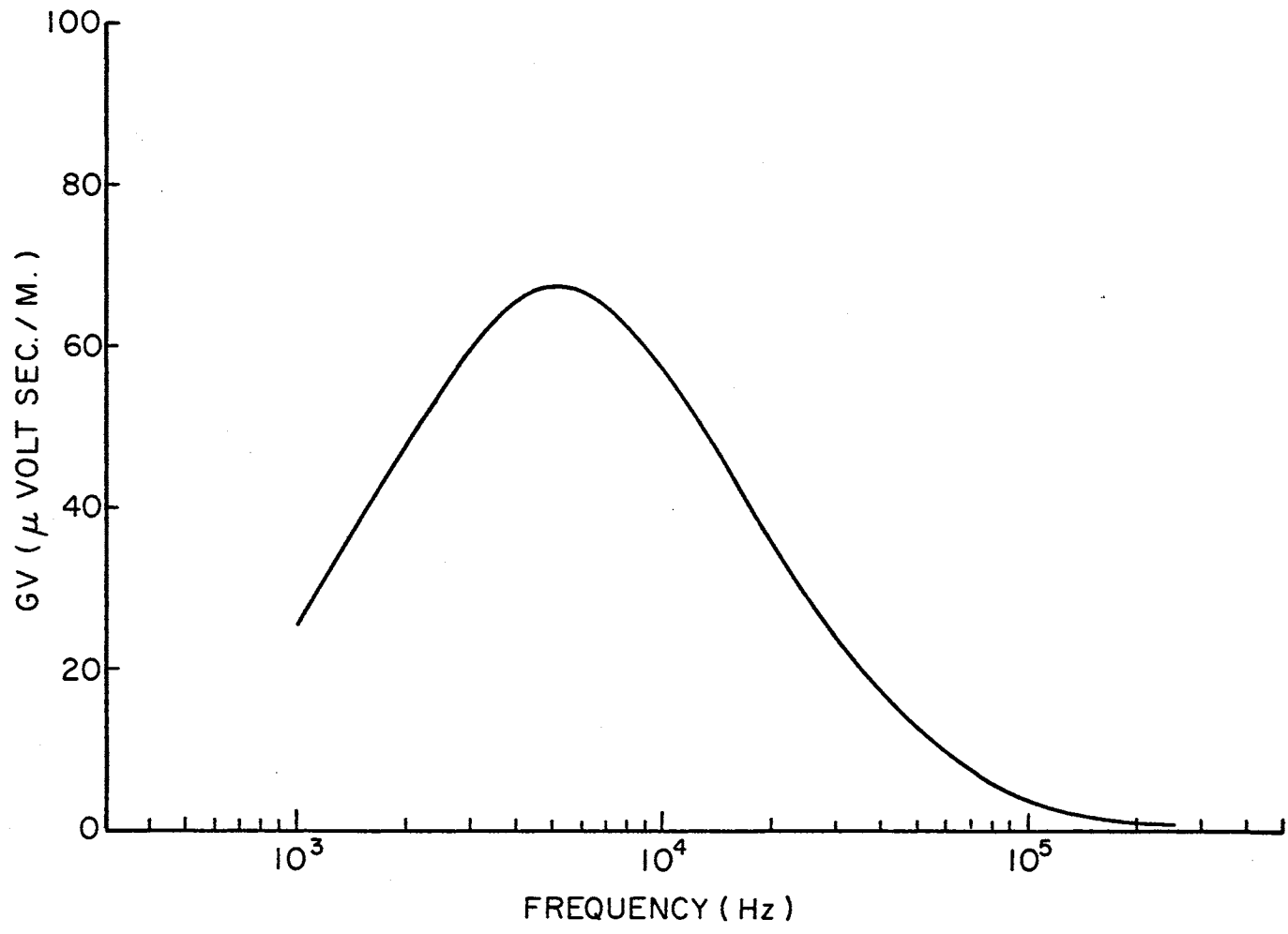
Figure 12. 2.66 Km Vertical Return Stroke With 10 M Dipoles

waveform $I_{LP}(t - T_{OL})U(t - T_{OL})$ advances down the channel from the cloud base toward the ground governed by the velocity expression

$$V_L(t) = V_{LO} \exp[-G_L(t - T_{OL})]U(t - T_{OL}) \qquad .$$

As in the case of the return stroke, continuity of current is assumed in all dipoles through which the velocity expression has allowed the current pulse to pass. The current pulse continues toward ground until it reaches the first dipole that has an index i which is a multiple of a specified integer, NDSP. Rather than proceeding through this dipole, the advance of the current is allowed to pause for DELAY seconds while this current pulse decays. The present programs are capable of selecting the values of DELAY from a normal distribution by specifying the mean, the standard deviation, and an odd integer IX to initialize the random selection.

Following this delay a second current waveform, identical in form to the first pulse, is assumed to exist in all dipoles through which the first pulse has passed while the tip of this pulse continues toward ground in accordance with the velocity expression $V_L(t)$ existing before the delay. When this second current pulse reaches the second dipole that is a multiple of NDSP, another delay is randomly selected to allow this current waveform to decay. This procedure is repeated until the final pulse has reached the ground.

As an example, consider a channel length approximated by NN 10 M dipoles. If the delays are chosen to occur every 50 M, NDSP is chosen as 5. Note that $T_{OL} \leq D(NN, 6) \leq \cdots \leq D(1, 6)$ for the leader process. That is, the leader is initiated at time T_{OL}; at some later time the dipole furthest removed from the ground is considered conducting, and

the final dipole to conduct is that touching the ground. For compact-ness, let T_i denote $D(i, 6)$, D_k denote the kth delay proceeding down the channel, IJ = (i+NDSP-1)/NDSP in integer arithmetic, and NWD = (IJ)(NDSP). IJ will have the value 1 for $1 \leq i \leq$ NDSP, 2 for NDSP < i $\leq$ 2 NDSP, etc. The total number of delays along the channel is given by NT = NN/NDSP in integer arithmetic. Assuming each current pulse has the form $I_{LP}(t)$ the current required for each dipole in the configura-tion $I_i(t)$ may be represented by the following expressions:

$$I_i(t) = I_{LP}[t-(T_{NWD} + \sum_{k=1}^{(NT+1-IJ)} D_k)]U[t-(T_i + \sum_{k=1}^{(NT+1-IJ)} D_k)], \quad 1 \leq i \leq NDSP$$

(4.3.1)

and

$$I_i(t) = I_{LP}[t-(T_{NWD} + \sum_{k=1}^{(NT+1-IJ)} D_k)]U[t-(T_i + \sum^{(NT+1-IJ)} D_k)]$$

$$+ \sum_{j=\ell(NDSP)}^{(NWD-NDSP)} I_{LP}[t-(T_j + \sum_{k=1}^{(NT+1-\ell)} D_k)]U[t-(T_j + \sum_{k=1}^{(NT+1-\ell)} D_k)],$$
$$\ell=1,2,\ldots$$

(4.3.2)

for NDSP < i $\leq$ (NN/NDSP)(NDSP). For (NN/NDSP)(NDSP) < i $\leq$ NN the above expression is correct if T_{NWD} is replaced by T_{NN}.

At first glance the above expressions are far from enlightening. Consider NN = 266 as a specific example with NDSP = 5 as before. The total number of delays along the channel is NT = 266/5 = 53. These de-lays occur just before the dipoles with indices i = 265,260,...,10,5 are considered conducting. Since NWD = 5 and (NT+1-IJ) = 53 for $1 \leq i \leq 5$, the first expression states the current in the first five dipoles, $1 \leq i \leq 5$, is a current pulse $I_{LP}(t)$ which is shifted in time to begin in the fifth dipole at the time required for the velocity expression to reach this dipole plus all the delays encountered along the channel.

Each of the remaining dipoles, $1 \leq i \leq 4$, conduct with this same current in such a manner as to maintain continuity of current with the dipoles above them.

For $6 \leq i \leq 10$, NWD = 10, (NT+1-IJ) = 52, and (NWD-NDSP) = 5. Thus the first term in the expression for $I_i(t)$ is

$$I_{LP}[t-(T_{10} + \sum_{k=1}^{52} D_k)]U[t-(T_i + \sum_{k=1}^{52} D_k)] \qquad ,$$

which is similar to the expression obtained for the first five dipoles. In this case only fifty-two delays exist in the channel above the tenth dipole. The sum in the expression for $I_i(t)$ is

$$\sum_{\substack{j=\ell5 \\ \ell=1,2,\ldots}}^{5} I_{LP}[t-(T_j + \sum_{k=1}^{(54-\ell)} D_k)]U[t-(T_j + \sum_{k=1}^{(54-\ell)} D_k)] \qquad .$$

Since $\ell = 1$ is the only value allowed for ℓ, the sum becomes

$$I_{LP}[t-(T_5 + \sum_{k=1}^{53} D_k)]U[t-(T_5 + \sum_{k=1}^{53} D_k)] \qquad ,$$

which is exactly the current in the fifth dipole, or the current required in all dipoles above the fifth to maintain its assumed current waveform.

Similar current waveforms are obtained from the $I_i(t)$ expressions for larger values of i. That is, one term is obtained for the assumed current pulse in that segment of the channel plus a sum of other terms to allow that segment to support the current flow in the segments below.

If the current pulses, $I_{LP}(t)$, are negative current pulses flowing down the channel, it is obvious that a negative charge is deposited along each 50 M length of the channel given by the integral of $I_{LP}(t)$ as required of the leader process.

The model of the leader process chosen to be presented here is

essentially the same as that discussed above. That is, a 2 2/3 Km
channel is approximated by two hundred sixty-six dipoles with 10 M
lengths and delays occurring every 50 M or five dipoles along the chan-
nel. Since the points at which the delays occur were arbitrarily chosen
with respect to the ground rather than the cloud base, the first delay
occurs after the first 10 M of the channel has been overtaken by the
velocity expression. The succeeding delays then occur at multiples of
50 M from the point of this first delay. To simplify the computations
the velocity expression was deleted in this model. That is, the current
pulse for a particular 50 M segment was assumed to exist on all dipoles
within that segment simultaneously after the appropriate number of de-
lays rather than starting at the upper dipole in this segment and pro-
gressing downward.

The waveform assumed for the current pulses is that suggested by
Steptoe (17),

$$I_{LP}(t) = I_0[\exp(-\alpha t) - \exp(-\beta t)] \qquad ,$$

where $I_0 = 2 \times 10^3$ amp, $\alpha = 2 \times 10^4$ sec^{-1}, and $\beta = 2 \times 10^5$ sec^{-1}. It
is noted by Arnold and Pierce (1) that typical delays are of the order
of 50 μsec, and that this form of pulse is significantly different from
zero after the delay, and thus the above expression is not a particu-
larly good model. They suggest that the current pulse produces a pulse
in the measured electric field of the form

$$E(t) = K[h_1^3 t \exp(-h_1^2 t^2) + h_2^3 t \exp(-h_2^2 t^2)] \qquad .$$

This expression was deduced empirically by Pierce (15), with $h_1 = 3.5 \times$
10^5 sec^{-1}, $h_2 = 1.2 \times 10^5$ sec^{-1}, and $K = 2.7 \times 10^{-12}$ volt sec^2/m at

100 Km from the channel. Uman and McLain (20) have considered the re-
lations between this field, the required leader currents, and the cur-
rent propagation velocity.

The results of this model are shown in Figure 13 for all delays
having the same value of 50 µsec, which Uman (19) refers to as a repre-
sentative time between steps. The observation point is located at
100 Km from the channel on the ground plane. Here it is noted that the
peaks occur at the fundamental frequency $1/50$ µsec^{-1} or 20 KHz and its
harmonics. Note these peaks dominate the spectrum when the delay term
is assumed deterministic.

Schonland (16) suggests that the delays are random with a mean of
50 µsec and a standard deviation of approximately 23 µsec. The field
resulting from the above model was calculated drawing the delays from a,
normal distribution with mean 50 µsec and standard deviation 23 µsec.
Figure 14 is the average of thirty-six of these computed spectra. That
is, IX, the parameter initializing the random selection, was set equal
to 1, the required fifty-three delays were selected by means of the sub-
routine GAUSS (see Appendix B), and the Fourier transform of the field
was computed. This procedure was repeated for IX = 3,5,...,71, and the
amplitudes of the resulting Fourier transforms were averaged.

Drawing the delays from such a normal distribution admits the pos-
sibility of negative delays which did in fact occur in the calculations
leading to Figure 14. The physical significance of these possible neg-
ative delays is not fully understood. To avoid this problem thirty-six
waveforms were calculated for the same values of IX as before with the
constraint that all negative delays would be rejected and the program
returned to the subroutine for the selection of another delay. The
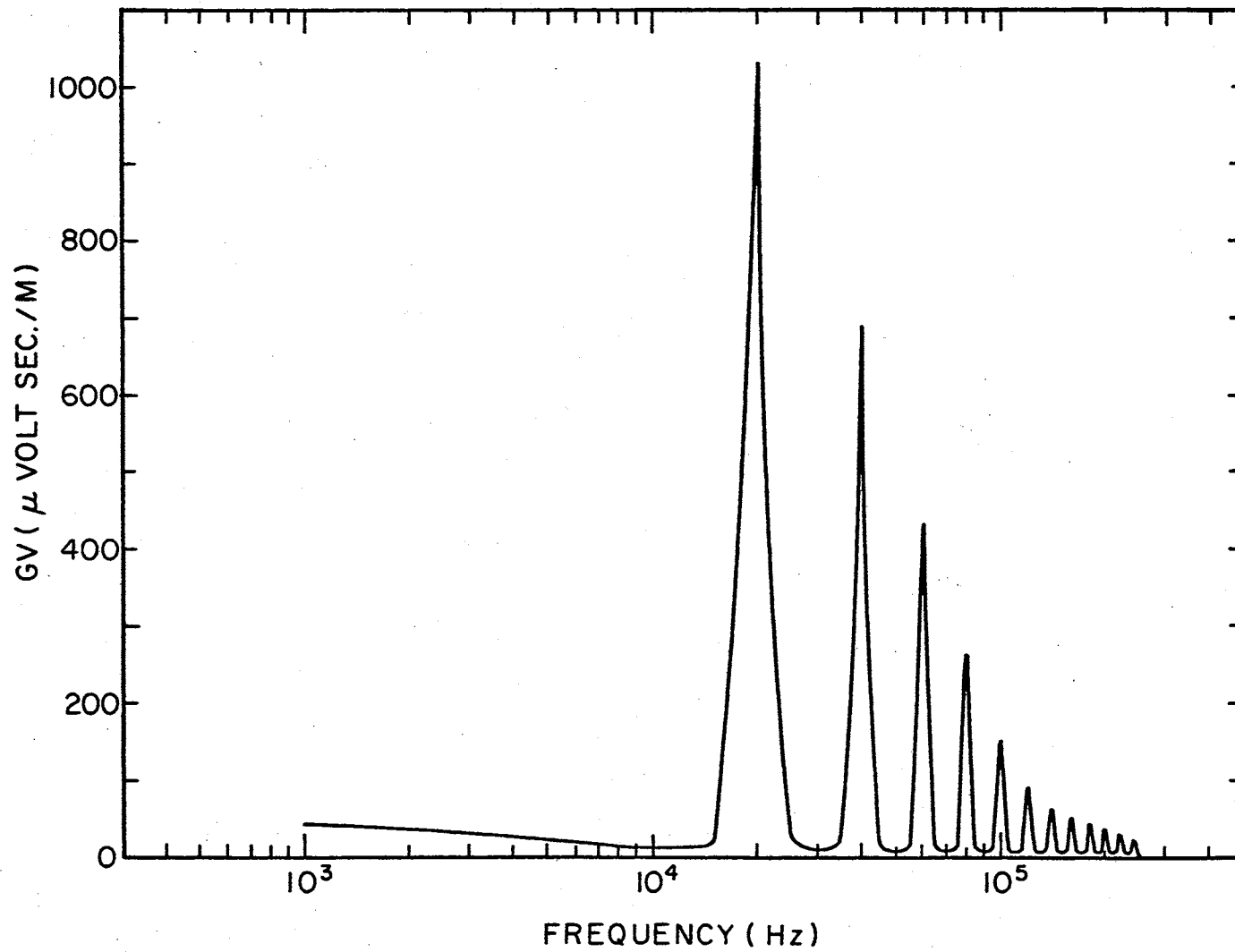
Figure 13.   2.66 Km Vertical Stepped Leader With 50 μsec Delays Every 50 M
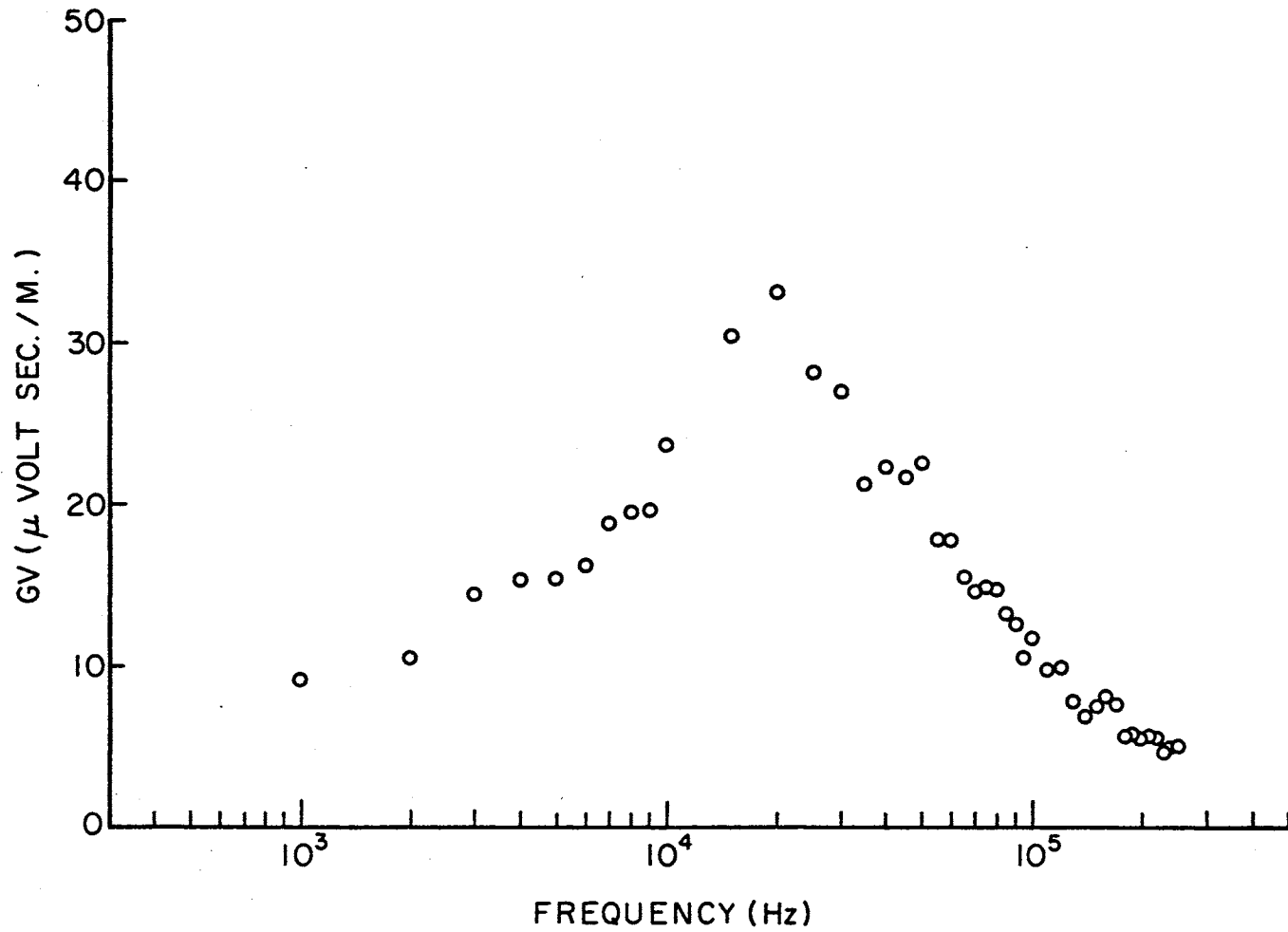
Figure 14. 2.66 Km Vertical Stepped Leader With Random Delays Every 50 M

average of the amplitudes of these waveforms is presented in Figure 15.

Arnold and Pierce (1) have calculated what they term the mean amplitude spectrum of the received field at 100 Km resulting from a series of sixty-four current pulses suggested by Steptoe, assuming a length of 100 M was energized by the current pulses. The time between pulses was assumed to be described by the same normal distribution. Their result, although presented on logarithmic scales, does not appear too different in shape than would Figures 14 and 15 on similar scales. The maximum value occurs at 20 KHz as it does in both Figures 14 and 15. However, the amplitude at this maximum is approximately 2.4 μvolt sec/M where Figures 14 and 15 indicate approximately 33 μvolt sec/M.

It is believed that this discrepancy in magnitude can be explained in terms of the differences in the two models of the stepped leader process. First Arnold and Pierce obtain an expression which states the mean amplitude spectrum is proportional to the square root of the number of pulses. Their calculations assumed sixty-four pulses while those of Figures 14 and 15 involved fifty-three. This implies, all other things being equal, that their results should be 10 per cent larger in magnitude than those obtained here. However, the main difference is in the length of channel each pulse is assumed to exist. Their model allows each pulse to occur only in the same 100 M segment. The present model allows the first pulse to occur in the upper 10 M of the channel, the second in the upper 60 M, the third in the upper 110 M, ..., and the last in the total 2.66 Km channel length. In the notation of Chapter II the magnitude of the received field is increased proportional to the effective dipole length. Or in the notation of Arnold and Pierce the magnitude of the received field is proportional to the second time
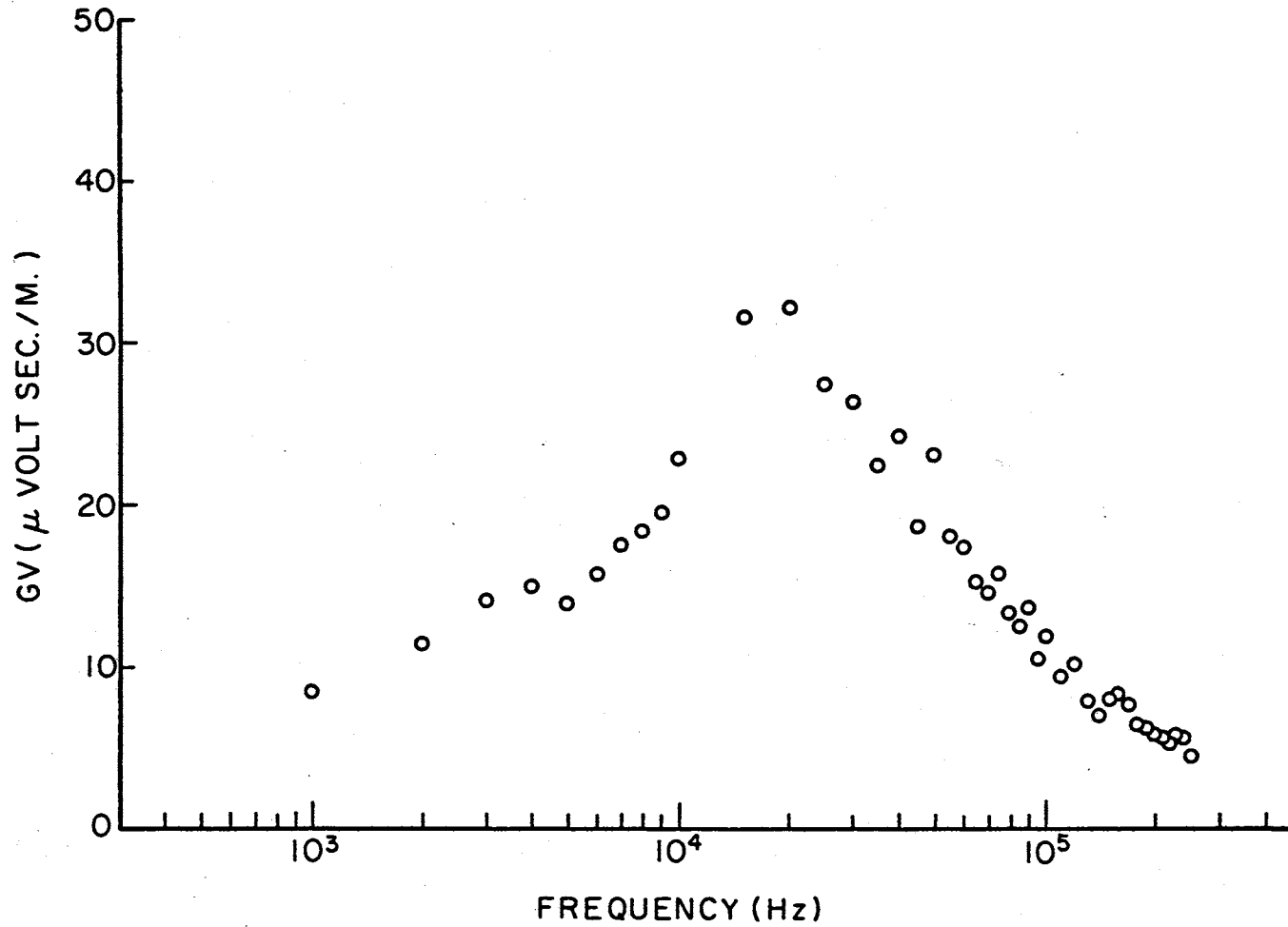
Figure 15.   2.66 Km Vertical Stepped Leader With Random Positive Delays Every 50 M

derivative of the dipole moment which they give as 200 dI/dt. The 200 results from an assumed separation of 100 M on the dipole approximating the segment and its image. In either event it is obvious that the magnitude obtained here should be considerably larger than those of Arnold and Pierce.

As an interesting point, Arnold and Pierce note that the magnitude experimentally obtained by Steptoe was actually an order of magnitude larger than their calculations. However, they mention that Steptoe's experimental conditions implied a bias toward stronger signals, and thus his observed results were for the strongest leader disturbances only rather than an average behavior.

4.4 Stepped Leader and Return Stroke. As stated previously, the effect of the leader process is to distribute a net negative charge along the main channel by means of a negative current progressing down the channel from the cloud to the ground. The return stroke which follows at some later time transports or partially transports this net negative charge to ground by a positive current flow progressing up the channel. This combined effect has been modeled by combining the models of the leader process and return stroke discussed in the preceding two sections. That is, the current existing in the ith dipole was assumed of the form

$$I_i(t) = I_L(t)\{U[t-D(i,6)]-U[t-T_{1,i}]\} + I_R(t)\{U[t-D(i,7)]-U[t-T_{2,i}]\} \quad ,$$
$$1 \leq i \leq N_n \quad (3.4.4)$$

in accordance with Section 3.4 with the understanding that $I_L(t)$ denotes that portion of the total leader current existing in the segment of the channel approximated by the ith dipole.

The Fourier transform of the charge on the ith dipole, $F_i(\omega)$, chosen for the calculations of this section is the sum of that given by Equation 4.2.7 for the return stroke plus $1/j\omega$ times the Fourier transform of the appropriate terms of Equation 4.3.2 for the contribution from the leader process. This procedure is in agreement with Equation 3.4.6.

Note the above implies that the Fourier transforms of the dipole charge have been summed assuming contributions from the leader process and the return stroke result from nonnegative currents. This may be explained by recalling that the positive reference on the dipoles was assumed along the positive coordinate axes which for vertical discharges, as being considered here, correspond to the positive z-axis. Now the leader process is to remove negative charge from the cloud and transport this charge down the channel. With the above notation this corresponds to a positive current flowing from the lower charge to the upper charge on each dipole. That is, for each dipole the lower charge becomes more negative and the upper charge becomes more positive indicating a transport of negative charge downward.

Similarly, the return stroke is to remove negative charge from the channel and transport this charge to ground. This is also accomplished by a positive current flowing from the lower charge to the upper on each dipole. Thus the effective current for the leader process and the return stroke is of the same sign.

The magnitude of the Fourier transform of the received field resulting from a combination of a stepped leader identical to that of Section 4.3 and a return stroke identical to that of Section 4.2 was calculated for a channel height of 2.66 Km at a distance of 100 Km from

the channel on the ground. T_{OL}, the initiation time for the leader

process, was assumed to be zero. T_{OR}, the initiation time for the re-

turn stroke, was calculated within the program to be the time the leader

current reached the ground. As before, the values of the delays were

selected from a normal distribution with a mean of 50 μsec and a stand-

ard deviation of 23 μsec. These results are presented in Figure 16 for

an average of twelve waveforms. The twelve values of IX assumed for

these computations were 1,3,5,...,23. The corresponding average magni-

tude resulting from the stepped leader alone is given in Figure 17.

Comparing these results with those of Figure 12 which represent

the return stroke alone one may conclude that for frequencies lower than

15 KHz the process assumed for the stepped leader does not appreciably

affect the average spectrum. At frequencies greater than 15 KHz the

average spectrum resulting from the combination is somewhat larger than

that of the return stroke alone. This is due to the energy of the

leader process in this range of frequencies. These results are as to

be expected. Hosever, the results are for average values, and one

should be cautioned that if a particular event were to be considered as

in observing actual storm data, the effect of the leader process may

drastically affect the spectrum as Figure 13 indicates for the extreme

case of all delays having identical values.

4.5 Streamer Process. In order to more completely represent the

effect of a discharge to ground one should include some process by which

charge can be transported from regions within the cloud to the upper tip

of the main channel. Horner (10,11) and Uman (19) give references on

the processes occurring between return strokes in a discharge. One pro-

cess that has been described consists of so-called junction streamers

100

80

GV (μ VOLT SEC./ M.)

60

40

20

0

10^3 10^4 10^5

FREQUENCY (Hz)
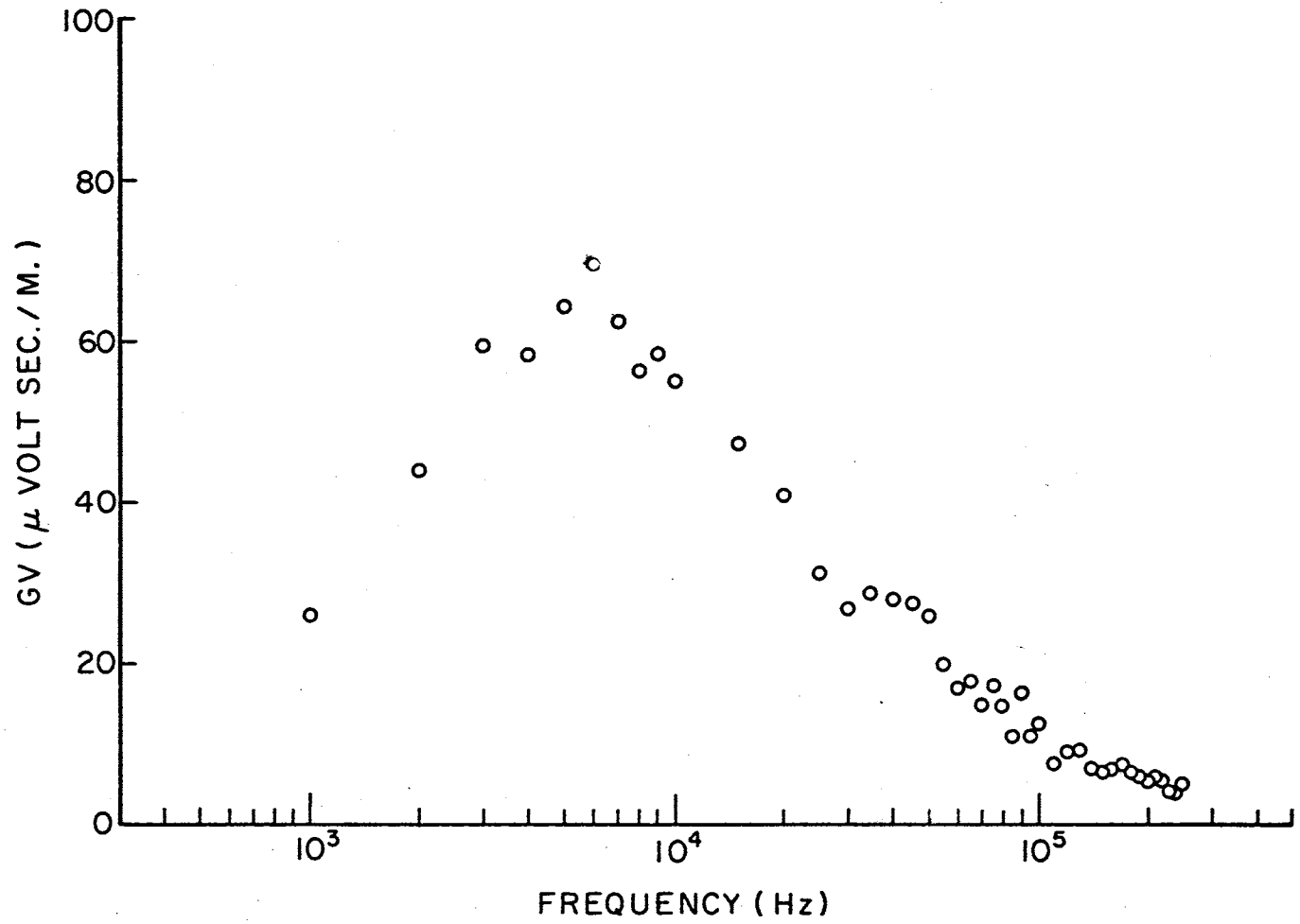
Figure 16.   Average Spectra for Stepped Leader and Return Stroke
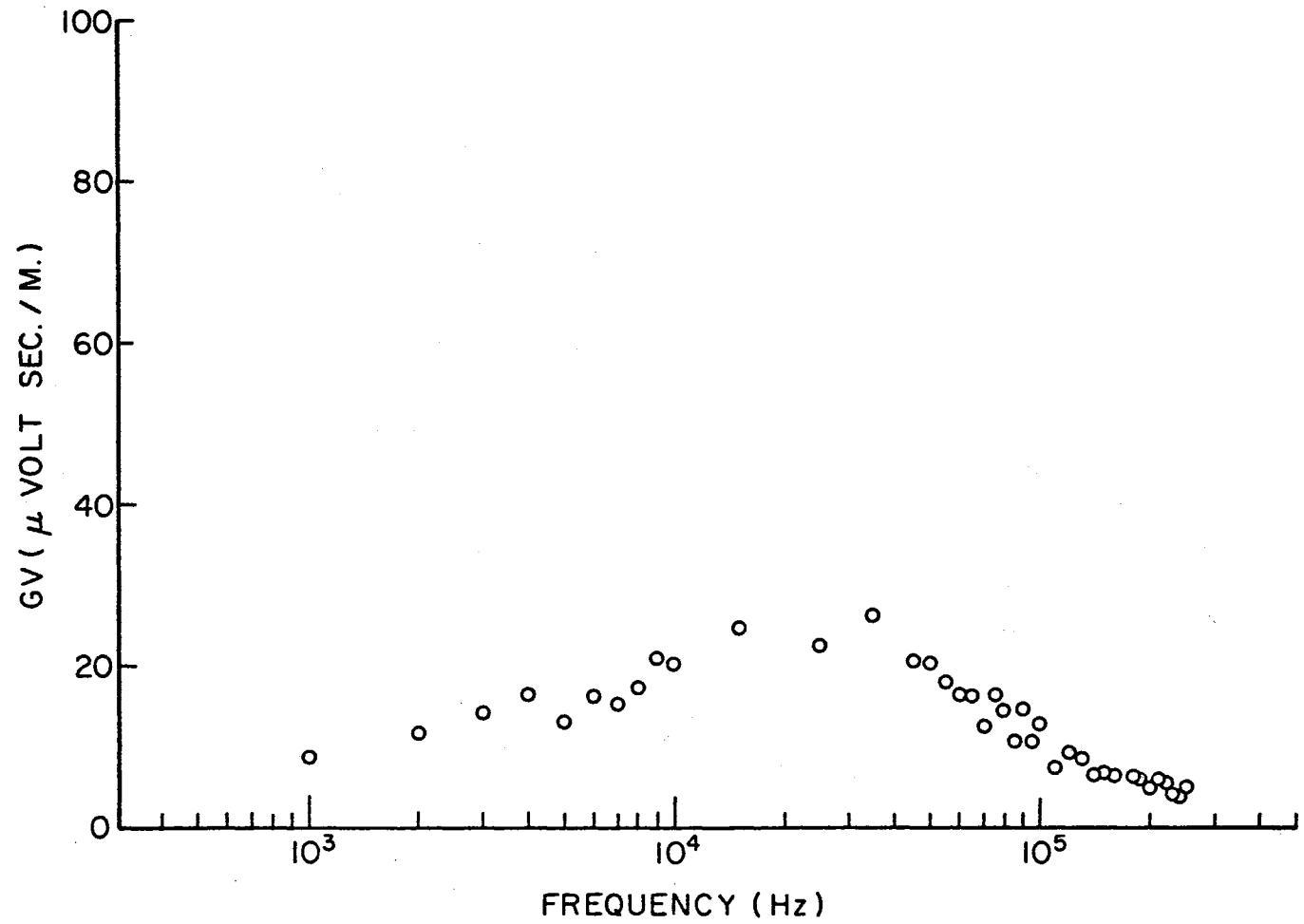
Figure 17. Average Spectra for Stepped Leader

extending from the upper tip of the main channel towards concentrations of charge in other parts of the cloud. When these streamers connect with these accumulations of charge a current pulse (K pulse) is experienced resulting from transportation of this charge to the channel tip.

No calculations have been made for this process in the present work. However, the computer models are capable of accepting such a process if one has a specific process in mind.

The possibilities are too numerous to list. However, the following brief example should suffice in indicating how one may incorporate such a process into the discharge model.

As a general example, the process might be approximated by a current waveform, representing the junction streamer, progressing from the upper tip of the main channel along a specified branch in accordance with the velocity expression

$$V_S(t) = V_{SO} \exp[-G_S(t - T_{OS})]U(t - T_{OS}) \qquad .$$

This current is allowed to advance along the branch until it reaches a point on the branch which is to represent an accumulation of charge. When this point is reached the K pulse resulting from this accumulation of charge may be modeled by superimposing an additional current on all dipoles between the channel tip and this point. This process may be repeated for the current progressing along the branch toward the next accumulation of charge. Such a process may be incorporated into the programs with no more difficulty than that of the leader process described in Section 4.3.

Also if the times between the K pulses are desired to be random, the same subroutine used for the delays in the leader process may be

used. With the desired mean and standard deviation corresponding to the K pulses specified, sample values would be drawn from this normal distribution. Kitagawa and Brook (12) indicate a mean of 8.5 msec and a standard deviation of 6 msec is appropriate for K pulses.

4.6 The Detected Field. Recall the procedure for calculating the time functions representing the narrow-band, half-wave linear detected field described in Sections 2.4 and 3.6. First the Fourier transform of the received waveform was passed through an ideal band-pass filter with bandwidth β about a selected center frequency ω_i. It was then shown mathematically that the time function representing the half-wave linear detection of this narrow band signal was proportional to the magnitude of the inverse Fourier transform of this narrow band signal shifted in the frequency domain from the interval $[\omega_c-\beta/2,\omega_c+\beta/2]$ to the interval $[0, \beta]$.

Figures 18, 19, and 20 are the time waveforms obtained from an identical return stroke as presented in Figure 12 for center frequencies of 10, 50, and 100 KHz, respectively. The bandwidths about each center frequency were chosen as 1 KHz.

These curves appear to have a modified (sin at)/t variation which has been shifted on the time axis. This is a direct result of the ideal band-pass assumption. That is, the frequency function has been multiplied by a pulse of width $2\pi \times 10^3$ radians/sec which requires the corresponding time function to be convolved with $(\sin \pi \times 10^3 t)/\pi t$. In fact one can see from the minimums of these plots that the variation is actually of the predicted form $(\sin \pi \times 10^3 t)/t$ corresponding to the 1 KHz bandwidth.

It is observed that the first maximum occurs at approximately
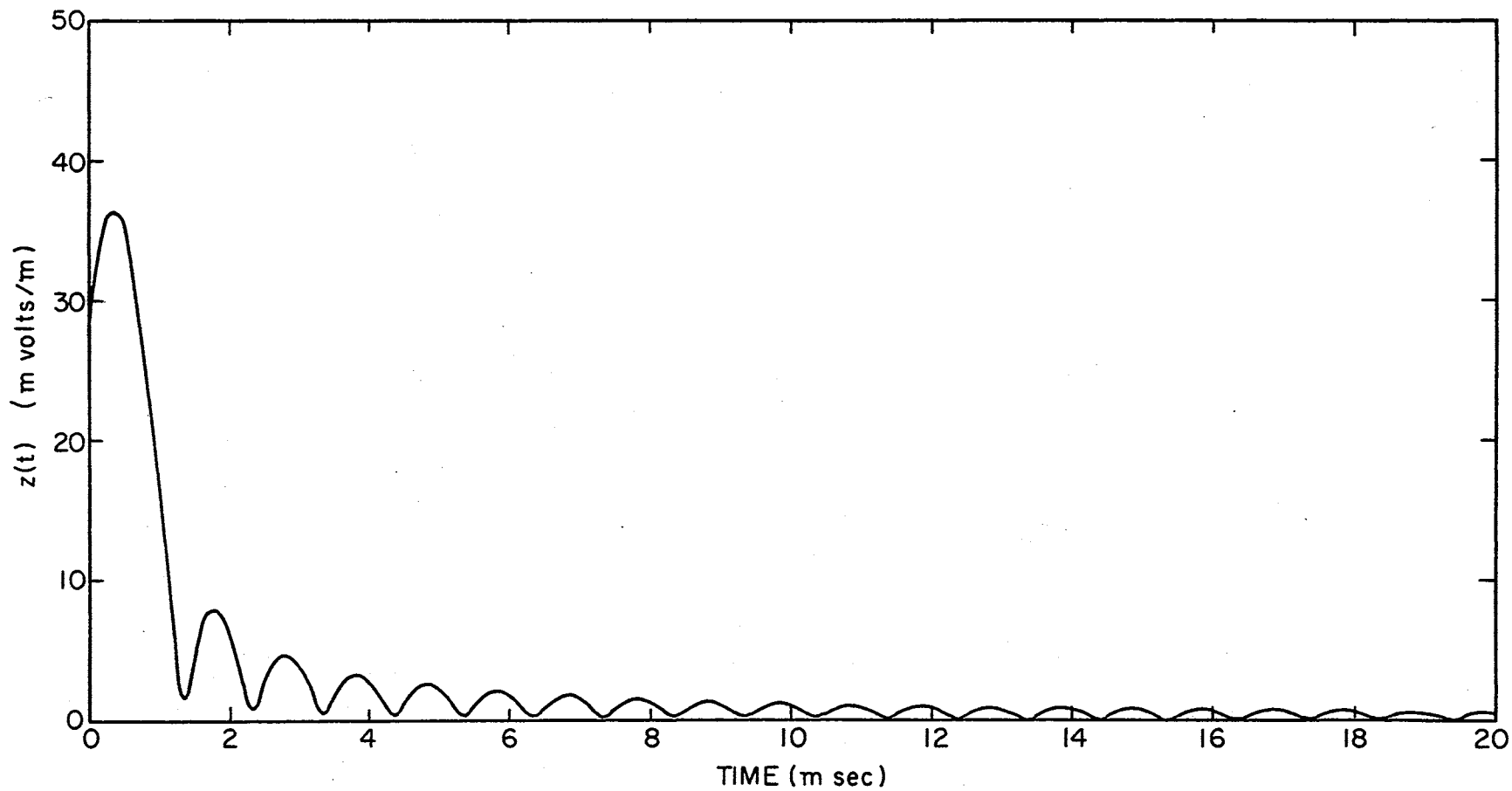
Figure 18. Detected Field for a Return Stroke, Center Frequency = 10 KHz
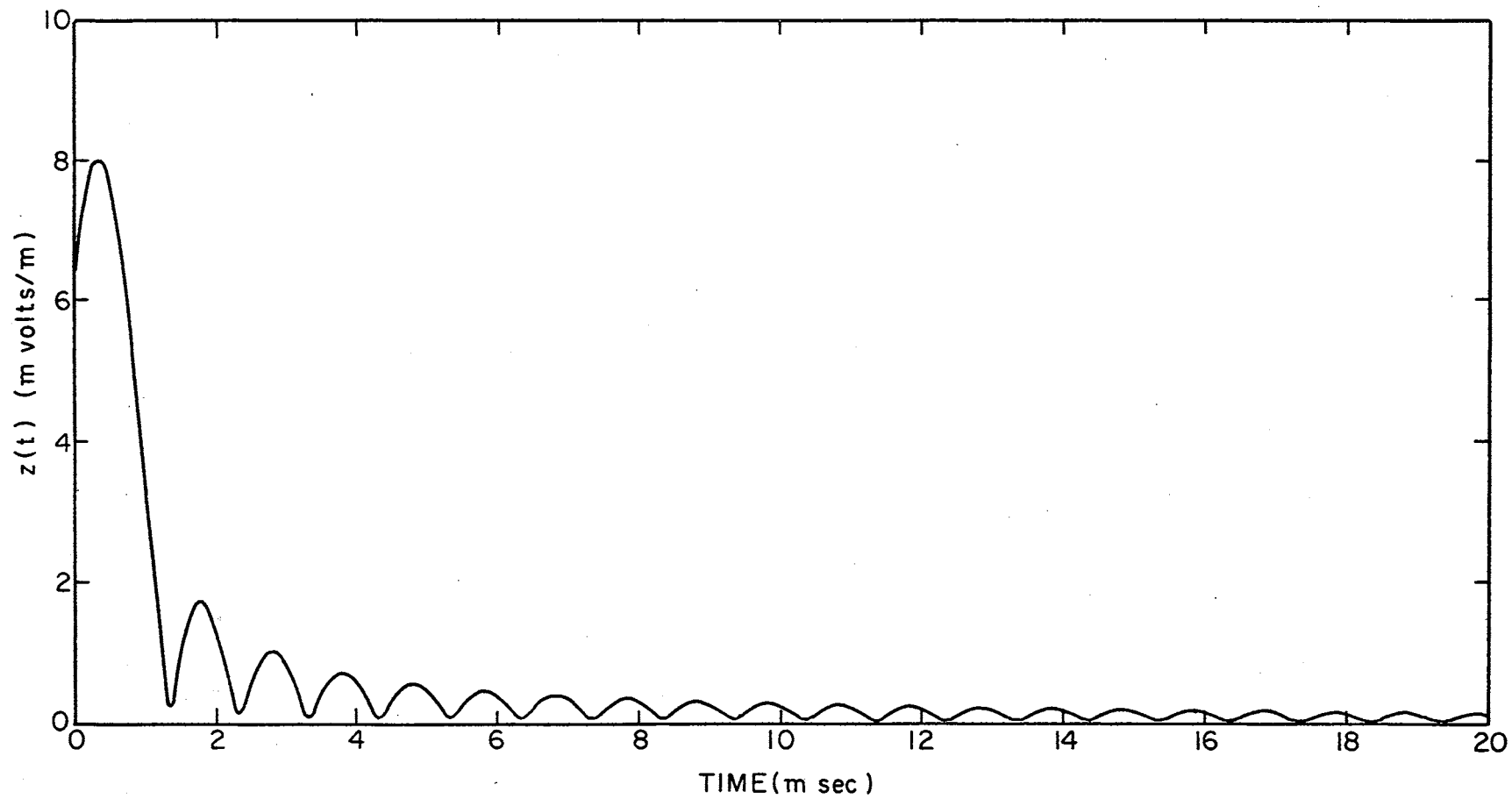
Figure 19. Detected Field for a Return Stroke, Center Frequency = 50 KHz
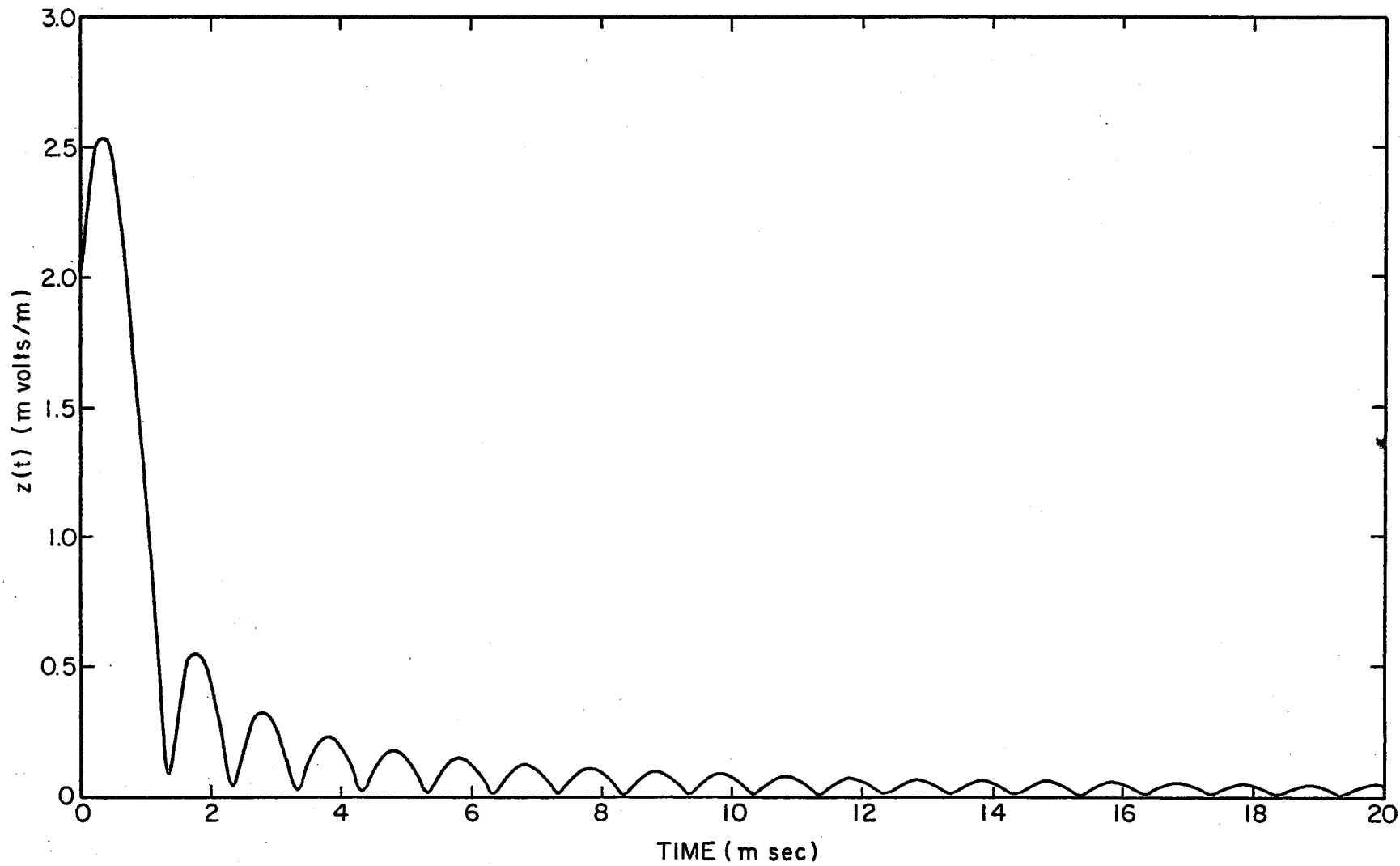
Figure 20. Detected Field for a Return Stroke, Center Frequency = 100 KHz

0.33 msec rather than the origin. This corresponds to the propagation
time required for radiation to reach the antenna. In these calculations
the return stroke was initialized at time $t = T_{OR} = 0$ sec. Thus the
antenna situated 100 Km from the channel would measure no response until
$t = T_{OR} + 10^5/3 \times 10^8$ or 0.33 msec.

The values of the time response existing before $t = 0.33$ msec is
again a problem associated with the ideal band-pass process. That is,
the $(\sin \pi \times 10^3 t)/t$ exists for $-\infty < t < \infty$. Or in other words, the
dual assumption of a finite bandwidth and a finite time interval is not
theoretically possible (2).

These problems may be slightly alleviated with the assumption of a
more realistic band-pass filter which the program will readily accept.
However, the problem of the infinite time record will remain since one
can only handle a finite number of samples.

Common problems in the algorithm utilized to invert the narrow-band
frequency function may be found in reference (4). One that is apparent
here is time resolution. In Section 3.6 it was mentioned that 256 sam-
ple values obtained from the frequency function over the 1 KHz bandwidth
and $2,304 = (2,560 - 256)$ zeros were introduced into the algorithm to
yield an output time function that should be accurate over the time in-
terval $0 \leq t < 256$ msec with a spacing of 0.1 msec. In the situation
modeled here the return stroke should essentially be zero after a dura-
tion of at most 10 time constants or 0.5 msec. Thus with the present
time domain spacing only five values are to represent the process we
desire to observe. Padding with additional zeros, say $(25,6000 - 256)$
will reduce the time increments to 0.01 msec at the obvious expense of
computer storage and cost.

Although the spacing of samples in the frequency domain was set at $10^3/256$ Hz in the present program to hopefully result in time representation valid to $256/10^3$ sec, this sampling rate could be reduced if shorter time intervals are to be considered. For example, a sample spacing of $10^3/64$ Hz in the frequency domain should result in a time representation valid to $64/10^3$ sec. With the addition of only (6,400 - 64) zeros the time increments are 0.01 msec.

It is implied that obtaining N equally spaced samples over the 1 KHz bandwidth will result in the associated time function which is valid for $0 \leq t < N$ msec. Personally the author would place a safety factor of 1/5 on this upper limit.

4.7 Summary. The results of the return stroke are in excellent agreement with those produced by other models.

The spectra obtained from the modeled leader process is reasonable with others if adjustment is made for the effective channel length. However, the randomness of the delays necessitates averaging.

The return stroke may be combined with a leader process with predictable results.

Although no calculations for a streamer process have been presented, the programs will readily accept reasonable models for this process.

The present program calculating the narrow-band, half-wave linear detected waveforms gives predictable results for the assumptions made. However, if these time waveforms are to determine anything about the received waveforms from some assumed process for a comparison with measured data, more realistic assumptions must be made for the narrow-band filter.

CHAPTER V

PARAMETER SELECTION

5.1 Introduction. Although the computer model developed in this
work is somewhat involved and capable of representing a multiplicity of
processes or combination of processes, the original intent was not to
develop an elaborate model of a lightning discharge in order to deter-
mine more about the mechanisms involved in the discharge process.
Rather, the purpose here was to develop a model which would be capable
of yielding some information relating parameters in the electromagnetic
radiation from thunderstorms to parameters within the storm. However,
in the development it was not known how accurate a description of the
processes would be required to yield such information. Thus, the pres-
ent model evolved.

Many hazards may be encountered when attempting to relate the re-
ceived electromagnetic data to the parameters of the discharge via a
model as developed here. For example, distances are not known accu-
rately, modes of propagation not included in the model exist, etc. One
of the most fundamental problems is the fact that the received field is
not unique to a particular source. Also problems in comparison exist
as a result of the randomness inherent in actual discharges.

In developing this model allowances have been made for the intro-
duction of many processes and random effects if meaningful assumptions
or hypotheses for the processes are available. However, the author

still has many questions on the processes and believes that trying to specify certain parameters too accurately while others just as critical to the results are unknown would not be optimum procedure.

The following is proposed. The return stroke calculations appear to be quite acceptable. Realizing this is far from the actual discharge, and also that this portion of the discharge changes from stroke to stroke not to mention flashes, use the return stroke waveforms as test signals, not to infer about the absolute signals that might be received from various discharges, but to infer what changes in the received signals could be expected for a very restricted set of changes in the discharge.

5.2 Effect of Channel Length. At the end of Section 4.2 it was noted that the spectra of Figures 8 and 12 resulted from an identical set of parameters on the modeled return stroke except for the assumed channel height. Figure 8 represented a channel height of 1 Km and had the maximum value of its spectrum at 10 KHz. Figure 12 represented the maximum channel height allowable by the velocity expression

$$V_R(t) = V_{RO} \exp[-G_R(t - T_{OR})]U(t - T_{OR}) \qquad ,$$

or $V_{RO}/G_R = 2.66$ Km. However, in the latter case a smooth curve with a maximum at 5 KHz was obtained for the spectrum.

The possibilities are that the higher frequency content of the 1 Km channel over the 2.66 Km channel results from the termination of the channel before the current has decayed sufficiently, or the channel height may also influence the frequency content. The termination of the channel will definitely influence the frequency content as evidenced by the local maximums at the higher frequencies of Figure 8.

To determine if channel height is also involved, the following calculations were performed. A return stroke current of the form

$$I_R(t) = \{3 \times 10^4[\exp(-2 \times 10^4\tau) - \exp(-2 \times 10^5\tau) + 2.5 \times 10^3 \exp(-10^3\tau)]U(\tau)$$

was assumed, where $\tau = (t - T_{OR})$. This is the same current assumed for the return strokes of Figures 7 through 12 with the addition of the last term. Since the effect of channel height was to be determined, G_R was equated to zero yielding $V_R(t) = V_{RO} = 8 \times 10^7$ m/sec. Thus the V_{RO}/G_R restriction on channel height was removed.

The results presented in Figures 21 through 26 represent the calculated field, assuming the dipoles are 10 M in length, at 100 Km from the channel on the ground for channel heights of 1.0, 1.5, 2.0, 2.5, 4.0, 5.0, and 9.99 Km, respectively.

The maximums of the spectra occur at approximately 11, 10, 8, 7.2, 5.8, 5, and 3.3 KHz, respectively. That is, increasing the channel height while holding constant all other parameters shifts the maximum of the spectrum to lower values of frequency.

Also note that the local maximums in Figure 27 are less pronounced than in the six previous graphs. The time required for the current to reach this height is approximately 125 μsec. Thus if 50 μsec is an effective decay time constant for the current waveform, this current has begun to decay significantly when the channel growth is terminated. Figure 26 which represents a channel height of 5 Km corresponding to a required time of 62.5 μsec or slightly over one time constant when the channel is terminated indicates the local maximums are quite pronounced as is to be expected.
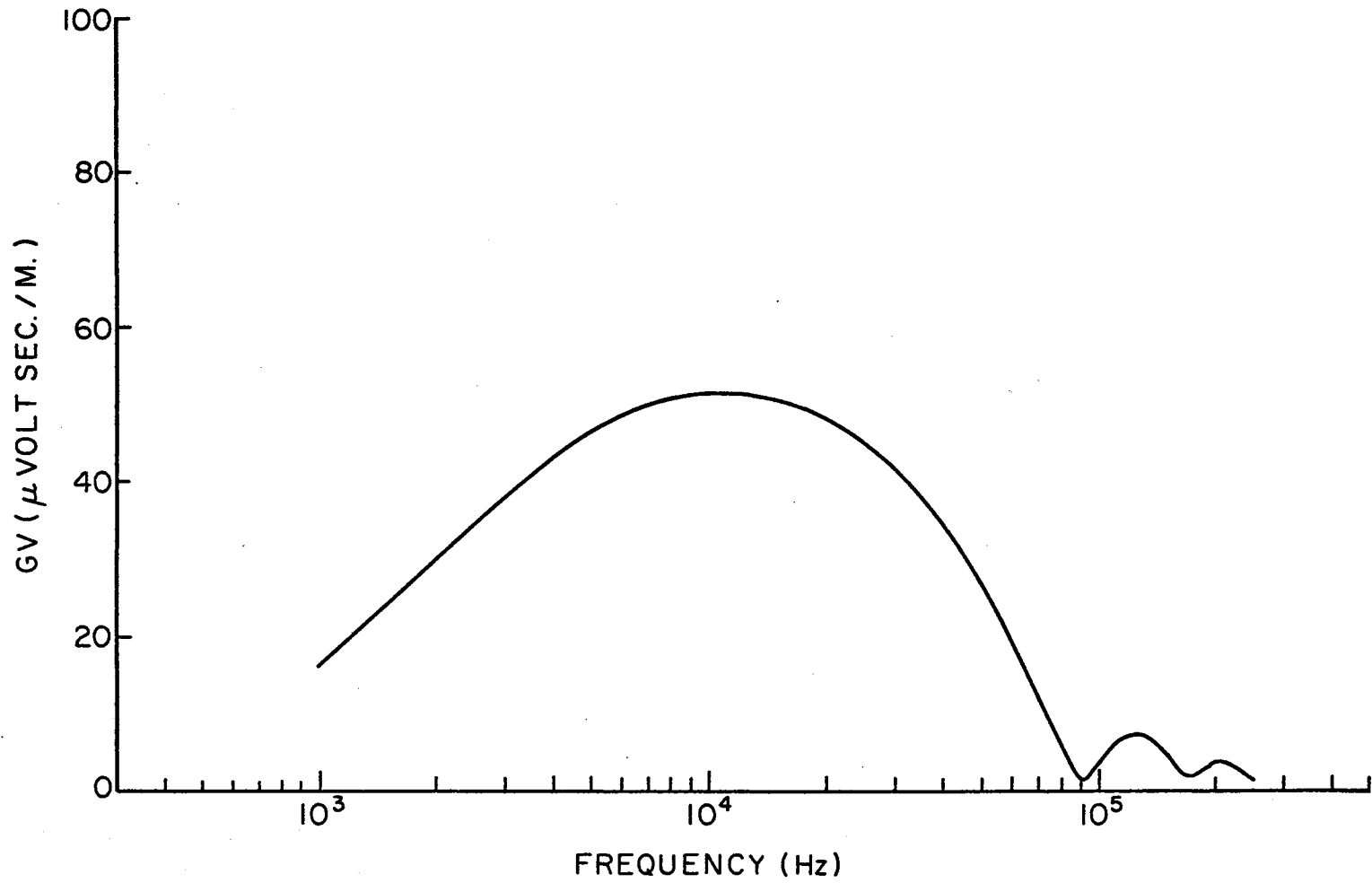
Figure 21. 1.0 Km Vertical Return Stroke
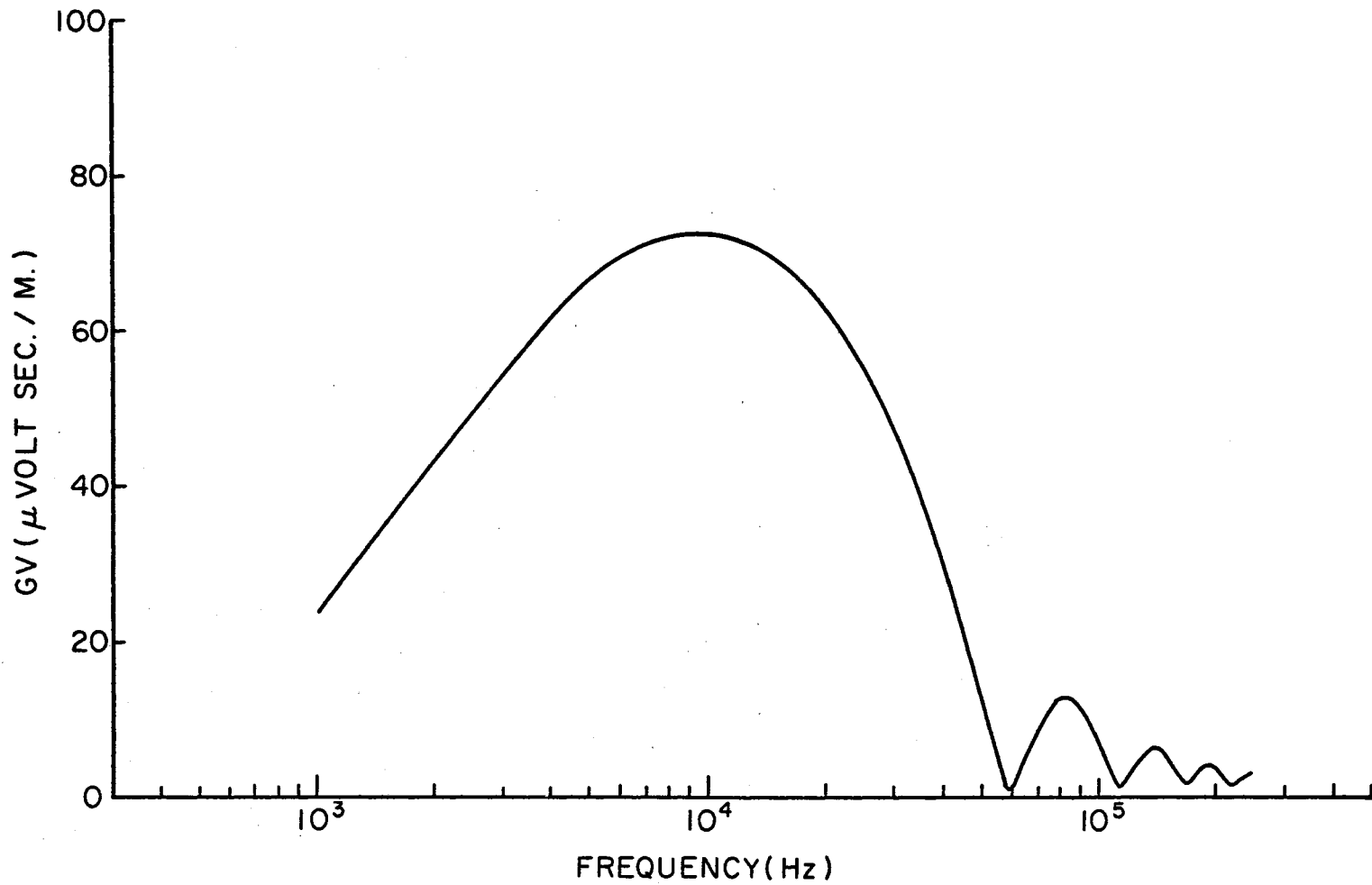
Figure 22. 1.5 Km Vertical Return Stroke
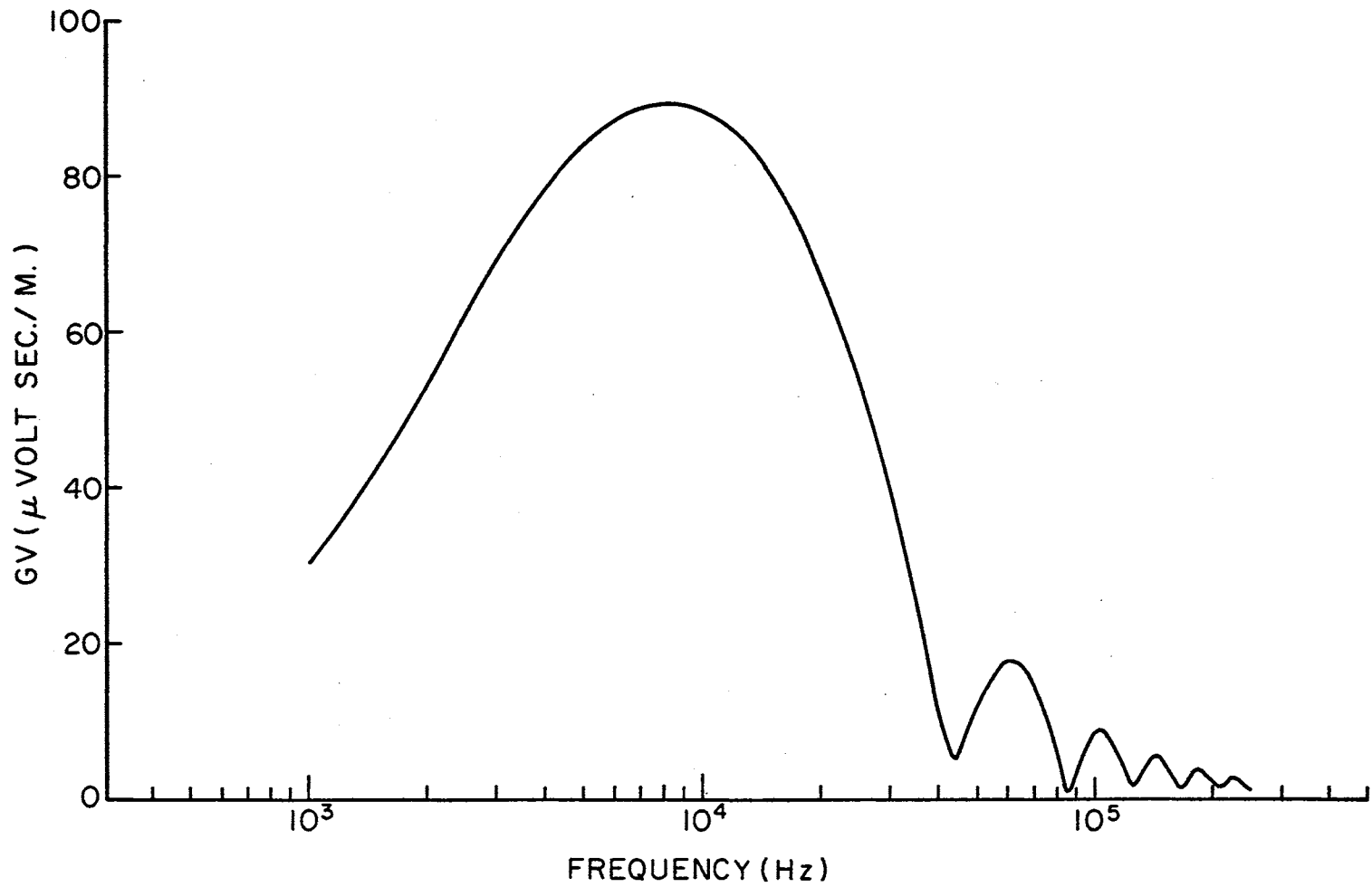
Figure 23.   2.0 Km Vertical Return Stroke

GV (μ VOLT SEC./ M.)

FREQUENCY (Hz)
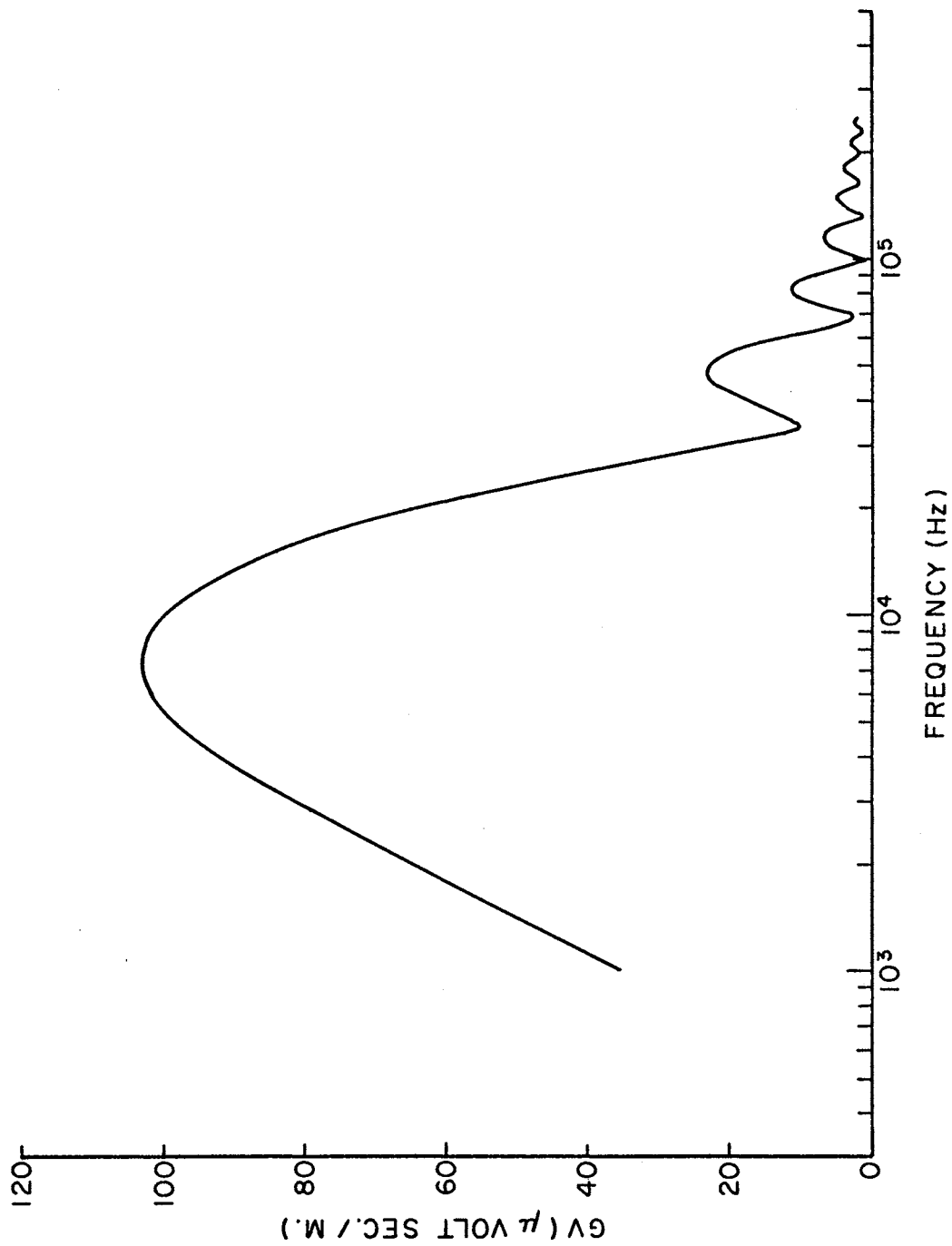
Figure 24. 2.5 Km Vertical Return Stroke
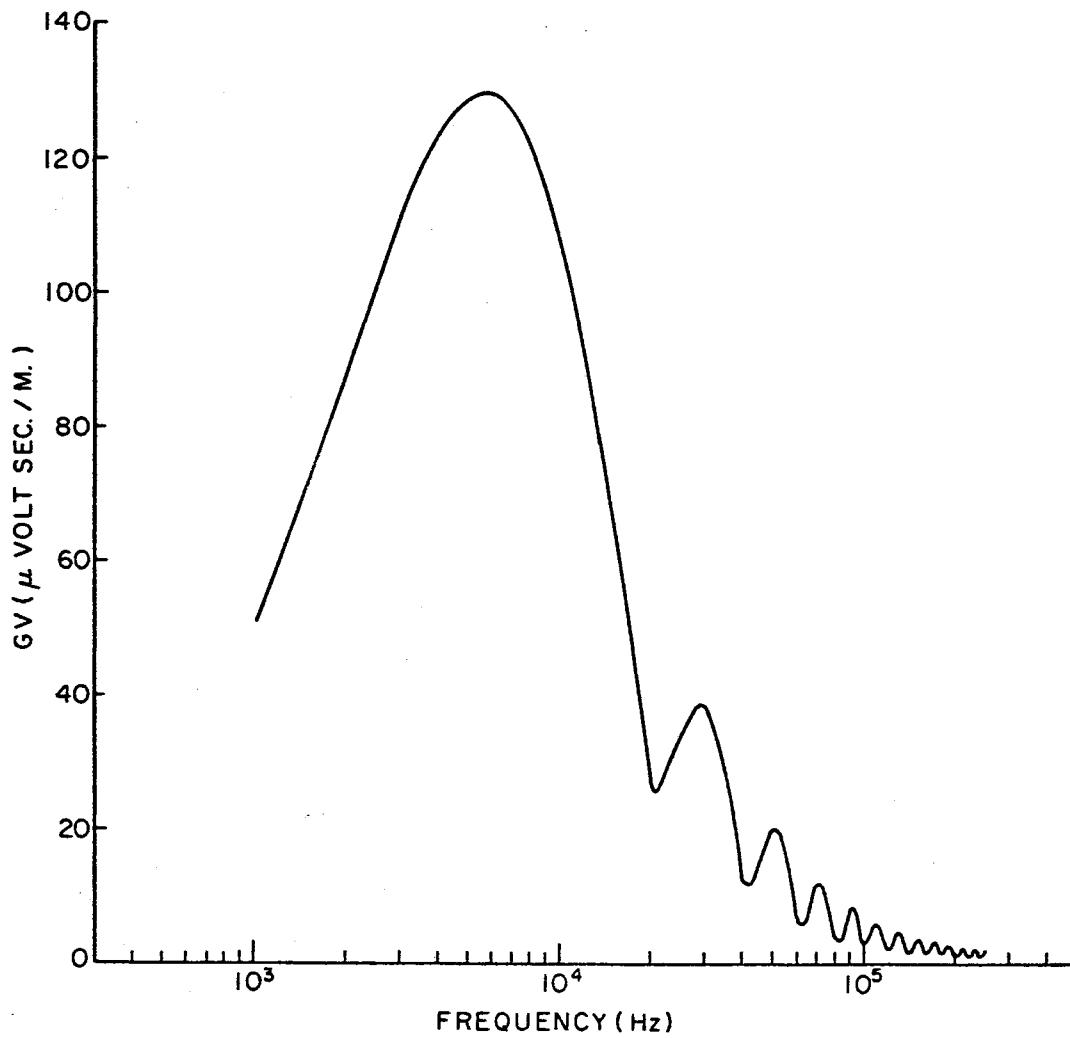
Figure 25. 4.0 Km Vertical Return Stroke
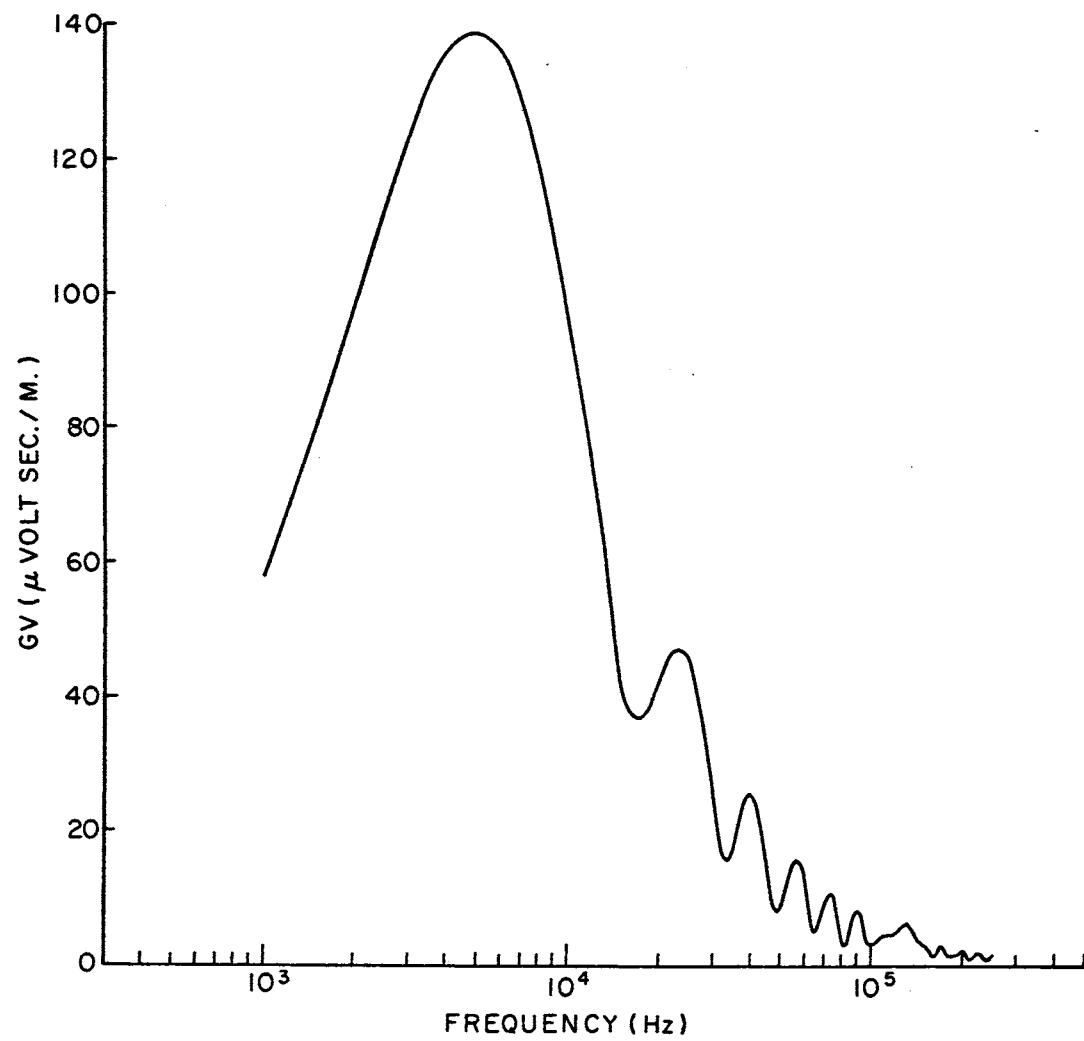
Figure 26. 5.0 Km Vertical Return Stroke
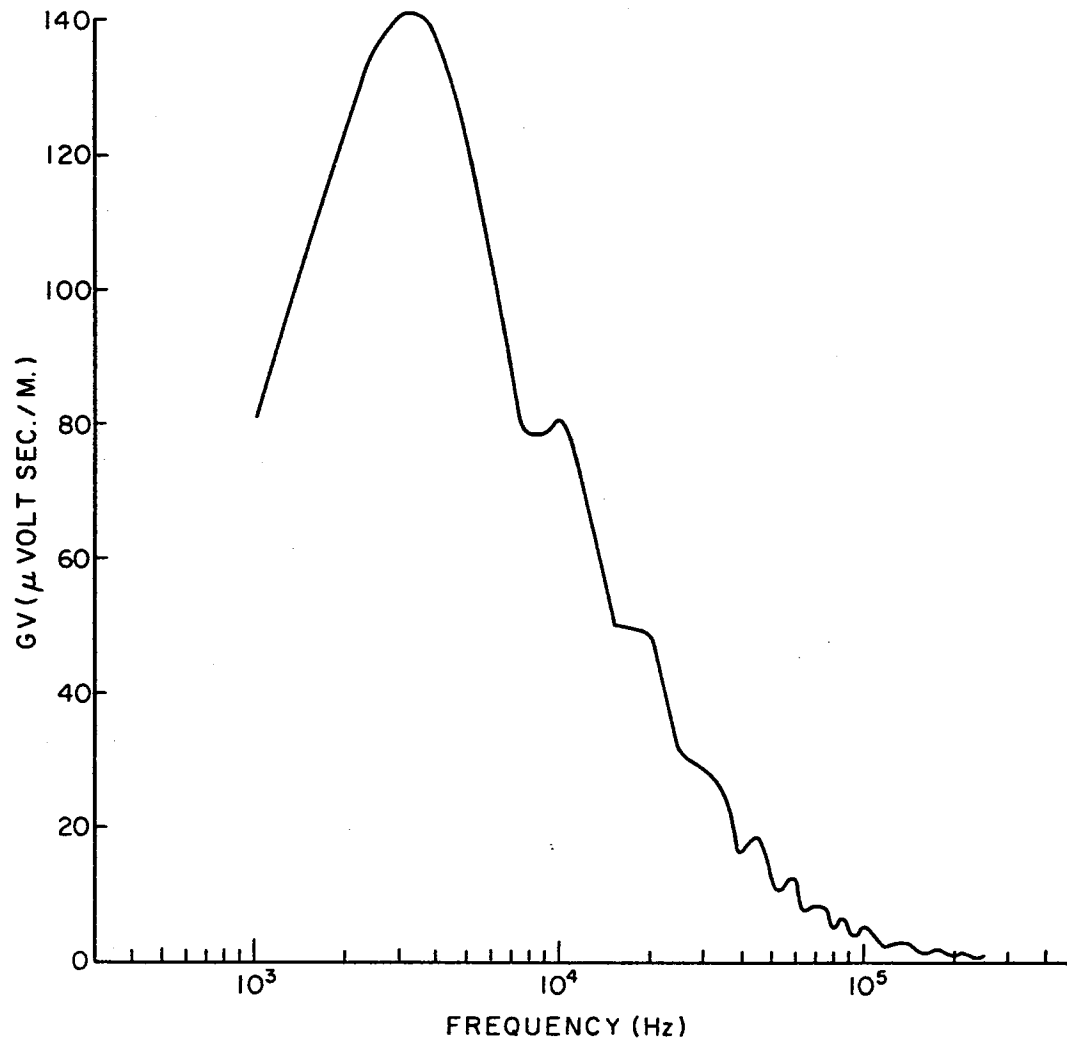
Figure 27. 9.99 Km Vertical Return Stroke

5.3 Effect of Channel Orientation (Far Field). In this section,
and the one following, the current on the channel and its propagation
velocity are fixed and only the geometry of the channel is varied. In
particular, the current form assumed is identical to that of the return
stroke modeled to obtain Figure 12. That is,

$$I_R(t) = I_0\{\exp[-\alpha(t - T_{OR}) - \exp[-\beta(t - T_{OR})]\}U(t - T_{OR} \qquad (4.2.5)$$

with

$$V_R(t) = V_{RO} \exp[-G_R(t - T_{OR})]U(t - T_{OR}) \qquad ,$$

where

$$I_0 = 3 \times 10^4 \text{ amp}, \qquad \alpha = 2 \times 10^4 \text{ sec}^{-1}, \qquad \beta = 2 \times 10^5 \text{ sec}^{-1}$$

$$V_{RO} = 8 \times 10^7 \text{ m/sec}, \qquad G_R = 3 \times 10^4 \text{ sec}^{-1}, \qquad T_{OR} = 0.0 \text{ sec} \qquad .$$

The length of the channel, approximated by dipoles of length 10 M, is
assumed to be the maximum length allowable for the velocity expression
with these parameters, 2.66 Km.

Seven channel orientations are considered. In each case the ini-
tial point of the channel, (X_0, Y_0, Z_0), has been adjusted such that
the X,Y-coordinates of the channel midpoint is centered over the origin.
Also four heights are considered for the initial points on each orien-
tation. These heights are Z_0 = 0, 3, 5, and 7 Km for the orientations
with any vertical component and Z_0 = 1, 3, 5, and 7 Km for the hori-
zontal orientations.

The observation point for the following figures is located 100 Km
from the discharge on the ground plane or (X_a, Y_a, Z_a) = (0, 100 Km, 0)
in accordance with Section 3.3.

Figure 28 represents the received field for a vertical channel with direction cosines (0, 0, 1). The solid curve corresponds to Z_0 = 0 which is the same situation modeled in Figure 12. The dashed curve represents the received field for an identical discharge with the initial point of the channel elevated to Z_0 = 7 Km. Calculations were performed with Z_0 = 3 and 5 Km. These graphs were not plotted since they were essentially the same as those presented with values lying between the two curves.

Figures 29, 30, and 31 represent channels inclined thirty degrees from the vertical. The direction cosines for these figures are (0, .5, .866), (-.5, 0, .866), and (0, -.5, .866), respectively. That is, the original vertical channel is first inclined toward the observer, then rotated a positive ninety degrees, and finally rotated an additional ninety degrees. Again the solid curves represent the values obtained for Z_0 = 0, the dashed curves represent the values obtained for Z_0 = 7 Km, and the values obtained for Z_0 = 3 and 5 Km fall between the two curves presented on each figure.

Figures 32, 33, and 34 represent horizontal channels. The direction cosines for these three figures are (0, 1, 0), (0, -1, 0), and (-1, 0, 0), respectively. In each figure the curves obtained for Z_0 = 1, 3, 5, and 7 Km are indicated.

Comparing Figures 28 through 31 there appears to be no significant difference existing between the four figures. From this, one may conclude that the observed field is relatively insensitivie to the channel orientation for small, less than thirty degrees, deviations from the vertical. Also, a comparison of the curves on each figure implies that the received field does not vary significantly as a fixed channel length

Figure 28. Vertical Channels, Far Field

Figure 29. Channels Inclined 30° From Vertical Toward Observer, Far Field
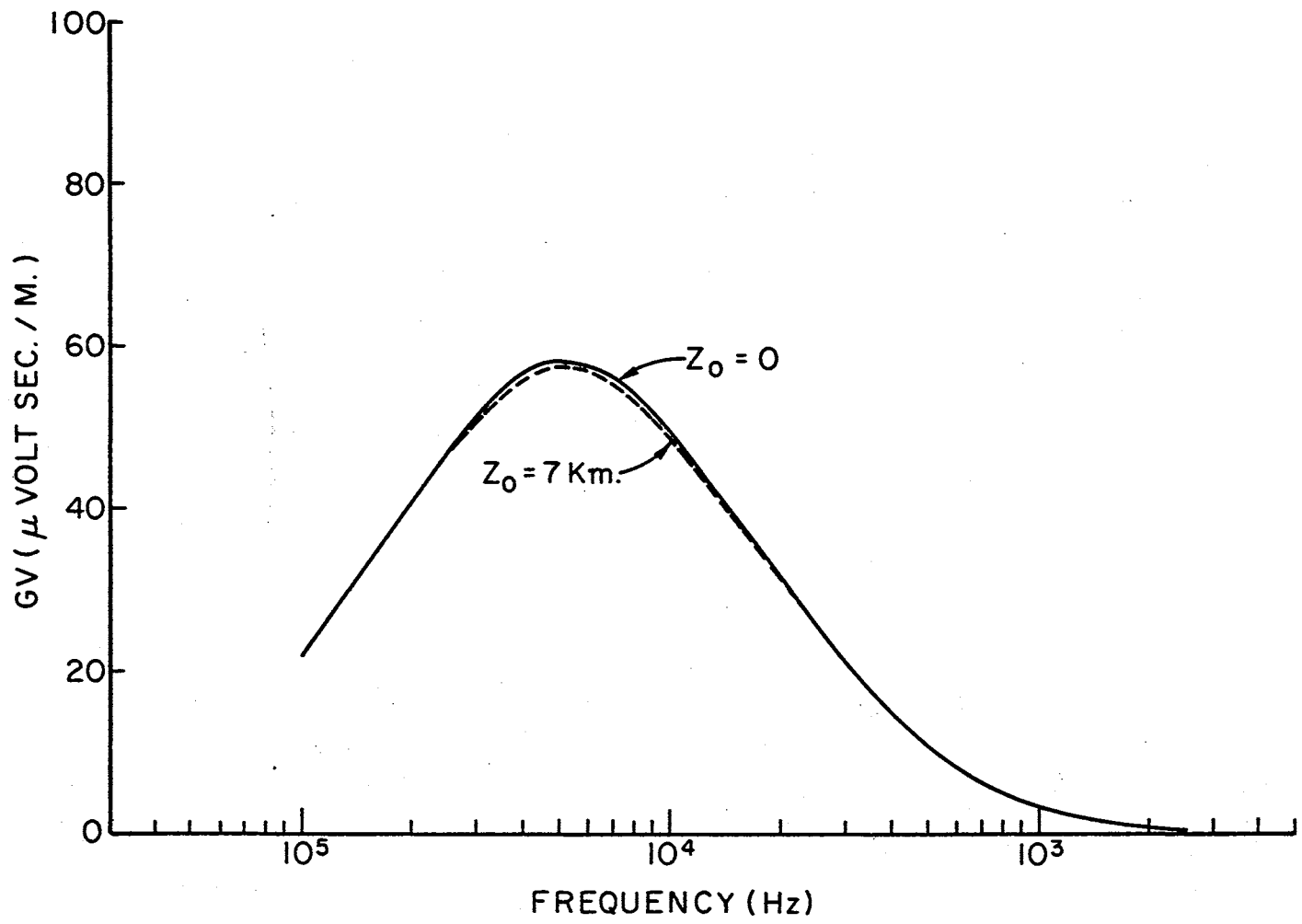
Figure 30. Channels Inclined Transverse to Observer, Far Field

Figure 31. Channels Inclined 30° From Vertical Away From Observer, Far Field
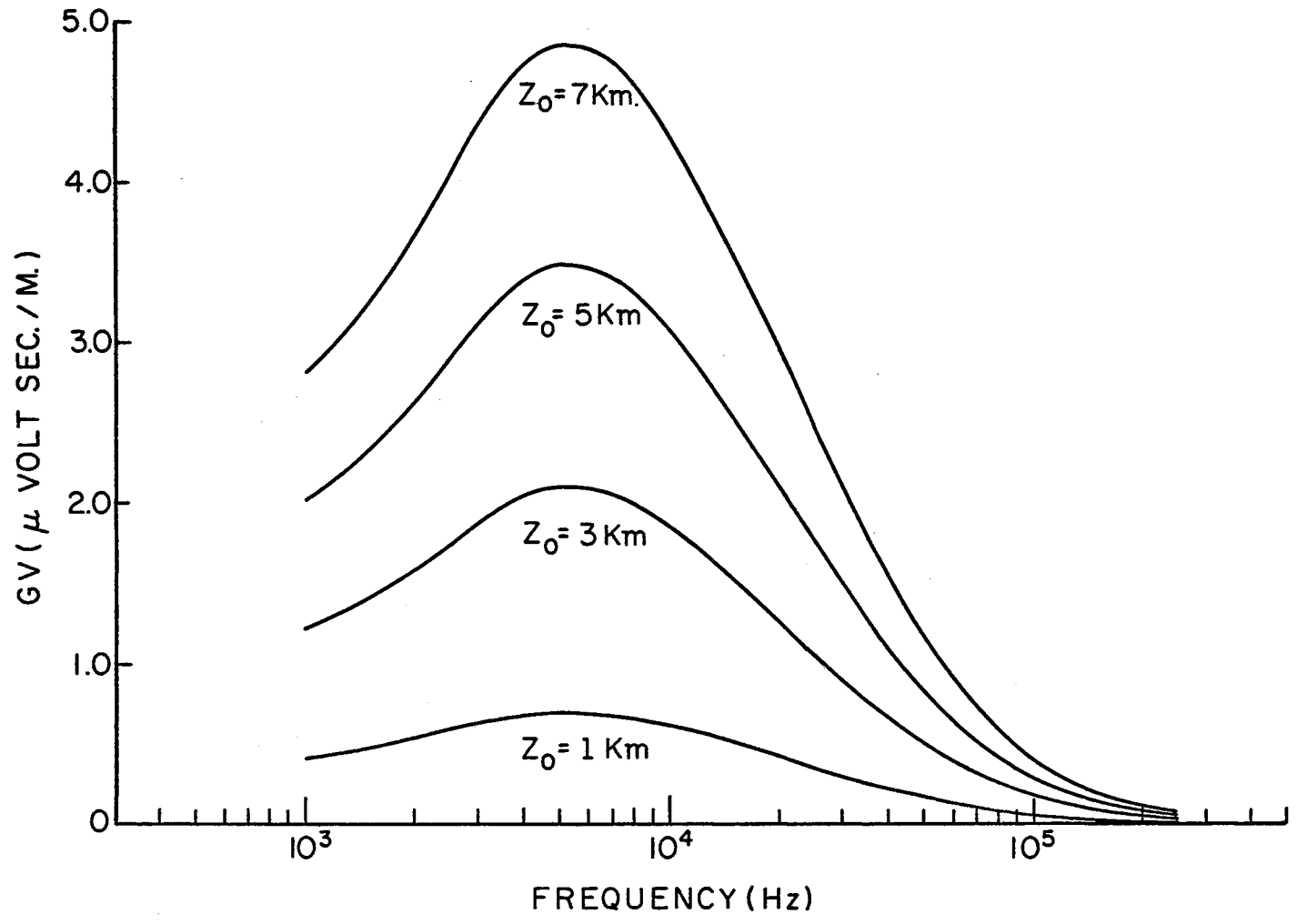
Figure 32. Horizontal Channels Directed Toward Observer, Far Field
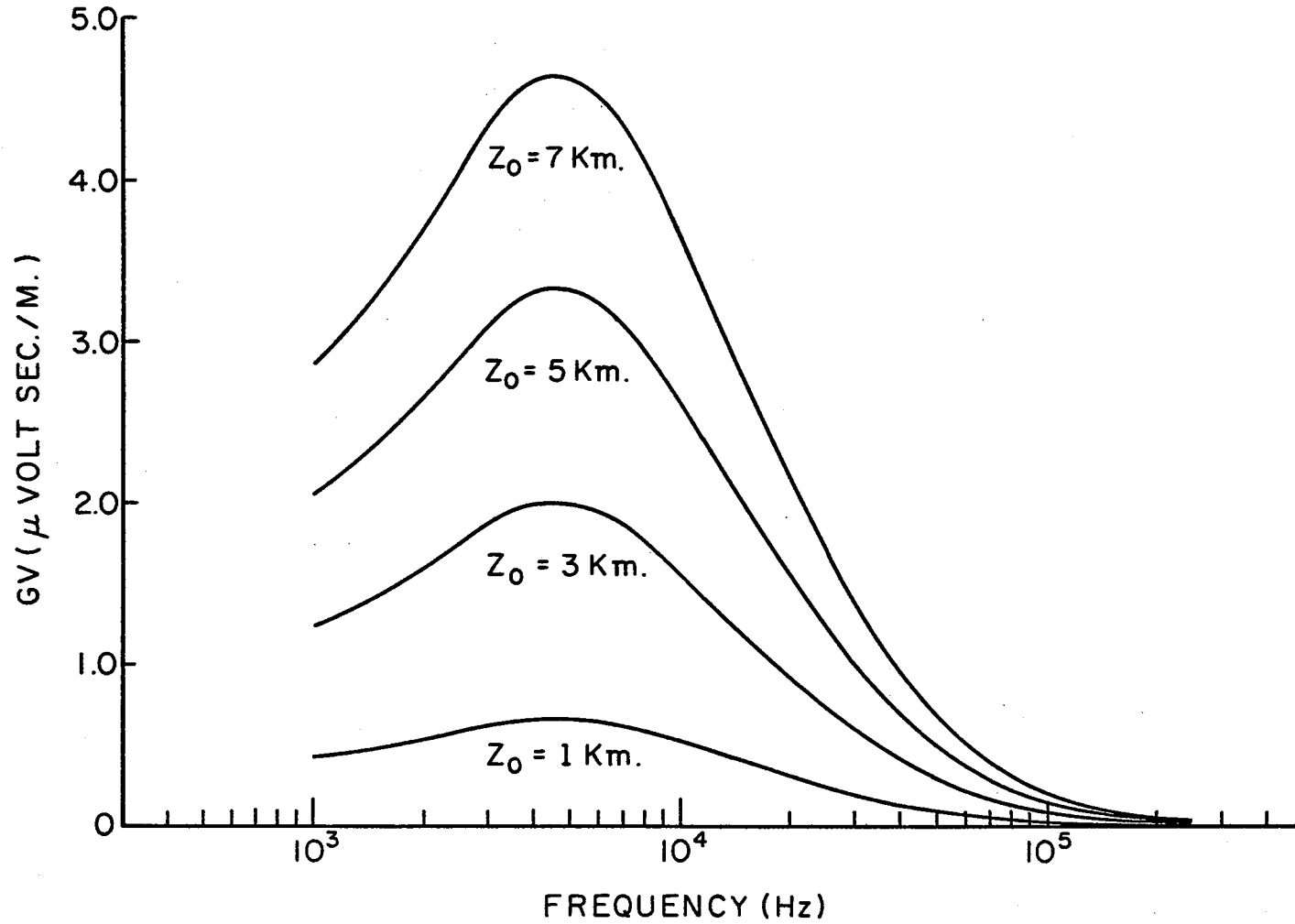
Figure 33. Horizontal Channels Directed Away From Observer, Far Field
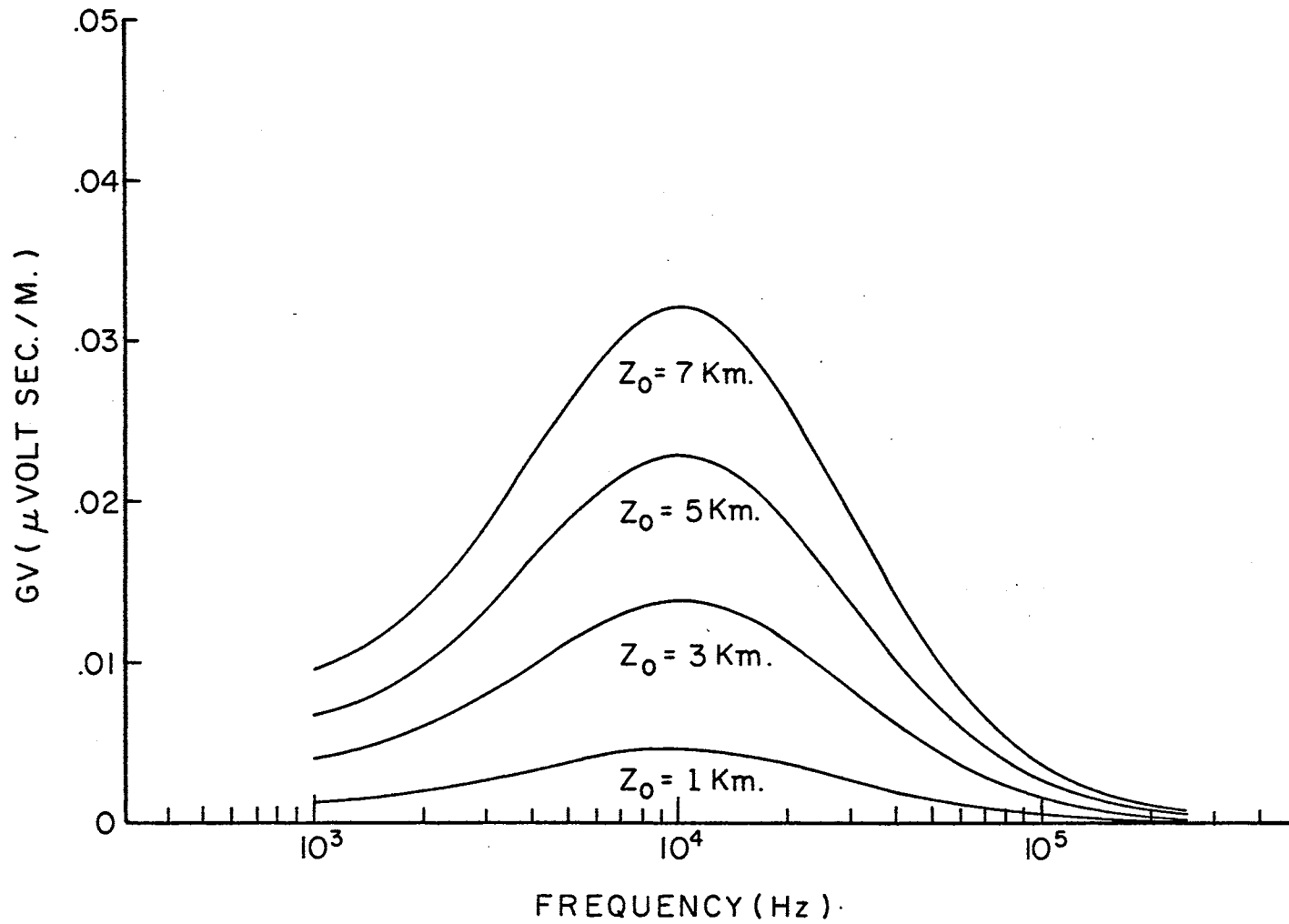
Figure 34. Horizontal Channels Directed Transverse to Observer, Far Field

with predominantly vertical orientation is translated along the vertical or Z-axis for the values considered here, $0 \leq Z_0 \leq 7$ Km. This lends support for those making the assumption of approximating the field produced from a current distribution on several different elements of the same length along the channel by the superposition of the currents on the same segment (1).

The curves of Figures 32 and 33 represent horizontal channel lengths in the same plane as the observation point, the Y,Z-plane. Again these results are not significantly different from the results of the preceding figures if the magnitudes are adjusted for the reduced channel length projected on the vertical antenna at the observation point.

Figure 34 represents a horizontal channel length parallel to the X-axis or perpendicular to and symmetric with respect to the Y,Z-plane. If all dipoles along the channel were assumed identical, the computed vertical component of the field should be identically zero. However, the assumption of the current progressing along the channel length requires different dipole moments on each. Although the resulting magnitude is small compared to Figures 32 and 33, the result is considered significant. That is, the general shape is the same as the horizontal discharges represented by Figures 32 and 33; however, the position of the maximum values have shifted from 5 KHz to 10 KHz. Or in other words, strictly horizontal discharges will produce vertical components of the field when measured in the far field on the ground. And the frequency content will be a function of the angle of observation projected on the ground plane.

Before proceeding to the next section, recall that for these

calculations the observation point was located at a distance of 100 Km from the channel on the ground, $(X_a, Y_a, Z_a) = (0, 100$ Km, $0)$.

5.4 Effect of Channel Orientation (Near Field). The discharge processes and geometries modeled in this section are identical to those discussed in the previous section. Only the observation point has been changed from $(X_a, Y_a, Z_a) = (0, 100$ Km, $0)$ to $(0, 10$ Km, 5 Km$)$. For a vertical discharge connecting with the ground, this corresponds to an observation point positioned 10 Km from the base of the discharge and elevated to an altitude of 5 Km. As before, the vertical antenna is parallel with the Z-axis and the horizontal antenna is parallel with the X-axis.

Figures 35, 36, and 39 represent channels with direction cosines $(0, 0, 1)$, $(0, .5, .866)$, and $(0, -.5, .866)$, respectively. These three figures correspond to the discharges modeled in Figures 28, 29, and 31, respectively. Figures 37 and 38 represent the vertical and horizontal components of the received fields from the discharges modeled in Figure 30 with direction cosines $(-.5, 0, .866)$.

The first obvious difference between the curves of this section and the preceding ones is the large increase in magnitude as the frequency approaches the lower values. This difference is explained by noting that the distance from the channel to the observation point is considerably less than a wavelength, λ, at these frequencies. Although the dependence of the electric field upon frequency, ω, and distance to the observation point, r, is masked in the equations of Chapter II, the electric field produced by one oscillating electric dipole (18) is proportional to the weighted sum of three terms $1/r^3$, ω/vr^2, and ω^2/v^2r, where v is the velocity of propagation. Near the dipole, r considerably
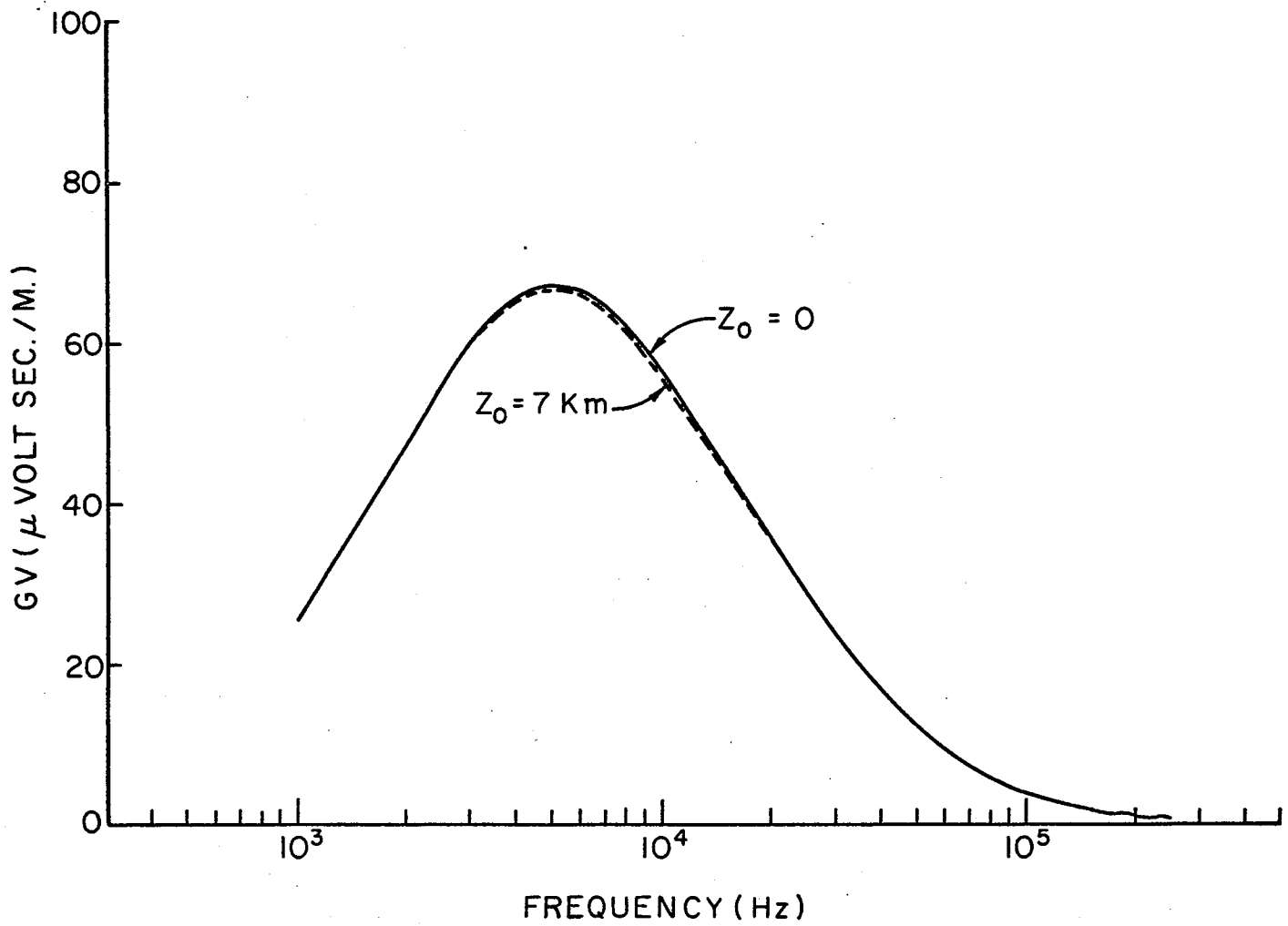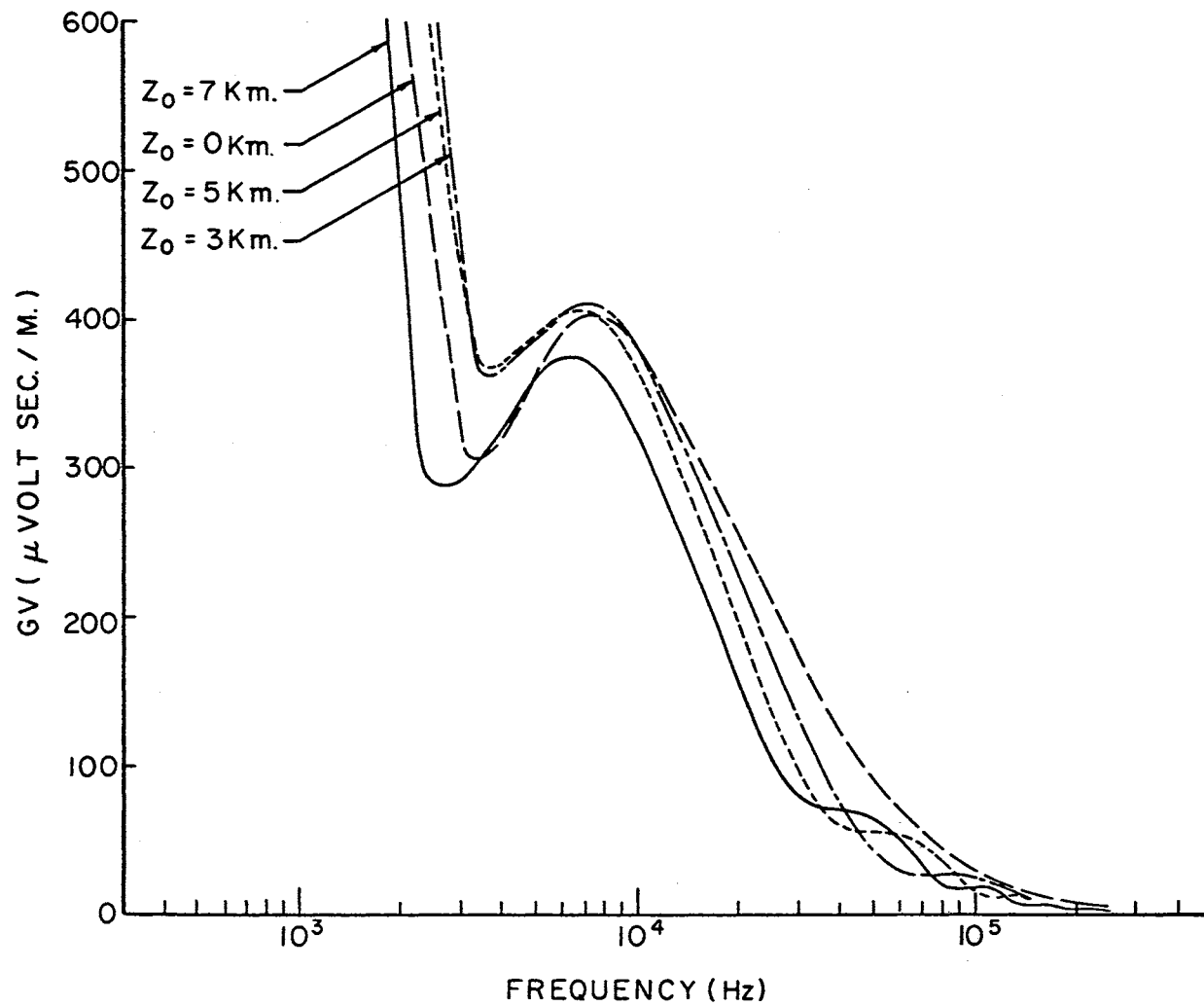
Figure 35. Vertical Channels
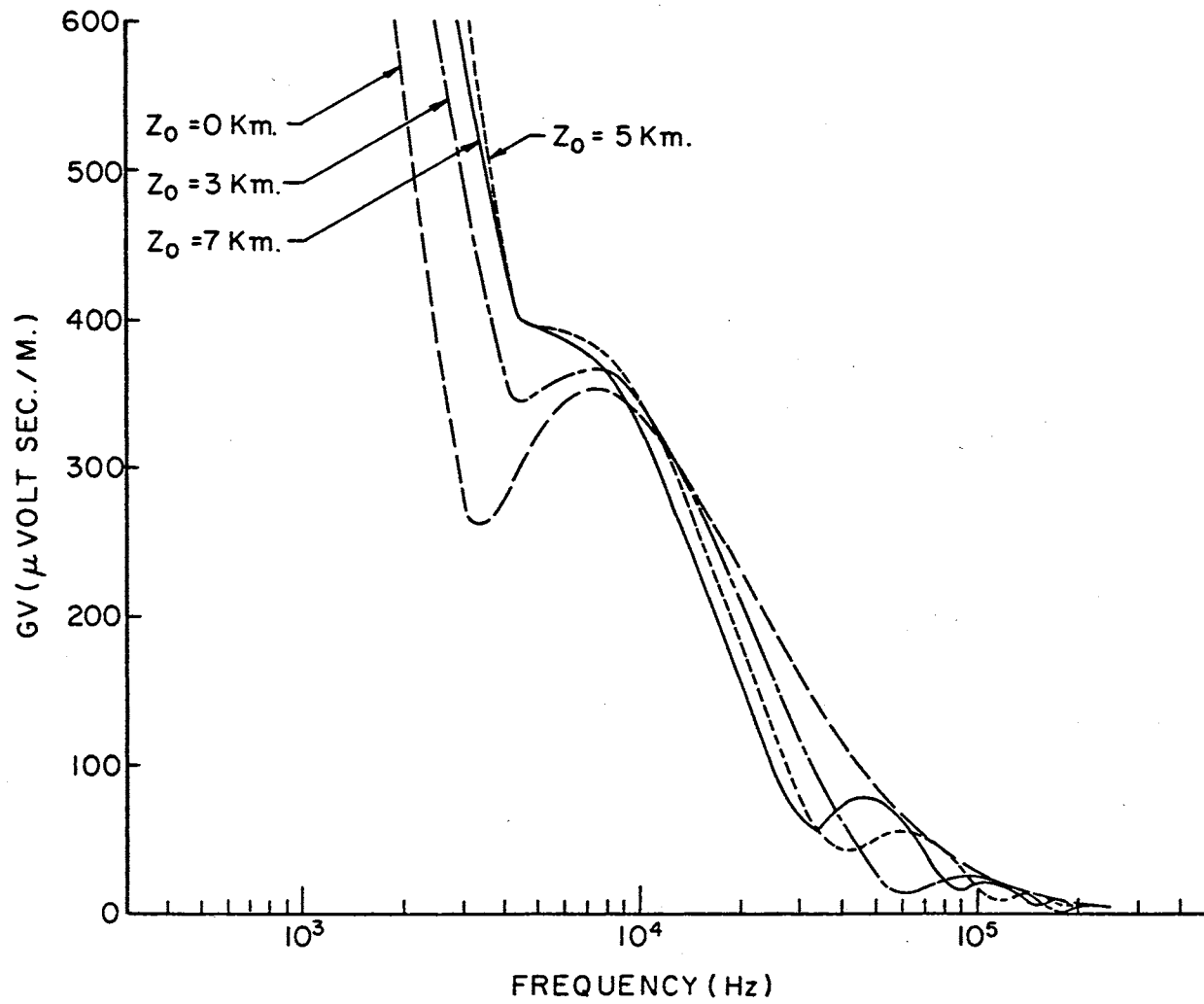
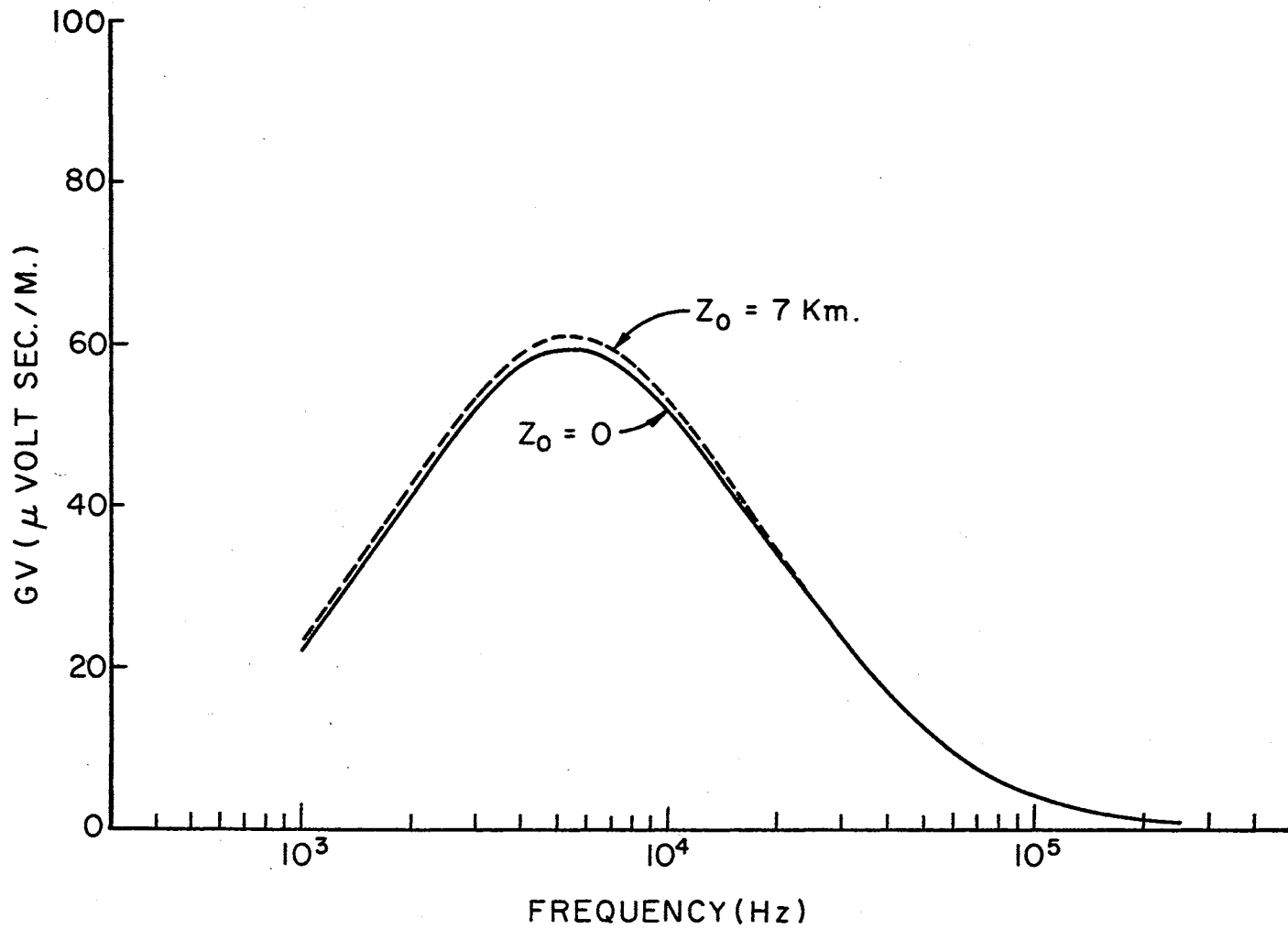Figure 36. Channels Inclined 30° From Vertical Toward Observer

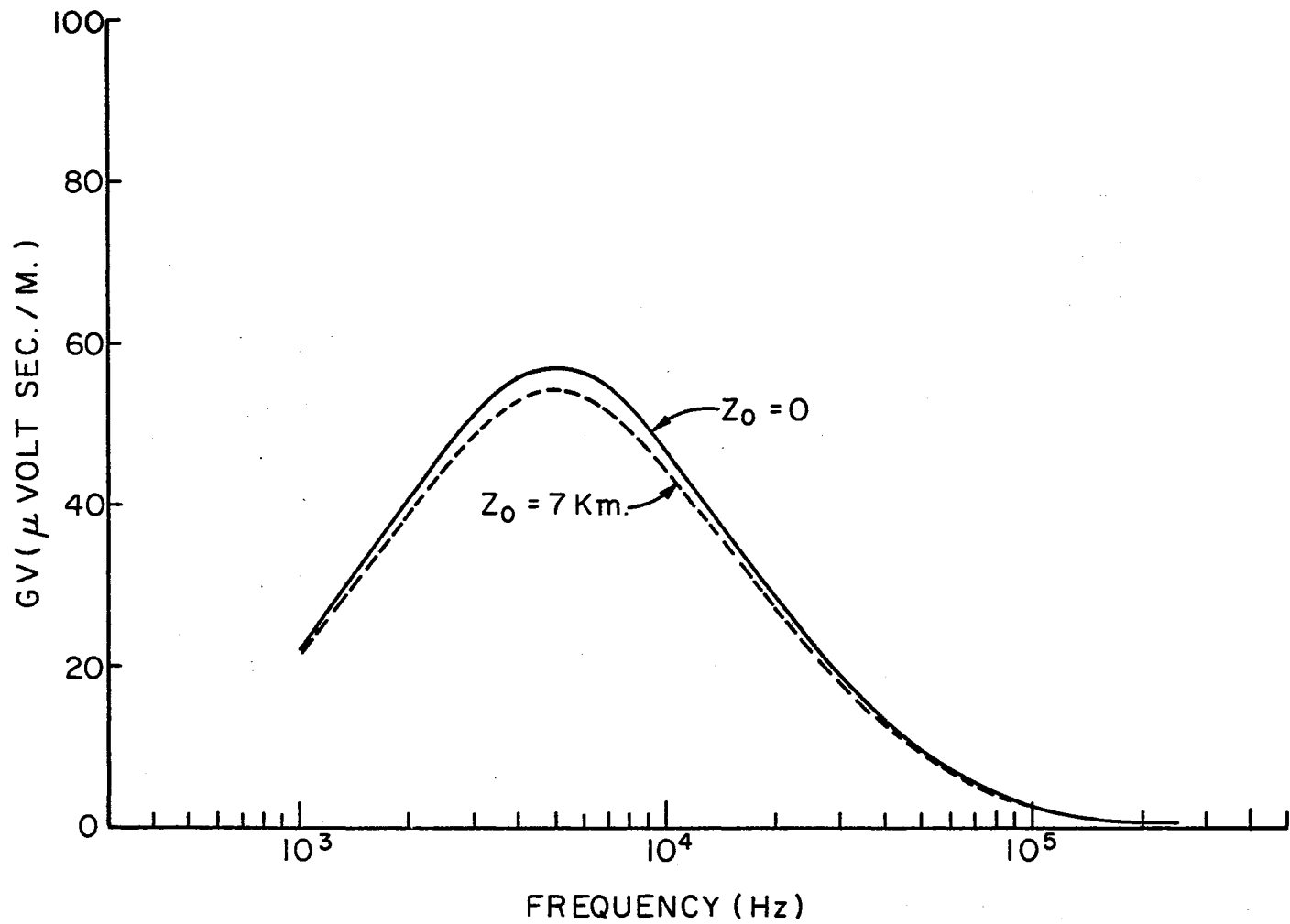Figure 37. Channels Inclined Transverse to Observer, Vertical Component
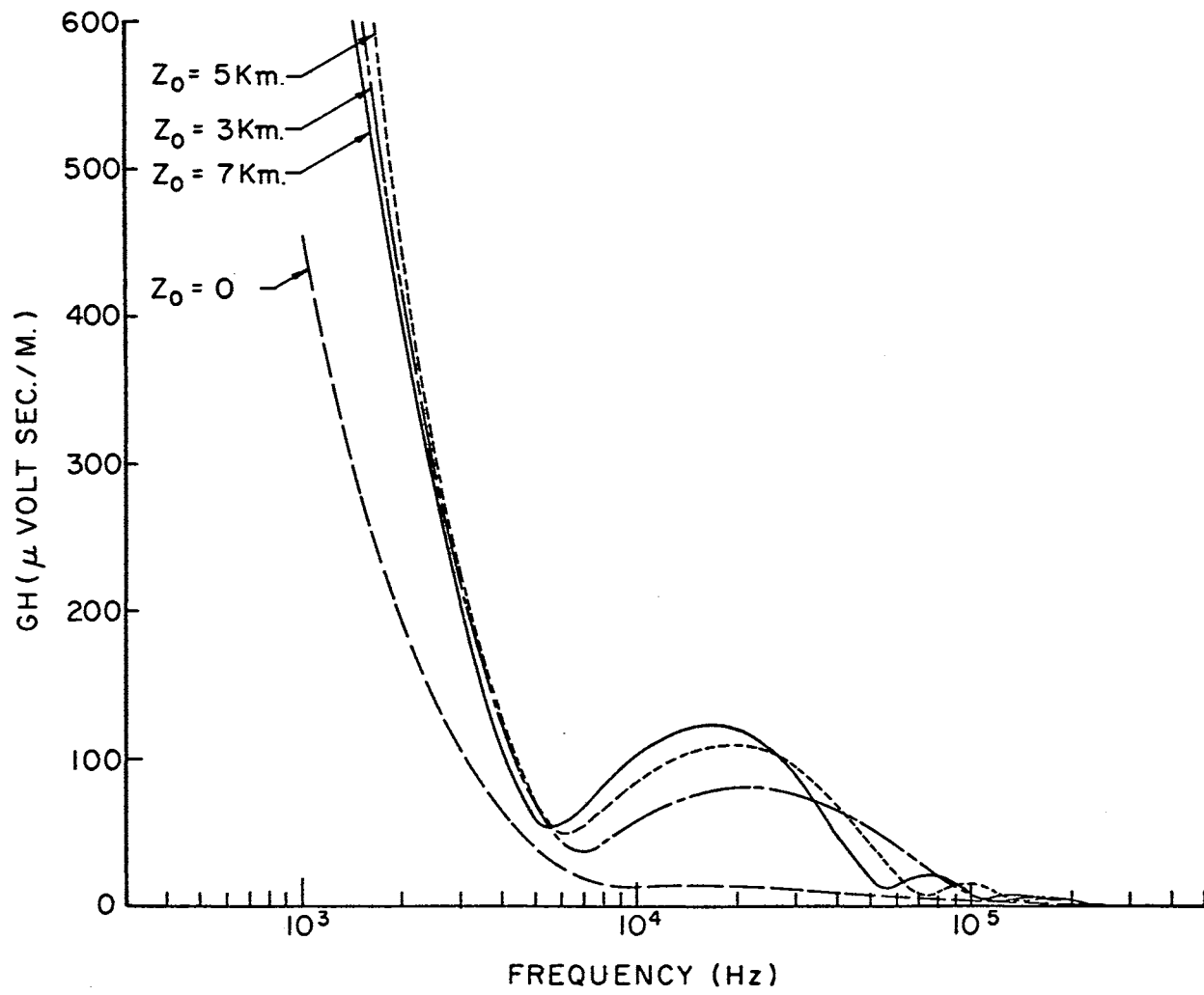
Figure 38. Channels Inclined Transverse to Observer, Horizontal Component
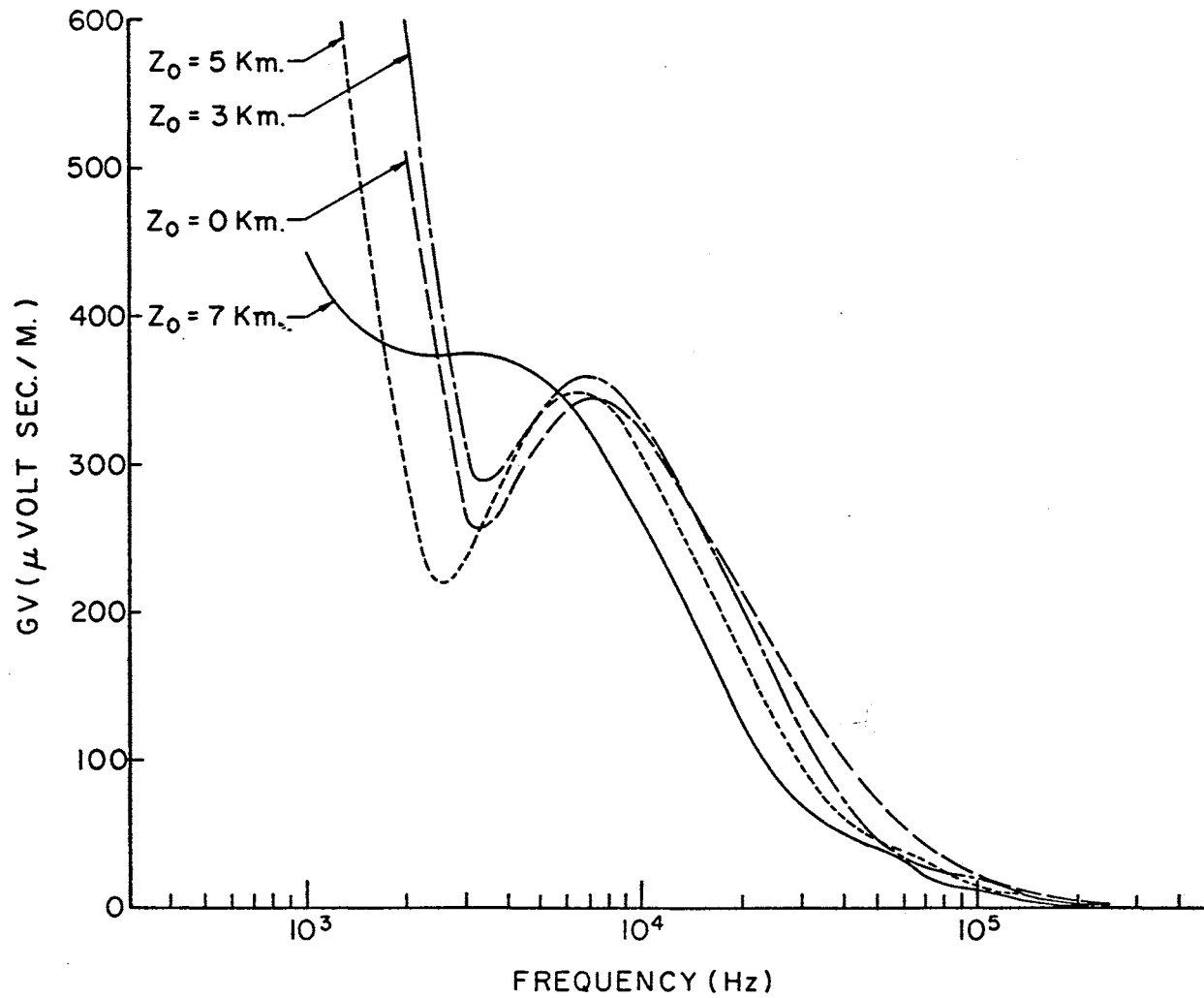
Figure 39. Channels Inclined 30° From Vertical Away From Observer

less than $\lambda/6$, the $1/r^3$ and $1/r^2$ terms begin to dominate the field. For fixed r, as the frequency is reduced further, the $1/r^3$ term becomes even more dominant. The Fourier transform of the charge on the ith dipole was assumed to be of the form

$$F_i(\omega) = I_i(\omega) \ [\pi\delta(\omega) + \frac{1}{j\omega}] \qquad ,$$

where $I_i(\omega)$ is the Fourier transform of the current waveform on that dipole. This results in a transform of the field produced by each dipole which tends toward $I_i(\omega)/j\omega$. For the current waveforms considered here the transforms $I_i(\omega)$ approach constant values as ω decreases. Thus the $1/\omega$ variation at the lower frequencies results. This problem is a direct result of the assumption that a charge remains on each dipole for an infinite length of time and is then removed or partially removed at some finite time. For example consider the unit step function U(t) which is analogous to the charge waveforms assumed. The Fourier transform is $\pi\delta(\omega) + 1/j\omega$. However, the unit pulse of duration 2T has the transform $(2\ \sin\omega T)/\omega$ which is well behaved as ω approaches zero. This unit pulse is analogous to a charge that is placed on the dipole at some finite time and removed at some later (finite) time. Also note that the maximum value of $(2\ \sin\omega T)/\omega$ depends on the duration T.

It is possible that in actual measurements the atmosphere may attenuate these lower frequency components. Horner (11) discusses the attenuation of atmospherics around 3 KHz. However, his discussion is limited to far field conditions, and the attenuation is considered resulting from waveguide modes of propagation. Extrapolation of this attenuation data to apply to the results of this section may be quite hazardous due to the distances involved. In any event the calculated

values are as to be expected for the means of propagation and the current waveforms assumed in the model.

Disregarding the frequencies below 4 KHz for the present and comparing Figures 28 and 35 which represent the vertical channels, it is noted the peaks in the spectra have been translated to higher frequencies in the near field. That is, a discharge which produces a peak in the spectrum at 5 KHz when measured at 100 Km on the ground will have considerably different frequency content when measured in the near field off the ground plane.

Also the far field calculations on the channels with vertical components of orientation yielded no appreciable difference in the spectra as the channel was elevated. However, the near field calculations indicate marked differences as evidenced by Figures 35 through 39. In addition to these differences the orientation modeled in Figure 30, direction cosines (-.5, 0, .866), allows a horizontal component of the field. Figure 37 represents the vertical component of this field when measured at (X_a, Y_a, Z_a) = (0, 10 Km, 5 Km). Figure 38 represents the corresponding horizontal component. The peaks of the horizontal components are located roughly at 20 KHz with magnitudes approximately one-fourth those of the vertical. Also note that the channel touching the ground, Z_0 = 0, is considerably less than the others around 20 KHz. Thus discharges inclined slightly, thirty degrees, from the vertical and elevated above the ground plane produce significant horizontal components of field. Also the maximum of the spectrum of the horizontal field occurs at a significantly greater frequency than that of the vertical field. That is, it appears that the higher frequency content for cloud discharges may not be a function of the process alone but rather how

they are observed.

Figures 40 and 41 represent the horizontal discharges with orienta-
tions (0, 1, 0) and (0, -1, 0) corresponding to Figures 32 and 33, re-
spectively. Figures 42 and 43 are the vertical and horizontal compo-
nents of the field for the horizontal discharges with orientation (-1,
0, 0) corresponding to Figure 34.

First, assume there does exist an attenuation of the spectra at
the lower frequencies, say around 3 KHz. One may see from Figures 40,
41, and 42 that the frequency of the maximums in the vertical spectra
may be determined by the form of this attenuation superimposed on the
spectra, the orientation, and the elevation of the discharge rather
than the discharge process alone. Also note that it is possible for
these maximums in the vertical spectra to occur at frequencies as high
as 20 KHz for the cases of Z_0 = 1 and 3 Km in Figures 40 and 41 and as
high as 30 KHz for the cases of Z_0 = 1 and 3 Km in Figure 42. In each
of these cases recall that the process is the same, and only the height
above ground and the direction of the discharge is being changed.

Of these three horizontal discharges, only the one with direction
cosines (-1, 0, 0) will produce a component of the horizontal field due
to the assumed direction on the horizontal antenna. This horizontal
component is shown in Figure 43. Again, as in Figure 38, the horizontal
component of the field exhibits maximums significantly larger than that
obtained from the identical discharge if it were strictly vertical. In
particular, the cases for Z_0 = 1, 3 and 5 Km have maximums at 30, 25,
and 20 KHz, respectively.
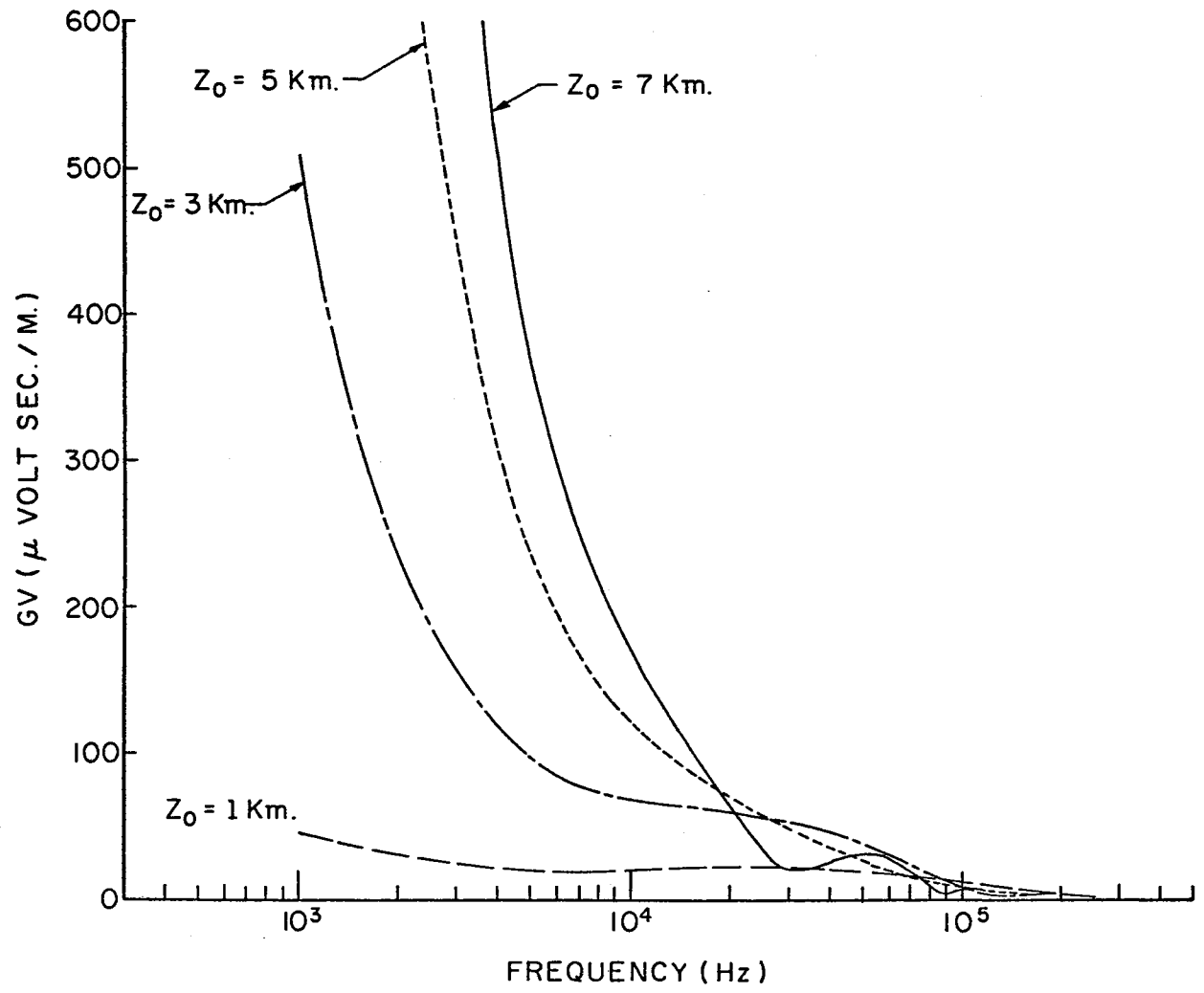
Figure 40. Horizontal Channels Directed Toward Observer
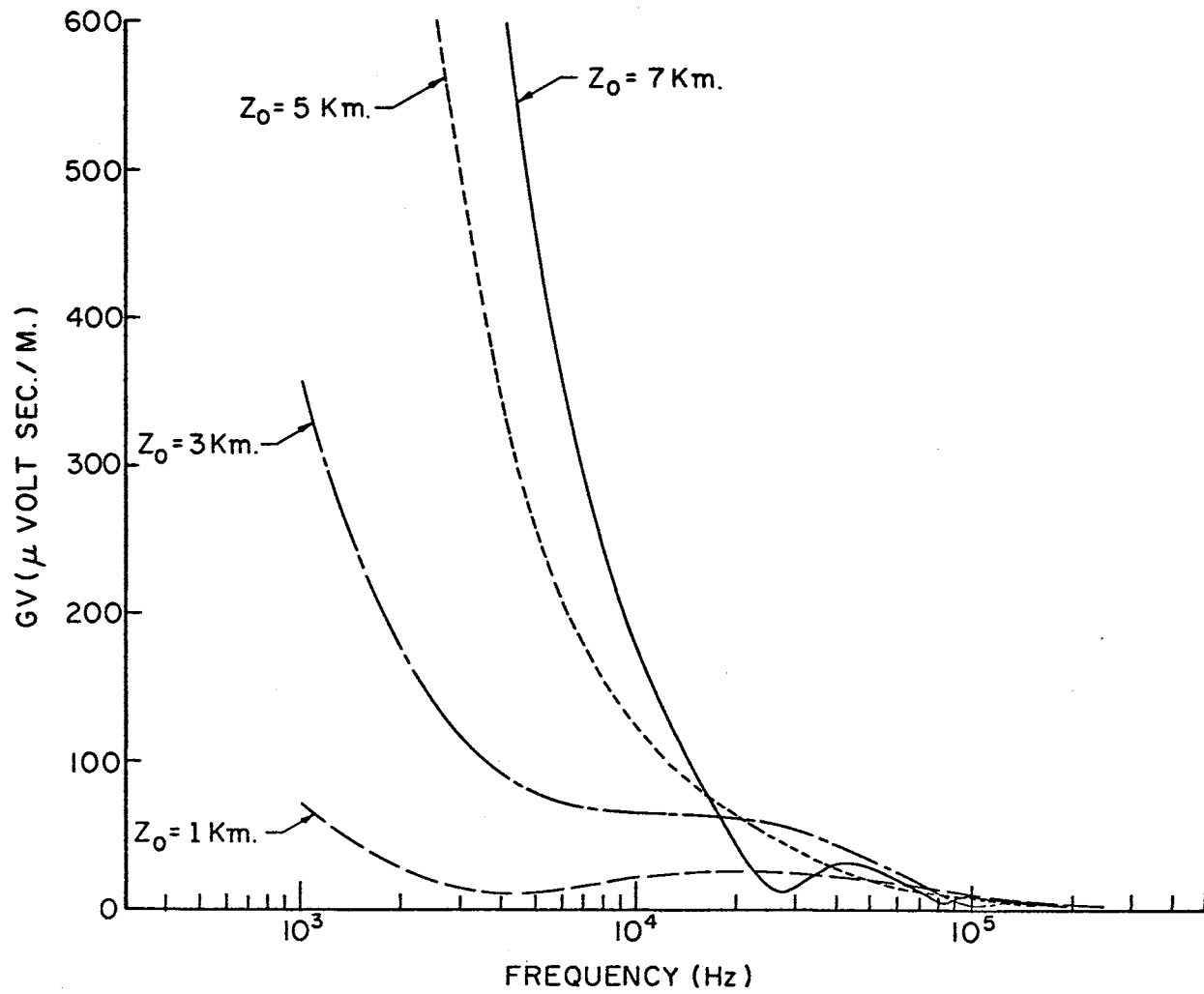
Figure 41. Horizontal Channels Directed Away From Observer
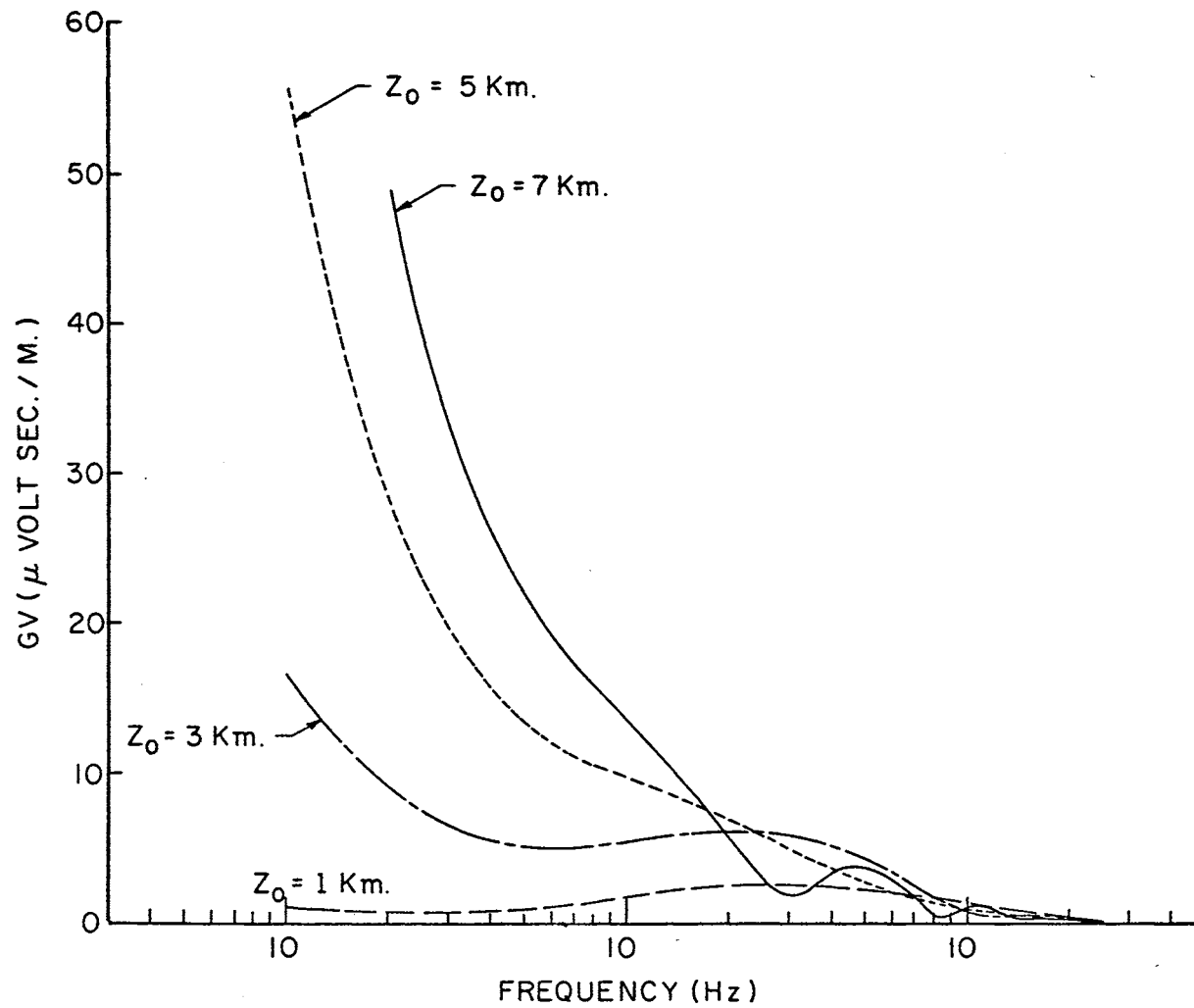
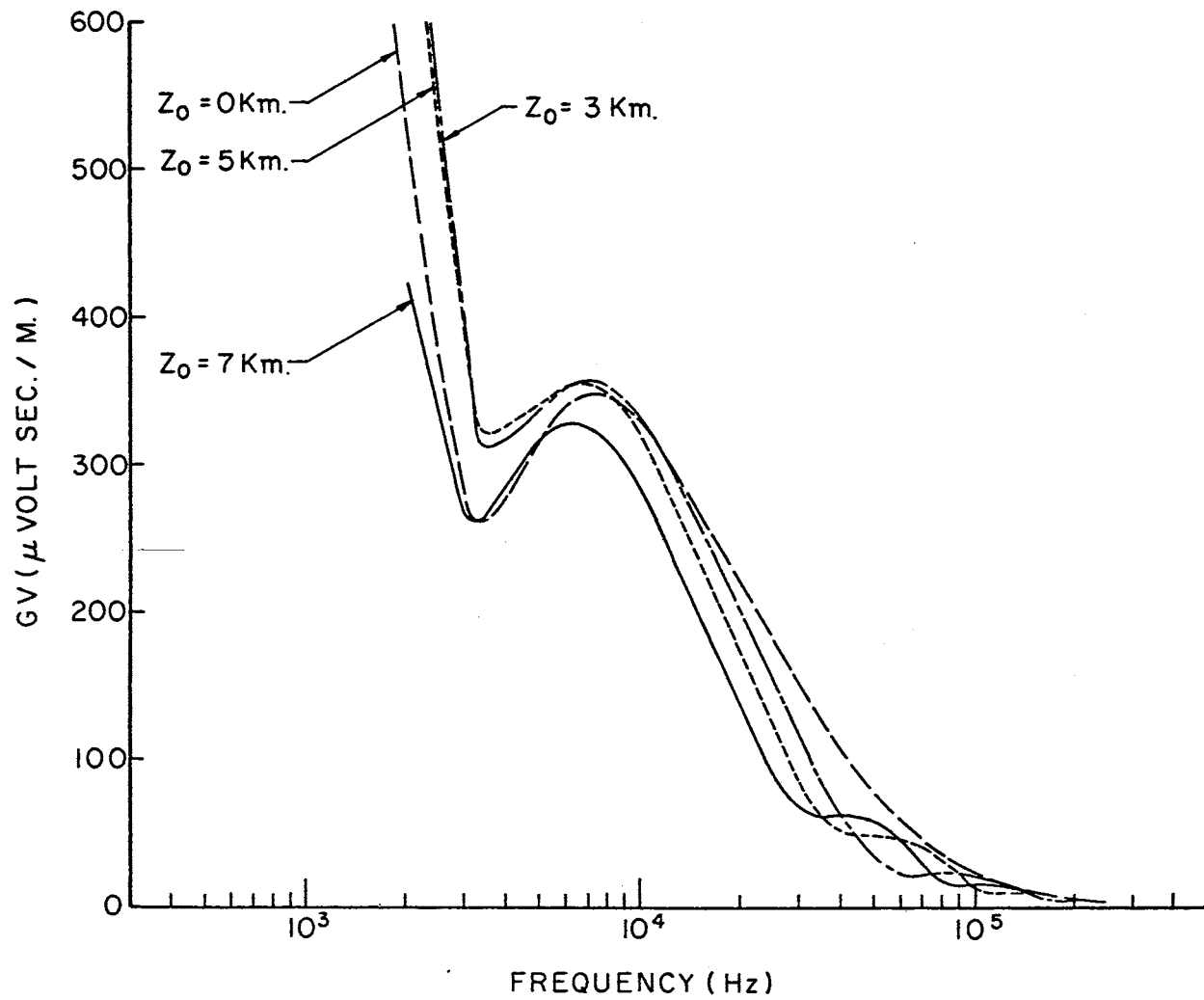Figure 42. Horizontal Channels Directed Transverse to Observer, Vertical Component
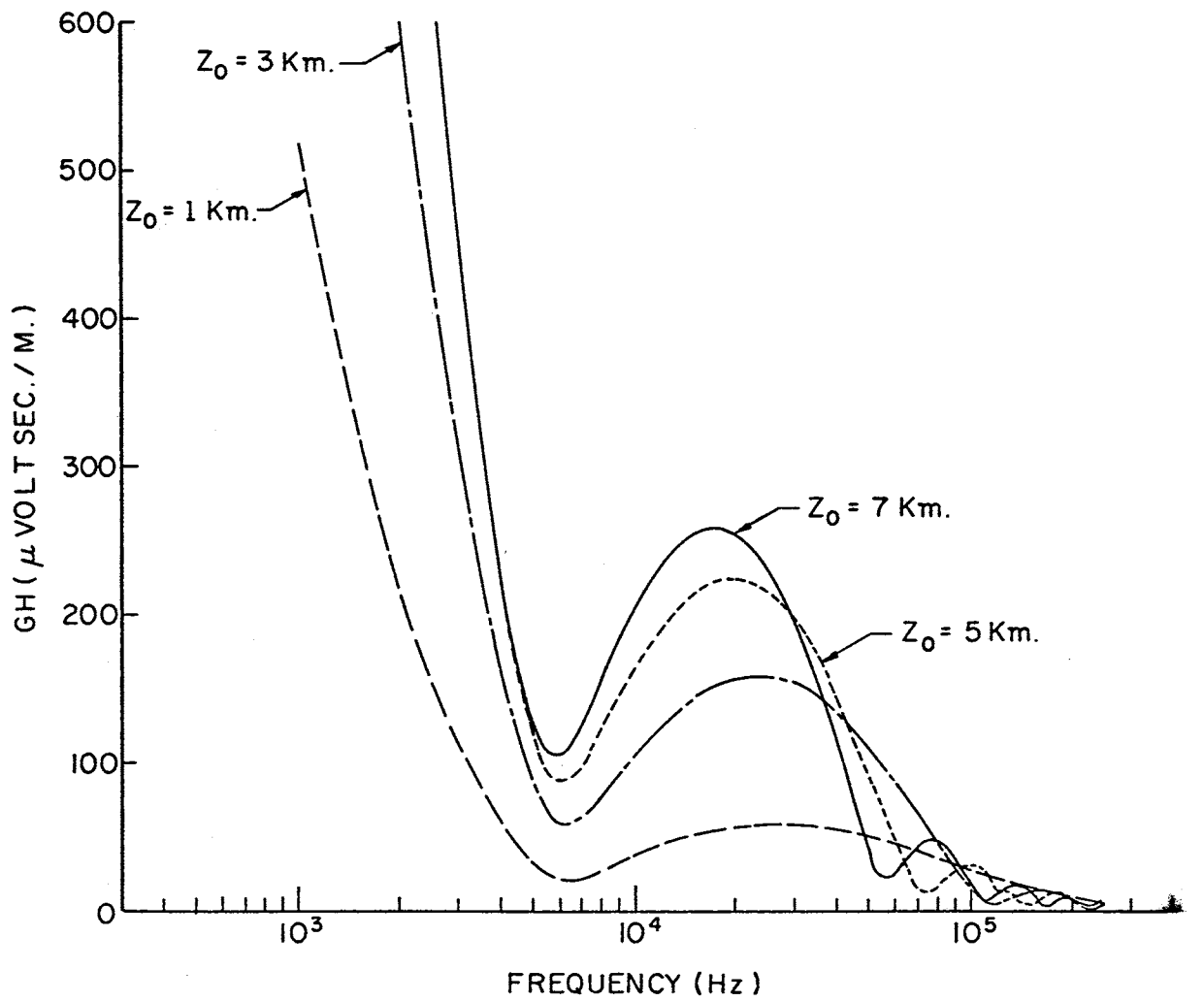
Figure 43. Horizontal Channels Directed Transverse to Observer, Horizontal Component

CHAPTER VI

SUMMARY AND CONCLUSIONS

A computer program has been developed to compute the Fourier trans-
form of the electric field produced by various models of lightning dis-
charges. This program produces results in agreement with other models
existing in the literature when equal assumptions are made on the pro-
cesses to be modeled. In addition, the computations of the present pro-
gram are not limited to far field conditions, and the observation point
may be located at any position desired either on or above the ground
plane. A multiplicity of discharges may be incorporated into the pro-
gram by simply specifying the geometry desired, the Fourier transform
of the assumed current waveforms, and the manner in which these current
waveforms are to progress through the geometry.

This program has been extended to calculate the time functions
approximating the narrow-band, half-wave linear detected fields produced
by the same discharge models the first program is capable of implement-
ing. The results of this program are in agreement with the assumptions
made for the detection system. However, if this program is to be uti-
lized for the comparison of computed time waveforms with measured data,
more realistic assumptions must be made for the band-pass filters in-
volved.

The intent of this work was not to develop an elaborate model of a
lightning discharge for the purpose of determining more about the

mechanisms involved in the discharge process. Rather, the purpose was
to develop a model which would be capable of yielding some information
relating parameters in the electromagnetic radiation received from
thunderstorms to possible parameters within the storm.

With this in mind, the Bruce and Golde current model for a return
stroke was chosen as a test signal and the Fourier transform of the re-
sulting field was calculated varying only the channel geometry and the
point of observation.

Calculations were performed to indicate that the position of the
maximum of the spectrum resulting from a cloud-to-ground discharge is
related to the discharge length if all other considerations are constant.

It was found that a vertical discharge to ground which produces a
peak in the received spectrum at 5 KHz when observed at 100 Km on the
ground plane is capable of producing a peak at 10 KHz measured at the
same observation point if the discharge is elevated above the ground
plane and tilted to a horizontal position.

Discharges which produce no significant differences when measured
in the far field were seen to be quite different when measured near the
discharge. This is especially true of the horizontal discharges modeled.

One of the major conclusions drawn from the computations is that
the predicted difference in the frequency content between cloud-to-
ground and intra cloud discharges is not entirely a function of the dif-
ferences in the processes. Rather the inclination of the discharges
and the angle from which they are observed significantly enter into the
resulting spectra.

From these results it appears that the location of the peaks in
the spectra is a significant parameter to consider in pattern

recognition. Realizing that the received field is not unique to a particular discharge and that randomness is inherent in actual discharges indicates that the positions of the maximums alone are not sufficient. However, it is suggested that consideration of the peaks of the horizontal and vertical data simultaneously will remove some uncertainties.

Before definite conclusions can be drawn from the calculated spectra, the actual attenuation must be investigated. Also to obtain well behaved spectra for near field calculations, it is necessary that each dipole charge be nonzero only over a finite time interval. The effect of this "duration" of charge should be investigated.

SELECTED BIBLIOGRAPHY

(1) Arnold, Helen R., and E. T. Pierce. "Leader and Junction Processes
     in the Lightning Discharge as a Source of VLF Atmospherics."
     RADIO SCIENCE Journal of Research NBS/USNC-URSI., Vol. 68D
     (July, 1964).

(2) Bendat, J. S. Principles and Applications of Random Noise Theory.
     New York: John Wiley & Sons, 1958.

(3) Bendat, J. S., and A. G. Piersol. Measurement and Analysis of
     Random Data. New York: John Wiley & Sons, 1966.

(4) Bergland, G. D. "A Guided Tour of the Fast Fourier Transform."
     IEEE Spectrum., Vol. 7 (July, 1969).

(5) Bruce, C. E. R., and R. H. Golde. "The Lightning Discharge."
     J. Inst. Elec. Engrs. (London), Vol. 88 (1941).

(6) Davenport, Wilbur B. and William L. Root. An Introduction to the
     Theory of Random Signals and Noise. New York: McGraw-Hill,
     1958.

(7) Dennis, A. S. and E. T. Pierce. "The Return Stroke of the Light-
     ning Flash to Earth as a Source of VLF Atmospherics." RADIO
     SCIENCE Journal of Research NBS/USNC-URSI., Vol. 68D, (July,
     1964).

(8) Hill, E. L. "Electromagnetic Radiation From Lightning Strokes."
     Journal of the Franklin Institute., Vol. 263, (February, 1957).

(9) Hill, R. D. "Electromagnetic Radiation From the Return Stroke as
     a Lightning Discharge." Journal of Geophysical Research.,
     Vol. 71 (April, 1966).

(10) Horner, F. (Ed.) Monograph on Radio Noise of Terrestrial Origin.
     New York: Elsevier Publishing Company, 1962.

(11) Horner, F. "Radio Noise From Thunderstorms." Advances in Radio
     Research., Vol. 2. Ed. J. A. Saxton. New York: Academic
     Press, 1964.

(12) Kitagawa, N. and M. Brook. "A Comparison of Intracloud and Cloud
     to Cloud Lightning Discharges." Journal of Geophysical
     Research., Vol. 65 (1960).

(13) Kraus, John D. Antennas. New York: McGraw-Hill, 1950.

(14)   Papoulis, Anthanasios. The Fourier Integral and Its Applications.
        New York: McGraw-Hill, 1962.

(15)   Pierce, E. T. "Electrostatic Field Changes due to Lightning
        Discharges." Quart. J. Roy. Meteorol. Soc., Vol. 81 (1955).

(16)   Schonland, B. F. J. "The Lightning Discharge." Handbuch der
        Physik., Vol. 22. Berlin: Springer-Verlang OHG (1956).

(17)   Steptoe, B. J. "Some Observations on the Spectrum and Propagation
        of Atmospherics." (unpub. Ph.D. thesis, University of London,
        England, 1958).

(18)   Stratton, Julis Adams. Electromagnetic Theory. New York:
        McGraw-Hill, 1941.

(19)   Uman, Martin A. Lightning. New York: McGraw-Hill, 1969.

(20)   Uman, Martin A., and D. Kenneth McLain. "Radiation Field and
        Current of the Lightning Stepped Leader." Journal of
        Geophysical Research., Vol. 75 (February, 1970).

APPENDIX A

DERIVATION OF THE FIELD EQUATIONS

A.1 Introduction. Consider an oscillating electric dipole located
at $(0, 0, h)$ in free space with direction cosines (ℓ, m, n) and its
image located at $(0, 0, -h)$ with orientation $(-\ell, -m, n)$. Assume the
resulting Hertz vector may be approximated by (see Sections 2.1 and 2.2):

$$\vec{\Pi}(x, y, z) = \frac{\Delta L}{4\pi\varepsilon} \{ (\frac{Q_1}{r_1} - \frac{Q_2}{r_2}) \ell \, \vec{a}_x + (\frac{Q_1}{r_1} - \frac{Q_2}{r_2}) m \, \vec{a}_y + (\frac{Q_1}{r_1} + \frac{Q_2}{r_2}) n \, \vec{a}_z \} \quad ,$$

where $\vec{a}_x$, $\vec{a}_y$, and $\vec{a}_z$ are unit vectors in the X, Y, and Z directions,
respectively; $Q(t)\Delta L$ is the magnitude of the dipole moment;

$$r_1 = \{x^2 + y^2 + (z - h)^2\}^{\frac{1}{2}} \quad ,$$

$$r_2 = \{x^2 + y^2 + (z + h)^2\}^{\frac{1}{2}} \quad ,$$

$$Q_1 = Q(t - \frac{r_1}{v}) = Q_0 \exp \{j\omega(t - \frac{r_1}{v})\} \quad ,$$

and

$$Q_2 = Q(t - \frac{r_2}{v}) = Q_0 \exp \{j\omega(t - \frac{r_2}{v})\} \quad .$$

The field components resulting from this assumed Hertz vector are cal-
culated at the observation point (x, y, z) in spherical coordinates.
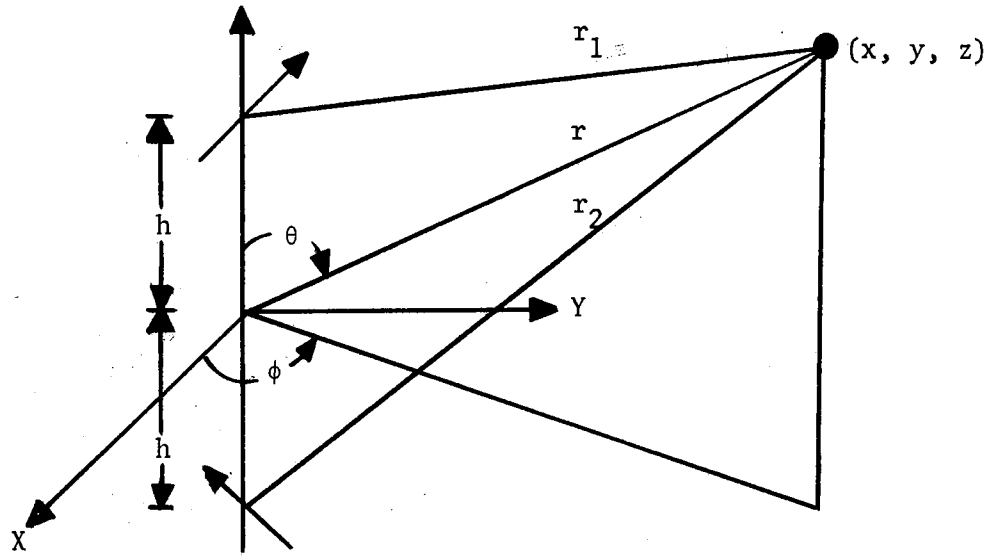
Figure 2. Dipole, Image, and Observation Point

A.2 Electric Intensity. The Hertz vector is converted to spherical coordinates by the equations

$$
\begin{bmatrix}
\pi_r(r, \theta, \phi, t) \\
\pi_\theta(r, \theta, \phi, t) \\
\pi_\phi(r, \theta, \phi, t)
\end{bmatrix}
=
\begin{bmatrix}
\sin\theta \cos\phi & \sin\theta \sin\phi & \cos\theta \\
\cos\theta \cos\phi & \cos\theta \sin\phi & -\sin\theta \\
-\sin\phi & \cos\phi & 0
\end{bmatrix}
\begin{bmatrix}
\pi_x(x, y, z, t) \\
\pi_y(x, y, z, t) \\
\pi_z(x, y, z, t)
\end{bmatrix},
$$

where $\vec{\pi} = \pi_r \vec{a}_r + \pi_\theta \vec{a}_\theta + \pi_\phi \vec{a}_\phi = \pi_x \vec{a}_x + \pi_y \vec{a}_y + \pi_z \vec{a}_z$. This transformation results in

$$
\pi_r = \frac{\Delta L}{4\pi\epsilon} \left\{ \left(\frac{Q_1}{r_1} - \frac{Q_2}{r_2}\right)(\ell \cos\phi + m \sin\phi) \sin\theta + \left(\frac{Q_1}{r_1} + \frac{Q_2}{r_2}\right)n \cos\theta \right\} \quad (A.2.1)
$$

$$
\pi_\theta = \frac{\Delta L}{4\pi\epsilon} \left\{ \left(\frac{Q_1}{r_1} - \frac{Q_2}{r_2}\right)(\ell \cos\phi + m \sin\phi) \cos\theta - \left(\frac{Q_1}{r_1} + \frac{Q_2}{r_2}\right)n \sin\theta \right\} \quad (A.2.2)
$$

$$\pi_\phi = \frac{\Delta L}{4\pi\epsilon} \{(\frac{Q_1}{r_1} - \frac{Q_2}{r_2})(-\ell \sin\phi + m \cos\phi)\} \qquad , \qquad (A.2.3)$$

where

$$r_1 = (r^2 + h^2 - 2 r h \cos\theta)^{\frac{1}{2}}$$

and,

$$r_2 = (r^2 + h^2 + 2 r h \cos\theta)^{\frac{1}{2}} \qquad .$$

The electric intensity is given by

$$\vec{E} = \nabla(\nabla \cdot \vec{\pi}) - \mu\epsilon\omega^2\vec{\pi} \qquad . \qquad (A.2.4)$$

Consider the term $\nabla \cdot \vec{\pi}$ given in spherical coordinates by

$$\nabla \cdot \vec{\pi} = \frac{1}{r^2} \frac{\partial}{\partial r} (r^2\pi_r) + \frac{1}{r \sin\theta} \frac{\partial}{\partial\theta} (\pi_\theta \sin\theta) + \frac{1}{r \sin\theta} \frac{\partial}{\partial\phi} (\pi_\phi)$$

$$\qquad (A.2.5)$$

$$= \frac{2}{r} \pi_r + \frac{\partial}{\partial r} (\pi_r) + \frac{1}{r} \frac{\partial}{\partial\theta} (\pi_\theta) + \frac{\cos\theta}{r \sin\theta} (\pi_\theta) + \frac{1}{r \sin\theta} \frac{\partial}{\partial\phi} (\pi_\phi)$$

Using the relations

$$\frac{\partial}{\partial r} (\frac{Q_i}{r_i}) = Q_i \{\frac{-j\omega}{r_i v} - \frac{1}{r_i^2}\} \frac{\partial r_i}{\partial r} \qquad (A.2.6)$$

and

$$\frac{\partial}{\partial\theta} (\frac{Q_i}{r_i}) = Q_i \{\frac{-j\omega}{r_i v} - \frac{1}{r_i^2}\} \frac{\partial r_i}{\partial\theta} \qquad (A.2.7)$$

for i = 1,2 with

$$\frac{\partial r_1}{\partial r} = \frac{r - h \cos\theta}{r_1} \qquad (A.2.8)$$

$$\frac{\partial r_2}{\partial r} = \frac{r + h \cos\theta}{r_2} \qquad (A.2.9)$$

$$\frac{\partial r_1}{\partial \theta} = \frac{r\ h\ \sin\theta}{r_1} \qquad\qquad (A.2.10)$$

$$\frac{\partial r_2}{\partial \theta} = -\frac{r\ h\ \sin\theta}{r_2} \qquad , \qquad (A.2.11)$$

the above equation results in

$$\nabla \cdot \vec{\pi} = \frac{\Delta L}{4\pi\varepsilon}\ \{[n\ h\ -\ r\ \sin\theta(\ell\ \cos\phi\ +\ m\ \sin\phi)][\frac{j\omega Q_1}{r_1^2 v} + \frac{Q_1}{r_1^3} - \frac{j\omega Q_2}{r_2^2 v} - \frac{Q_2}{r_2^3}]$$

$$-\ n\ r\ \cos\theta\ [\frac{j\omega Q_1}{r_1^2} + \frac{Q_1}{r_1^3} + \frac{j\omega Q_2}{r_2^2} + \frac{Q_2}{r_2^3}]\} \qquad . \qquad (A.2.12)$$

The expression for $\nabla(\nabla \cdot \vec{\pi})$ is

$$\nabla(\nabla \cdot \vec{\pi}) = \vec{a}_r \frac{\partial}{\partial r}\ (\nabla \cdot \vec{\pi}) + \vec{a}_\theta \frac{1}{r}\frac{\partial}{\partial \theta}\ (\nabla \cdot \vec{\pi}) + \vec{a}_\phi \frac{1}{r\ \sin\theta}\frac{\partial}{\partial \theta}\ (\nabla \cdot \vec{\pi}) \qquad .$$

$$(A.2.13)$$

Noting that

$$\frac{\partial}{\partial r}\ \{\frac{j\omega Q_i}{v\ r_i^2} + \frac{Q_i}{r_i^3}\} = \{\frac{\omega^2 Q_i}{v^2 r_i^2} - \frac{j3\omega Q_i}{v\ r_i^3} - \frac{3Q_i}{r_i^4}\} \frac{\partial r_i}{\partial r}$$

$$\frac{\partial}{\partial \theta}\ \{\frac{j\omega Q_i}{v\ r_i^2} + \frac{Q_i}{r_i^3}\} = \{\frac{\omega^2 Q_i}{v^2 r_i^2} - \frac{j3\omega Q_i}{v\ r_i^3} - \frac{3Q_i}{r_i^4}\} \frac{\partial r_i}{\partial \theta}$$

for $i = 1,2$, and using the expressions for $\partial r_i/\partial r$ and $\partial r_i/\partial \theta$ given by Equations A.2.8 through A.2.11, $\nabla(\nabla \cdot \vec{\pi})$ is obtained and added to $-\mu\varepsilon\omega^2\vec{\pi}$ in accordance with A.2.4 to obtain the electric intensity. The spherical components E_r, E_θ, and E_ϕ of $\vec{E} = E_r\vec{a}_r + E_\theta\vec{a}_\theta + E_\phi\vec{a}_\phi$ may be expressed in the following form:

$$E_r = \frac{\Delta L}{4\pi\epsilon} \{ \sin\theta(\ell \cos\phi + m \sin\phi)[-Q_{1,2}(2,3;-2,-3) + \mu\epsilon\omega^2 Q_{1,2}(1;-1)$$

$$+ n \cos\theta[-Q_{1,2}(2,3;2,3) + \mu\epsilon\omega^2 Q_{1,2}(1;1)]$$

$$+ Q_1(3,4,5)(r - h \cos\theta)[r n \cos\theta - h n + r \sin\theta(\ell \cos\phi + m \sin\phi)]$$

$$+ Q_2(3,4,5)(r + h \cos\theta)[r n \cos\theta + h n - r \sin\theta(\ell \cos\phi + m \sin\phi)]\} \quad ,$$

$$(A.2.14)$$

$$E_\theta = \frac{\Delta L}{4\pi\epsilon} \{ \cos\theta(\ell \cos\phi + m \sin\phi)[-Q_{1,2}(2,3;-2,-3) + \mu\epsilon\omega^2 Q_{1,2}(1;-1)$$

$$+ n \sin\theta[Q_{1,2}(2,3;2,3) - \mu\epsilon\omega^2 Q_{1,2}(1;1)]$$

$$- h \sin\theta[h n - r \sin\theta(\ell \cos\phi + m \sin\phi)][Q_1(3,4,5) + Q_2(3,4,5)]$$

$$+ h n r \sin\theta \cos\theta[Q_1(3,4,5) - Q_2(3,4,5)]\} \quad ,$$

$$(A.2.15)$$

$$E_\phi = \frac{\Delta L}{4\pi\epsilon} \{ (\ell \sin\phi - m \cos\phi)[Q_{1,2}(2,3;-2,-3) - \mu\epsilon\omega^2 Q_{1,2}(1;-1)]\} \quad ,$$

$$(A.2.16)$$

where,

$$Q_{1,2}(1; \pm 1) = \frac{Q_1}{r_1} \pm \frac{Q_2}{r_2} \qquad (A.2.17)$$

$$Q_i(3,4,5) = -(\tfrac{\omega}{v})^2 \frac{Q_i}{r_i^3} + j3(\tfrac{\omega}{v}) \frac{Q_i}{r_i^4} + e \frac{Q_i}{r_i^5} , \quad i = 1,2 \qquad (A.2.18)$$

$$Q_{1,2}(2,3; \pm 2, \pm 3) = j(\tfrac{\omega}{v}) \frac{Q_1}{r_1^2} + \frac{Q_1}{r_1^3} \pm j(\tfrac{\omega}{v}) \frac{Q_2}{r_2^2} \pm \frac{Q_2}{r_2^3} . \qquad (A.2.19)$$

In addition to these calculations, the following has been performed as a check on these results. A Hertz vector was defined for the original dipole in terms of a spherical coordinate system which had the dipole at its origin, and the field conditions were calculated. The same was performed for the image dipole and its coordinate system. The two fields were superimposed and converted to the coordinate system used in the first calculations, and the results were found to agree with those

given above.

The field components may be partitioned according to the form

$$E_r = (ER1X + ER2X) + j(ER1Y + ER2Y)$$

$$E_\theta = (E\theta1X + E\theta2X) + j(E\theta1Y + E\theta2Y)$$

$$E_\phi = (E\phi1X + E\phi2X) + j(E\phi1Y + E\phi2Y) \qquad ,$$

where the indices 1 and 2 indicate the contribution due to the dipole
and the image, respectively; X and Y denote the real and imaginary
parts. With the following substitutions the partitioned

$$DRLM = \ell \cos\phi + m \sin\phi$$

$$RMH = r - h \cos\theta$$

$$RPH = r + h \cos\theta$$

$$RNMH = r \ n \cos\theta - h \ n + DRLM \ r \sin\theta$$

$$RNPH = r \ n \cos\theta + h \ n - DRLM \ r \sin\theta$$

components of the electric intensity may be written as:

$$ER1X = \frac{\Delta LQ_1}{4\pi\epsilon} \ \{ \frac{\mu\epsilon\omega^2}{r_1} \ [\sin\theta \ DRLM + n \cos\theta]$$

$$+ \frac{1}{r_1^3} \ [-\sin\theta \ DRLM - n \cos\theta - (\frac{\omega}{v})^2 \ RMH \ RNMH] + \frac{1}{r_1^5} \ [3 \ RMH \ RNMH] \}$$

$$\text{(A.2.20)}$$

$$ER1Y = \frac{\Delta LQ_1}{4\pi\epsilon} \ \{ \frac{1}{r_1^2} \ (\frac{\omega}{v}) \ [-\sin\theta \ DRLM - n \cos\theta] + \frac{1}{r_1^4} \ (\frac{\omega}{v}) \ [3 \ RMH \ RNMH] \} \qquad ,$$

$$\text{(A.2.21)}$$

$$E\theta 1X = \frac{\Delta LQ_1}{4\pi\varepsilon} \{\frac{\mu\varepsilon\omega^2}{r_1} [\cos\theta \ DRLM - n \sin\theta]$$

$$+ \frac{1}{r_1^3} [-\cos\theta \ DRLM + n \sin\theta - (\frac{\omega}{v})^2 h \sin\theta \ RNMH] + \frac{1}{r_1^5} [3 \ h \sin\theta \ RNMH]\}$$

$$(A.2.22)$$

$$E\theta 1Y = \frac{\Delta LQ_1}{4\pi\varepsilon} \{\frac{1}{r_1^2} (\frac{\omega}{v}) [-\cos\theta \ DRLM + n \sin\theta] + \frac{1}{r_1^4} (\frac{\omega}{v}) [3 \ h \sin\theta \ RNMH]\} \quad ,$$

$$(A.2.23)$$

$$E\phi 1X = \frac{\Delta LQ_1}{4\pi\varepsilon} \{ [- \frac{\mu\varepsilon\omega^2}{r_1} + \frac{1}{r_1^3}] [\ell \sin\phi - m \cos\phi]\} \quad , \quad (A.2.24)$$

$$E\phi 1Y = \frac{\Delta LQ_1}{4\pi\varepsilon} \{\frac{1}{r_1^2} (\frac{\omega}{v}) [\ell \sin\phi - m \cos\phi]\} \quad , \quad (A.2.25)$$

$$ER2X = \frac{\Delta LQ_2}{4\pi\varepsilon} \{\frac{\mu\varepsilon\omega^2}{r_2} [-\sin\theta \ DRLM + n \cos\theta]$$

$$+ \frac{1}{r_2^3} [\sin\theta \ DRLM - n \cos\theta - (\frac{\omega}{v})^2 RPH \ RNPH] + \frac{1}{r_2^5} [3 \ RPH \ RNPH]\} \quad ,$$

$$(A.2.26)$$

$$ER2Y = \frac{\Delta LQ_2}{4\pi\varepsilon} \{\frac{1}{r_2^2} (\frac{\omega}{v}) [\sin\theta \ DRLM - n \cos\theta] + \frac{1}{r_2^4} (\frac{\omega}{v}) [3 \ RPH \ RNPH]\} \quad ,$$

$$(A.2.27)$$

$$E\theta 2X = \frac{\Delta LQ_2}{4\pi\varepsilon} \{\frac{\mu\varepsilon\omega^2}{r_2} [-\cos\theta \ DRLM - n \sin\theta]$$

$$+ \frac{1}{r_2^3} [\cos\theta \ DRLM + n \sin\theta + (\frac{\omega}{v})^2 h \sin\theta \ RNPH] + \frac{1}{r_2^5} [-3 \ h \sin\theta \ RNPH]\}$$

$$(A.2.28)$$

$$E\theta 2Y = \frac{\Delta LQ_2}{4\pi\varepsilon} \{\frac{1}{r_2^2} (\frac{\omega}{v}) [\cos\theta \ DRLM + n \sin\theta] + \frac{1}{r_2^4} (\frac{\omega}{v}) [-3 \ h \sin\theta \ RNPH]\} \quad ,$$

$$(A.2.29)$$

$$E\phi 2X = \frac{\Delta LQ_2}{4\pi\varepsilon} \{ [\frac{\mu\varepsilon\omega^2}{r_2} - \frac{1}{r_2^3}] [\ell \sin\phi - m \cos\phi]\} \quad , \quad (A.2.30)$$

$$E\phi 2Y = \frac{\Delta LQ_2}{4\pi\varepsilon} \{\frac{1}{r_2^2} (\frac{\omega}{v}) (-\ell \sin\phi + m \cos\phi)\} \quad . \quad (A.2.31)$$

A.3 Transformation Equations. Equations A.2.20 through A.2.31 express the electric intensity resulting from the assumed Hertz vector with reference to a particular spherical coordinate system. The origin of this system is considered to be on the ground plane directly beneath the dipole. Superposition of the approximated fields from various dipoles requires the components to be expressed with reference to a common coordinate system.

Consider the origin of the initial coordinate system located at the point $(x_0, y_0, z_0) = (x_e, y_e, 0)$ in the reference system (X_0, Y_0, Z_0). The observation point (x, y, z) is located at $(x_0, y_0, z_0) = (x + x_e, y + y_e, z)$. For this translation of coordinate systems the transformation of the vector $\vec{A} = A_r \vec{a}_r + A_\theta \vec{a}_\theta + A_\phi \vec{a}_\phi$ into the vector $\vec{A} = A_{r_0} \vec{a}_{r_0} + A_{\theta_0} \vec{a}_{\theta_0} + A_{\phi_0} \vec{a}_{\phi_0}$ is given by

$$
\begin{aligned}
A_{r_0} = A_r\{&(\sin\theta \cos\phi) \sin\theta_0 \cos\phi_0 + (\sin\theta \sin\phi) \sin\theta_0 \sin\phi_0 \\
&+ (\cos\theta) \cos\theta_0\} + A_\theta\{(\cos\theta \cos\phi) \sin\theta_0 \cos\phi_0 \\
&+ (\cos\theta \sin\phi) \sin\theta_0 \sin\phi_0 - (\sin\theta) \cos\theta_0\} + A_\phi\{-(\sin\phi) \sin\theta_0 \sin\phi_0 \\
&+ (\cos\phi) \sin\theta_0 \sin\phi_0\}
\end{aligned}
$$

$$(A.3.1)$$

$$
\begin{aligned}
A_{\theta_0} = A_r\{&(\sin\theta \cos\phi) \cos\theta_0 \cos\phi_0 + (\sin\theta \sin\phi) \cos\theta_0 \sin\phi_0 \\
&- (\cos\theta) \sin\theta_0\} + A_\theta\{(\cos\theta \cos\phi) \cos\theta_0 \cos\phi_0 \\
&+ (\cos\theta \sin\phi) \cos\theta_0 \sin\phi_0 + (\sin\theta) \sin\theta_0\} + A_\phi\{(-\sin\phi) \cos\theta_0 \cos\phi_0 \\
&+ (\cos\phi) \cos\theta_0 \sin\phi_0\}
\end{aligned}
$$

$$(A.3.2)$$

and

$$
\begin{aligned}
A_{\phi_0} = A_r\{&-(\sin\theta \cos\phi) \sin\phi_0 + (\sin\theta \sin\phi) \cos\phi_0 + A_\theta\{-(\cos\theta \cos\phi) \sin\phi_0 \\
&+ (\cos\theta \sin\phi) \cos\phi_0\} + A_\phi\{(\sin\phi) \sin\phi_0 + (\cos\phi) \cos\phi_0\} \quad , \quad (A.3.3)
\end{aligned}
$$

where

$$\cos\theta = \frac{r_0}{r} \cos\theta_0 \qquad ,$$

$$\sin\theta = \{1 - (\frac{r_0}{r})^2 \cos^2\theta_0\}^{\frac{1}{2}} \qquad ,$$

$$\sin\phi = \frac{(r_0 \sin\theta_0 \sin\phi_0 - y_e)}{(r^2 - r_0^2 \cos^2\theta_0)^{\frac{1}{2}}} \qquad ,$$

$$\cos\phi = \frac{(r_0 \sin\theta_0 \cos\phi_0 - x_e)}{(r^2 - r_0^2 \cos^2\theta_0)^{\frac{1}{2}}} \qquad .$$

A.4 Magnetic Induction. The magnetic induction vector will not
be used in this work. However, its calculation is simple with the par-
tials in Section A.2 available and will be given for reference.

The magnetic induction vector is given by

$$\vec{B} = j\omega\mu\varepsilon \, \nabla x \vec{\pi} \qquad , \qquad (A.4.1)$$

where

$$\nabla x \vec{\pi} = \vec{a}_r \{\frac{\cos\theta \, \pi_\phi}{r \sin\theta} + \frac{1}{r} \frac{\partial(\pi_\theta)}{\partial\theta} - \frac{1}{r \sin\theta} \frac{\partial(\pi_\theta)}{\partial\phi}\}$$

$$+ \vec{a}_\theta \{\frac{1}{r \sin\theta} \frac{\partial(\pi_r)}{\partial\phi} - \frac{1\pi_\phi}{r} - \frac{\partial(\pi_\phi)}{\partial r} + \vec{a}_\phi \frac{1\pi_\theta}{r} + \frac{\partial(\pi_\theta)}{\partial r} - \frac{1}{r} \frac{\partial(\pi_r)}{\partial\theta}\} \qquad .$$

Utilizing the partials given by Equations A.2.6 through A.2.11, the
spherical components B_r, B_θ, and B_ϕ of $\vec{B} = B_r\vec{a}_r + B_\theta\vec{a}_\theta + B_\phi\vec{a}_\phi$ are

$$B_r = \frac{\Delta L}{4\pi} (j\omega\mu) \, h \, \sin\theta \, (\ell \sin\phi - m \cos\phi) \, Q_{1,2}(2,3;2,3) \qquad (A.4.2)$$

$$B_\theta = \frac{\Delta L}{4\pi} (j\omega\mu)(-\ell \sin\phi + m \cos\phi)[r \, Q_{1,2}(2,3;-2,-3) - h \cos\theta \, Q_{1,2}(2,3;2,3)]$$
$$(A.4.3)$$

$$B_\phi = \frac{\Delta L}{4\pi} \; (j\omega\mu)\{Q_{1,2}(2,3;2,3)[r \; n \; \sin\theta + h(\ell \; \cos\phi + m \; \sin\phi)]$$

$$- \; Q_{1,2}(2,3;-2,-3) \; r \; \cos\theta \; (\ell \; \cos\phi + m \; \sin\phi)\} \qquad . \qquad (A.4.4)$$

A.5 Magnetic Dipoles. As in the electric dipole calculations, the field due to a magnetic dipole above the earth's surface may be calculated by considering the actual dipole and its image radiating in free space. Thus, according to the principle of complementary solutions, the field expressions for the magnetic dipoles may be obtained from those of the electric dipole by the relations

$$\vec{E} = - \sqrt{\frac{1}{\mu\varepsilon}} \; \vec{B} \qquad , \qquad (A.5.1)$$

and

$$\vec{B} = \sqrt{\mu\varepsilon} \; \vec{E} \qquad . \qquad (A.5.2)$$

There is only one additional point to note. For an electric dipole with orientation $(1_e, m_e, n_e)$, the image will have orientation $(-1_e, -m_e, n_e)$, but for a magnetic dipole with orientation $(1_m, m_m, n_m)$, its image, due to an assumed infinite conducting plane, will have orientation $(1_m, m_m, -n_m)$. Thus, in the above expressions replace 1 by -1, m by -m, and n by -n when these are associated with the r_2 terms.

APPENDIX B

$\vec{G}(\omega)$ PROGRAM

Two versions of the program to compute the vertical and horizontal components of $\vec{G}(\omega)$ are listed in this appendix. The first is the standard program (Table I). The cards between the comment card CALCULATION OF FOURIER COEF. FOR INPUT TIME FUNCTIONS and 50 CONTINUE are the cards required to compute the Fourier transform of the return stroke current indicated by Equation 4.2.7.

The second program (Table II) listed is essentially the same as the first. This version of the program was used to compute the averaged magnitude of the Fourier transform resulting from the combination stepped leader and return stroke discussed in Section 4.4 with twelve data sets. The modifications included are the following. The four cards following 17 CONTINUE and the card 32 CONTINUE have been added to bypass the calculations involving the stepped leader velocity and thus let its progress be determined solely by the random delays. Also the card TOR=D(1,6) has been added in the calculation of the return stroke on time calculations so that the return stroke will begin when the stepped leader touches the ground as opposed to some fixed TOR specified by the input data. The cards between CALCULATION OF FOURIER COEF. FOR INPUT TIME FUNCTIONS and 50 CONTINUE have been modified to account for the addition of the leader current.

The matrix DD has been added to store the magnitudes of the Fourier

transforms so that they will be available for averaging after the twelve data sets have been considered.

TABLE I

$\vec{G}(\omega)$ PROGRAM WITH RETURN STROKE

```
//OGM2    JOB (10174,440-38-2220,008,50),'GUY MARNEY',MSGLEVEL=1,CLASS=A
// EXEC FORTGCLG,REGION.GO=110K
//FORT.SYSIN DD *
      DIMENSION D(1000,7),NS(30),DRL(30),DRM(30),DRN(30),DEL(30),XK(4,25
     16),DATA(2,2560),N(1),WORK(2,256)
      DO 999 III=1,5
      READ(5,101)XO,YO,ZO,LO,NB
  101 FORMAT(3E14.5,1X,I3,1X,I1)
      LONB=LO+NB
      DO 201 I=1,LONB
  201 READ(5,102)NS(I),DRL(I),DRM(I),DRN(I),DEL(I)
      NN=0
      DO 1 I=1,LO
      NN=NN+NS(I)
    1 CONTINUE
  102 FORMAT(I3,4E14.5)
      READ(5,103)XA,YA,ZA
  103 FORMAT(3E14.5)
      READ(5,104)VS,GS,VL,GL,VR,GR
  104 FORMAT(4E14.5/2E14.5)
      READ(5,105)TOS,TOL,TOR,IX
  105 FORMAT(3E14.5,I9)
      WRITE(6,107)
  107 FORMAT(5X,'XO',12X,'YO',12X,'ZO',9X,'LO',1X,'NB',4X,'XA',12X,'YA',
     112X,'ZA')
      WRITE(6,108)XO,YO,ZO,LO,NB,XA,YA,ZA
  108 FORMAT(3E14.5,1X,I3,1X,I1,3E14.5)
      WRITE(6,109)
  109 FORMAT(5X,'VS',12X,'GS',12X,'VL',12X,'GL',12X,'VR',12X,'GR')
      WRITE(6,110)VS,GS,VL,GL,VR,GR
  110 FORMAT(6E14.5)
      WRITE(6,111)
  111 FORMAT(5X,'TOS',12X,'TOL',12X,'TOR',12X,'IX')
      WRITE(6,105)TOS,TOL,TOR,IX
      WRITE(6,112)
  112 FORMAT('NS(I)',4X,'DRL(I)',8X,'DRM(I)',8X,'DRN(I)',8X,'DEL(I)')
  115 FORMAT(3X,I3,4E14.5)
      DO 204 I=1,LONB
  204 WRITE(6,115)NS(I),DRL(I),DRM(I),DRN(I),DEL(I)
      WRITE(6,113)
  113 FORMAT(1H1,6X,'G',13X,'T',9X,'J')
C
C
C     CALCULATION OF DIPOLE CENTERS
C
      I=1
      DO 10 L=1,LONB
      NK=NS(L)
      DO 10 M=1,NK
      IF (L.LE.LO) GO TO 2
      GO TO 6
    2 IF (M.EQ.1) GO TO 3
      GO TO 8
    3 IF (L.EQ.1) GO TO 4
      X=D(I-1,1)+(DEL(L-1)*DRL(L-1)+DEL(L)*DRL(L))/2.0
      Y=D(I-1,2)+(DEL(L-1)*DRM(L-1)+DEL(L)*DRM(L))/2.0
      Z=D(I-1,3)+(DEL(L-1)*DRN(L-1)+DEL(L)*DRN(L))/2.0
      GO TO 9
    4 X=XO+(DEL(1)*DRL(1))/2.0
      Y=YO+(DEL(1)*DRM(1))/2.0
```

TABLE I (Continued)

```
        Z=ZO+(DEL(1)*DRN(1))/2.0
        GO TO 9
    6 IF (M.EQ.1) GO TO 7
        GO TO 8
    7 X=D(NN,1)+(DEL(LO)*DRL(LO)+DEL(L)*DRL(L))/2.0
        Y=D(NN,2)+(DEL(LO)*DRM(LO)+DEL(L)*DRM(L))/2.0
        Z=D(NN,3)+(DEL(LO)*DRN(LO)+DEL(L)*DRN(L))/2.0
        GO TO 9
    8 X=D(I-1,1)+DEL(L)*DRL(L)
        Y=D(I-1,2)+DEL(L)*DRM(L)
        Z=D(I-1,3)+DEL(L)*DRN(L)
    9 CONTINUE
        D(I,1)=X
        D(I,2)=Y
        D(I,3)=Z
        I=I+1
   10 CONTINUE
C
C       CALCULATION OF R(DIPOLE) AND R(IMAGE)
C
        ND=0
        DO 11 I=1,LONB
        ND=ND+NS(I)
   11 CONTINUE
        DO 12 I=1,ND
        D(I,4)=SQRT((D(I,1)-XA)**2+(D(I,2)-YA)**2+(D(I,3)-ZA)**2)
        D(I,5)=SQRT((D(I,1)-XA)**2+(D(I,2)-YA)**2+(D(I,3)+ZA)**2)
   12 CONTINUE
C
C       STREAMER TON(S)
C
        IF (NB.EQ.0) GO TO 17
        IS=1
        IF (GS.EQ.0.0) IS=2
        I=NN+1
        LO1=LO+1
        DO 16 L=LO1,LONB
        NK=NS(L)
        T=TOS
        DO 16 M=1,NK
        GO TO (13,14),IS
   13 VO=VS*EXP(-GS*(T-TOS))
        DT=(1.0/GS)*ALOG(VO/(VO-GS*DEL(L)))
        GO TO 15
   14 DT=DEL(L)/VS
   15 T=T+DT
        D(I,6)=T
        I=I+1
   16 CONTINUE
C
C       STEPPED LEADER TON(S)
C
   17 CONTINUE
        IF (VL.EQ.0.0) GO TO 22
        IL=1
        IF (GL.EQ.0.0) IL=2
        I=NN
        T=TOL
        DO 21 L=1,LO
```

TABLE I (Continued)

```
      LL=(L0+1)-L
      NK=NS(LL)
      DO 21 M=1,NK
      GO TO (18,19),IL
   18 TAU=T-TOL
      VO=VL*EXP(-GL*TAU)
      DT=(1.0/GL)*ALOG(VO/(VO-GL*DEL(LL)))
      GO TO 20
   19 DT=DEL(LL)/VL
   20 D(I,6)=T+DT
      T=T+DT
      I=I-1
   21 CONTINUE
      NDSP=5
      DELA=0.0
      I=NN
      DO 30 KK=1,NN
      IJ=I/NDSP
      IJJ=(I-1)/NDSP
      DELAY=0.0
      IF (IJJ.LT.IJ) GO TO 28
      GO TO 29
   28 S=2.30000E-05
      AM=5.00000E-05
      CALL GAUSS(IX,S,AM,DELAY)
      IF (DELAY.LT.0.0) GO TO 28
      WRITE(6,888)DELAY
  888 FORMAT(E14.5)
   29 CONTINUE
      DELA=DELA+DELAY
      D(I,6)=D(I,6)+DELA
      I=I-1
   30 CONTINUE
C
C     RETURN STROKE TON(S)
C
   22 IF (VR.EQ.0.0) GO TO 27
      I=1
      T=TOR
      IR=1
      IF (GR.EQ.0.0) IR=2
      DO 26 L=1,LO
      NK=NS(L)
      DO 26 M=1,NK
      GO TO (23,24),IR
   23 VO=VR*EXP(-GR*(T-TOR))
      DT=(1.0/GR)*ALOG(VO/(VO-GR*DEL(L)))
      GO TO 25
   24 DT=DEL(L)/VR
   25 T=T+DT
      D(I,7)=T
      I=I+1
   26 CONTINUE
   27 CONTINUE
C
C     SET FO=(10-.5)KH FOR J=1,(50-.5)KH FOR J=2,(100-.5)KH FOR J=3,
C     (150-.5)KH FOR J=4,(200-.5)KH FOR J=5,(250-.5)KH FOR J=6.
C
      DO 99 J=1,6
```

TABLE I (Continued)

```
     GO TO (41,42,43,44,45,46),J
  41 FO=9.5E+03
     GO TO 47
  42 FO=4.95E+04
     GO TO 47
  43 FO=9.95E+04
     GO TO 47
  44 FO=1.495E+05
     GO TO 47
  45 FO=1.995E+05
     GO TO 47
  46 FO=2.495E+05
  47 CONTINUE
     NF=256
     DELF=1000.0/256.0
     DO 57 K=1,NF
     W=(2.0*3.14159265358979323846)*(FO+(K-1)*DELF)
C
C    CALCULATION OF FIELD COMPONENTS
C
     V=2.998E+08
     C1=(1.0)/((0.7958E+06)*(0.1129E+12))
     C2=(4.0)*(3.1416)*(8.854E-12)
     FX=0.0
     FY=0.0
     GHX=0.0
     GHY=0.0
     GVX=0.0
     GVY=0.0
     I=1
     DO 50 L=1,LONB
     NK=NS(L)
     DO 50 M=1,NK
     R=SQRT((D(I,1)-XA)**2+(D(I,2)-YA)**2+(ZA)**2)
     COSTH=ZA/R
     SINTH=SQRT(1.0-(COSTH)**2)
     COSPH=(XA-D(I,1))/(R*SINTH)
     SINPH=(YA-D(I,2))/(R*SINTH)
     DRLM=((DRL(L))*COSPH)+((DRM(L))*SINPH)
     RMH=R-(D(I,3)*COSTH)
     RPH=R+(D(I,3)*COSTH)
     RNMH=(R*DRN(L)*COSTH)-(D(I,3)*DRN(L))+(R*SINTH*DRLM)
     RNPH=(R*DRN(L)*COSTH)+(D(I,3)*DRN(L))-(R*SINTH*DRLM)
     A=DEL(L)/C2
     ER1X=A*((C1*(W**2)*(SINTH*DRLM+DRN(L)*COSTH)/D(I,4))+((-SINTH*DRLM
    1-DRN(L)*COSTH-((W/V)**2)*RMH*RNMH)/(D(I,4)**3))+((3.0*RMH*RNMH)/(D
    2(I,4)**5)))
     ETH1X=A*((C1*(W**2)*(COSTH*DRLM-DRN(L)*SINTH)/D(I,4))+((-COSTH*DRL
    1M+DRN(L)*SINTH-((W/V)**2)*D(I,3)*SINTH*RNMH)/(D(I,4)**3))+((3.0*D(
    2I,3)*SINTH*RNMH)/(D(I,4)**5)))
     EPH1X=A*(((-C1*(W**2)/D(I,4))+(1.0/(D(I,4)**3)))*(DRL(L)*SINPH-DRM
    1(L)*COSPH))
     ER1Y=A*(((W/V)*(-SINTH*DRLM-DRN(L)*COSTH)/(D(I,4)**2))+((W/V)*(3.0
    1*RMH*RNMH)/(D(I,4)**4)))
     ETH1Y=A*(((W/V)*(-COSTH*DRLM+DRN(L)*SINTH)/(D(I,4)**2))+((W/V)*(3.
    10*D(I,3)*SINTH*RNMH)/(D(I,4)**4)))
     EPH1Y=A*((W/V)*(DRL(L)*SINPH-DRM(L)*COSPH)/(D(I,4)**2))
     ER2X=A*((C1*(W**2)*(-SINTH*DRLM+DRN(L)*COSTH)/D(I,5))+((SINTH*DRLM
    1-DRN(L)*COSTH-((W/V)**2)*RPH*RNPH)/(D(I,5)**3))+((3.0*RPH*RNPH)/(D
```

TABLE I (Continued)

```
2(I,5)**5)))
 ETH2X=A*((C1*(W**2)*(-COSTH*DRLM-DRN(L)*SINTH)/D(I,5))+((COSTH*DRL
1M+DRN(L)*SINTH+((W/V)**2)*D(I,3)*SINTH*RNPH)/(D(I,5)**3))+((-3.0*D
2(I,3)*SINTH*RNPH)/(D(I,5)**5)))
 EPH2X=A*(((C1*(W**2)/D(I,5))-(1.0/(D(I,5)**3)))*(DRL(L)*SINPH-DRM(
1L)*COSPH))
 ER2Y=A*(((W/V)*(SINTH*DRLM-DRN(L)*COSTH)/(D(I,5)**2))+((W/V)*(3.0*
1RPH*RNPH)/(D(I,5)**4)))
 ETH2Y=A*(((W/V)*(COSTH*DRLM+DRN(L)*SINTH)/(D(I,5)**2))+((W/V)*(-3.
10*D(I,3)*SINTH*RNPH)/(D(I,5)**4)))
 EPH2Y=A*((W/V)*(-DRL(L)*SINPH+DRM(L)*COSPH)/(D(I,5)**2))
C
C    THE COMMON COORDINATE SYSTEM (XO,YO,ZO) IS
C
 XO=XO
 YO=YO
 ZO=0.0
 RO=SQRT((XO-XA)**2+(YO-YA)**2+(ZA)**2)
 COSTHO=(ZA)/(RO)
 SINTHO=SQRT(1.0-(COSTHO)**2)
 COSPHO=(XA-XO)/(RO*SINTHO)
 SINPHO=(YA-YO)/(RO*SINTHO)
C
C    TRANSFORMATION COEFFICIENTS
C
 TRR=(SINTH*COSPH)*SINTHO*COSPHO+(SINTH*SINPH)*SINTHO*SINPHO+(COSTH
1)*COSTHO
 TTR=(COSTH*COSPH)*SINTHO*COSPHO+(COSTH*SINPH)*SINTHO*SINPHO-(SINTH
1)*COSTHO
 TPR=-(SINPH)*SINTHO*COSPHO+(COSPH)*SINTHO*SINPHO
 TRT=(SINTH*COSPH)*COSTHO*COSPHO+(SINTH*SINPH)*COSTHO*SINPHO-(COSTH
1)*SINTHO
 TTT=(COSTH*COSPH)*COSTHO*COSPHO+(COSTH*SINPH)*COSTHO*SINPHO+(SINTH
1)*SINTHO
 TPT=-(SINPH)*COSTHO*COSPHO+(COSPH)*COSTHO*SINPHO
 TRP=-(SINTH*COSPH)*SINPHO+(SINTH*SINPH)*COSPHO
 TTP=-(COSTH*COSPH)*SINPHO+(COSTH*SINPH)*COSPHO
 TPP=(SINPH)*SINPHO+(COSPH)*COSPHO
C
C    TRANSFORMATION EQUATIONS
C
 ER1XT=(ER1X)*(TRR)+(ETH1X)*(TTR)+(EPH1X)*(TPR)
 ET1XT=(ER1X)*(TRT)+(ETH1X)*(TTT)+(EPH1X)*(TPT)
 EP1XT=(ER1X)*(TRP)+(ETH1X)*(TTP)+(EPH1X)*(TPP)
 ER1YT=(ER1Y)*(TRR)+(ETH1Y)*(TTR)+(EPH1Y)*(TPR)
 ET1YT=(ER1Y)*(TRT)+(ETH1Y)*(TTT)+(EPH1Y)*(TPT)
 EP1YT=(ER1Y)*(TRP)+(ETH1Y)*(TTP)+(EPH1Y)*(TPP)
 ER2XT=(ER2X)*(TRR)+(ETH2X)*(TTR)+(EPH2X)*(TPR)
 ET2XT=(ER2X)*(TRT)+(ETH2X)*(TTT)+(EPH2X)*(TPT)
 EP2XT=(ER2X)*(TRP)+(ETH2X)*(TTP)+(EPH2X)*(TPP)
 ER2YT=(ER2Y)*(TRR)+(ETH2Y)*(TTR)+(EPH2Y)*(TPR)
 ET2YT=(ER2Y)*(TRT)+(ETH2Y)*(TTT)+(EPH2Y)*(TPT)
 EP2YT=(ER2Y)*(TRP)+(ETH2Y)*(TTP)+(EPH2Y)*(TPP)
C
C    CALCULATION OF EH (REAL AND IMAG.) AND EV (REAL AND IMAG.)
C
 EH1X=EP1XT
 EH1Y=EP1YT
 EH2X=EP2XT
```

TABLE I (Continued)

```
      EH2Y=EP2YT
      EV1X=(ER1XT)*(COSTHO)-(ET1XT)*(SINTHO)
      EV1Y=(ER1YT)*(COSTHO)-(ET1YT)*(SINTHO)
      EV2X=(ER2XT)*(COSTHO)-(ET2XT)*(SINTHO)
      EV2Y=(ER2YT)*(COSTHO)-(ET2YT)*(SINTHO)
C
C     CALCULATION OF FOURIER COEF. FO INPUT TIME FUNCTIONS
C
      IF (L.LE.LO) GO TO 48
      FX=0.0
      FY=0.0
      GO TO 49
   48 CONTINUE
      AL=2.00000E+04
      BE=2.00000E+05
      GA=1.00000E+03
      CURO=3.00000E+04
      CUR1=0.0
      T1=D(I,7)
      AT1=-AL*T1
      BT1=-BE*T1
      GT1=-GA*T1
      WT1=W*T1
      ST1=SIN(WT1)
      CT1=COS(WT1)
      CW=(CURO*((1.0/BE)*EXP(BT1)-(1.0/AL)*EXP(AT1))/W)-CUR1*(1.0/GA)*EX
     1P(GT1)/W
      AW=(1.0/(AL**2+W**2))
      BW=(1.0/(BE**2+W**2))
      GW=(1.0/(GA**2+W**2))
      FAX=CURO*EXP(AT1)*AW
      FBX=-CURO*EXP(BT1)*BW
      FGX=CUR1*EXP(GT1)*GW
      FAY=-(W/AL)*EXP(AT1)*AW*CURO
      FBY=(W/BE)*EXP(BT1)*BW*CURO
      FGY=-(W/GA)*EXP(GT1)*GW*CUR1
      FABX=FAX+FBX+FGX
      FABY=-CW+FAY+FBY+FGY
      FX=FABX*CT1+FABY*ST1
      FY=-FABX*ST1+FABY*CT1
   49 CONTINUE
      F1X=FX*COS(W*D(I,4)/V)+FY*SIN(W*D(I,4)/V)
      F2X=FX*COS(W*D(I,5)/V)+FY*SIN(W*D(I,5)/V)
      F1Y=-FX*SIN(W*D(I,4)/V)+FY*COS(W*D(I,4)/V)
      F2Y=-FX*SIN(W*D(I,5)/V)+FY*COS(W*D(I,5)/V)
C
      GHX=GHX+(F1X*EH1X-F1Y*EH1Y)+(F2X*EH2X-F2Y*EH2Y)
      GHY=GHY+(F1X*EH1Y+F1Y*EH1X)+(F2X*EH2Y+F2Y*EH2X)
      GVX=GVX+(F1X*EV1X-F1Y*EV1Y)+(F2X*EV2X-F2Y*EV2Y)
      GVY=GVY+(F1X*EV1Y+F1Y*EV1X)+(F2X*EV2Y+F2Y*EV2X)
      I=I+1
   50 CONTINUE
C
C     SET MAGNITUDE AND PHASE OF BAND-PASS FILTER
C
      H1=1.0
      H1PH=0.0
C
C     CALCULATION OF FILTER OUTPUT
```

TABLE I (Continued)

```
C
      HX=H1*COS(H1PH)
      HY=H1*SIN(H1PH)
      XHX=GHX*HX-GHY*HY
      XHY=GHX*HY+GHY*HX
      XVX=GVX*HX-GVY*HY
      XVY=GVX*HY+GVY*HX
      XK(1,K)=XHX
      XK(2,K)=XHY
      XK(3,K)=XVX
      XK(4,K)=XVY
   57 CONTINUE
C
C
      DO 58 L=1,256
      DATA(1,L)=XK(1,L)
      DATA(2,L)=XK(2,L)
   58 CONTINUE
      DO 59 I=257,2560
      DATA(1,I)=0.0
      DATA(2,I)=0.0
   59 CONTINUE
      N(1)=2560
      CALL FOURT(DATA,N,1,+1,+1,WORK,256)
      DO 60 I=1,512
      T=(I-1)*(.0001)
      EH=SQRT((DATA(1,I)**2)+(DATA(2,I)**2))
      EH=EH/(3.1416*.128)
   60 WRITE(6,250)EH,T,J
  250 FORMAT(2E14.5,I3)
      DO 61 L=1,256
      DATA(1,L)=XK(3,L)
      DATA(2,L)=XK(4,L)
   61 CONTINUE
      DO 62 I=257,2560
      DATA(1,I)=0.0
      DATA(2,I)=0.0
   62 CONTINUE
      N(1)=2560
      CALL FOURT(DATA,N,1,+1,+1,WORK,256)
      DO 63 I=1,512
      T=(I-1)*(.0001)
      EV=SQRT((DATA(1,I)**2)+(DATA(2,I)**2))
      EV=EV/(3.1416*.128)
   63 WRITE(6,250)EV,T,J
   99 CONTINUE
  999 CONTINUE
      CALL EXIT
      END
      SUBROUTINE GAUSS(IX,S,AM,V)
      A=0.0
      DO 80 I=1,12
      CALL RANDU(IX,IY,Y)
      IX=IY
   80 A=A+Y
      V=(A-6.0)*S+AM
      RETURN
      END
      SUBROUTINE RANDU(IX,IY,YFL)
```

TABLE I (Continued)

```
      IY=IX*65539
      IF(IY)85,86,86
   85 IY=IY+2147483647+1
   86 YFL=IY
      YFL=YFL*.4656613E-9
      RETURN
      END
//GO.SYSIN DD *
//
```

TABLE II

$\vec{G}(\omega)$ PROGRAM WITH STEPPED LEADER AND RETURN STROKE

```
//OGM1    JOB  (10174,440-38-2220,010,10),'GUY MARNEY',MSGLEVEL=1,CLASS=A
// EXEC FORTGCLG,REGION.GO=80K
//FORT.SYSIN DD *
      DIMENSION D(1000,7),N(30),DRL(30),DRM(30),DRN(30),DEL(30)
      DO 999 III=1,12
      READ(5,101)XO,YO,ZO,LO,NB
  101 FORMAT(3E14.5,1X,I3,1X,I1)
      LONB=LO+NB
      DO 201 I=1,LONB
  201 READ(5,102)N(I),DRL(I),DRM(I),DRN(I),DEL(I)
      NN=0
      DO 1 I=1,LO
      NN=NN+N(I)
    1 CONTINUE
  102 FORMAT(I3,4E14.5)
      READ(5,103)XA,YA,ZA
  103 FORMAT(3E14.5)
      READ(5,104)VS,GS,VL,GL,VR,GR
  104 FORMAT(4E14.5/2E14.5)
      READ(5,105)TOS,TOL,TOR,IX
  105 FORMAT(3E14.5,I9)
      WRITE(6,107)
  107 FORMAT(5X,'XO',12X,'YO',12X,'ZO',9X,'LO',1X,'NB',4X,'XA',12X,'YA',
     112X,'ZA')
      WRITE(6,108)XO,YO,ZO,LO,NB,XA,YA,ZA
  108 FORMAT(3E14.5,1X,I3,1X,I1,3E14.5)
      WRITE(6,109)
  109 FORMAT(5X,'VS',12X,'GS',12X,'VL',12X,'GL',12X,'VR',12X,'GR')
      WRITE(6,110)VS,GS,VL,GL,VR,GR
  110 FORMAT(6E14.5)
      WRITE(6,111)
  111 FORMAT(5X,'TOS',12X,'TOL',12X,'TOR',12X,'IX')
      WRITE(6,105)TOS,TOL,TOR,IX
      WRITE(6,112)
  112 FORMAT(5X,'N(I)',4X,'DRL(I)',8X,'DRM(I)',8X,'DRN(I)',8X,'DEL(I)')
  115 FORMAT(3X,I3,4E14.5)
      DO 204 I=1,LONB
  204 WRITE(6,115)N(I),DRL(I),DRM(I),DRN(I),DEL(I)
      WRITE(6,113)
  113 FORMAT(1H1,5X,'GH',12X,'GHP',11X,'GV',12X,'GVP',16X,'F')
  114 FORMAT(5E14.5)
C
C     CALCULATION OF DIPOLE CENTERS
C
      I=1
      DO 10 L=1,LONB
      NK=N(L)
      DO 10 M=1,NK
      IF (L.LE.LO) GO TO 2
      GO TO 6
    2 IF (M.EQ.1) GO TO 3
      GO TO 8
    3 IF (L.EQ.1) GO TO 4
      X=D(I-1,1)+(DEL(L-1)*DRL(L-1)+DEL(L)*DRL(L))/2.0
      Y=D(I-1,2)+(DEL(L-1)*DRM(L-1)+DEL(L)*DRM(L))/2.0
      Z=D(I-1,3)+(DEL(L-1)*DRN(L-1)+DEL(L)*DRN(L))/2.0
      GO TO 9
    4 X=XO+(DEL(1)*DRL(1))/2.0
      Y=YO+(DEL(1)*DRM(1))/2.0
```

TABLE II (Continued)

```
      Z=ZO+(DEL(1)*DRN(1))/2.0
      GO TO 9
    6 IF (M.EQ.1) GO TO 7
      GO TO 8
    7 X=D(NN,1)+(DEL(LO)*DRL(LO)+DEL(L)*DRL(L))/2.0
      Y=D(NN,2)+(DEL(LO)*DRM(LO)+DEL(L)*DRM(L))/2.0
      Z=D(NN,3)+(DEL(LO)*DRN(LO)+DEL(L)*DRN(L))/2.0
      GO TO 9
    8 X=D(I-1,1)+DEL(L)*DRL(L)
      Y=D(I-1,2)+DEL(L)*DRM(L)
      Z=D(I-1,3)+DEL(L)*DRN(L)
    9 CONTINUE
      D(I,1)=X
      D(I,2)=Y
      D(I,3)=Z
      I=I+1
   10 CONTINUE
C
C
C     CALCULATION OF R(DIPOLE) AND R(IMAGE)
C
      ND=0
      DO 11 I=1,LONB
      ND=ND+N(I)
   11 CONTINUE
      DO 12 I=1,ND
      D(I,4)=SQRT((D(I,1)-XA)**2+(D(I,2)-YA)**2+(D(I,3)-ZA)**2)
      D(I,5)=SQRT((D(I,1)-XA)**2+(D(I,2)-YA)**2+(D(I,3)+ZA)**2)
   12 CONTINUE
C
C
C
C     STREAMER TON(S)
C
      IF (NB.EQ.0) GO TO 17
      IS=1
      IF (GS.EQ.0.0) IS=2
      I=NN+1
      LO1=LO+1
      DO 16 L=LO1,LONB
      NK=N(L)
      T=TOS
      DO 16 M=1,NK
      GO TO (13,14),IS
   13 VO=VS*EXP(-GS*(T-TOS))
      DT=(1.0/GS)*ALOG(VO/(VO-GS*DEL(L)))
      GO TO 15
   14 DT=DEL(L)/VS
   15 T=T+DT
      D(I,6)=T
      I=I+1
   16 CONTINUE
C
C     STEPPED LEADER TON(S)
C
   17 CONTINUE
      IF (VL.EQ.0.0) GO TO 22
      IL=1
      IF (GL.EQ.0.0) IL=2
      I=NN
      T=TOL
```

TABLE II (Continued)

```
            DO 21 L=1,LO
            LL=(LO+1)-L
            NK=N(LL)
            DO 21 M=1,NK
            GO TO (18,19),IL
        18  TAU=T-TOL
            VO=VL*EXP(-GL*TAU)
            DT=(1.0/GL)*ALOG(VO/(VO-GL*DEL(LL)))
            GO TO 20
        19  DT=DEL(LL)/VL
        20  D(I,6)=T+DT
            T=T+DT
            I=I-1
        21  CONTINUE
            NDSP=5
            DELA=0.0
            I=NN
            DO 30 KK=1,NN
            IJ=I/NDSP
            IJJ=(I-1)/NDSP
            DELAY=0.0
            IF (IJJ.LT.IJ) GO TO 28
            GO TO 29
        28  S=2.30000E-05
            AM=5.00000E-05
            CALL GAUSS(IX,S,AM,DELAY)
            IF (DELAY.LT.0.0) GO TO 28
            WRITE(6,888)DELAY
       888  FORMAT(E14.5)
        29  CONTINUE
            DELA=DELA+DELAY
            D(I,6)=D(I,6)+DELA
            I=I-1
        30  CONTINUE
    C
    C       RETURN STROKE TON(S)
    C
        22  IF (VR.EQ.0.0) GO TO 27
            I=1
            T=TOR
            IR=1
            IF (GR.EQ.0.0) IR=2
            DO 26 L=1,LO
            NK=N(L)
            DO 26 M=1,NK
            GO TO (23,24),IR
        23  VO=VR*EXP(-GR*(T-TOR))
            DT=(1.0/GR)*ALOG(VO/(VO-GR*DEL(L)))
            GO TO 25
        24  DT=DEL(L)/VR
        25  T=T+DT
            D(I,7)=T
            I=I+1
        26  CONTINUE
        27  CONTINUE
    C
    C       SET FREQUENCY FOR FIELD CALCULATIONS, W=ANGULAR FREQUENCY
    C
            DO 66 J=1,43
```

TABLE II (Continued)

```
      IF (J.GT.10) GO TO 70
      W=(6283.2)*(J)
      GO TO 72
   70 IF (J.GT.28) GO TO 71
      W=(6283.2)*(5*J-40)
      GO TO 72
   71 W=(6283.2)*(10*J-180)
   72 CONTINUE
      F=W/(6.2832)
C
C     CALCULATION OF FIELD COMPONENTS
C
      V=2.998E+08
      C1=(1.0)/((0.7958E+06)*(0.1129E+12))
      C2=(4.0)*(3.1416)*(8.854E-12)
      FX=0.0
      FY=0.0
      GHX=0.0
      GHY=0.0
      GVX=0.0
      GVY=0.0
      I=1
      DO 50 L=1,LONB
      NK=N(L)
      DO 50 M=1,NK
      R=SQRT((D(I,1)-XA)**2+(D(I,2)-YA)**2+(ZA)**2)
      COSTH=ZA/R
      SINTH=SQRT(1.0-(COSTH)**2)
      COSPH=(XA-D(I,1))/(R*SINTH)
      SINPH=(YA-D(I,2))/(R*SINTH)
      DRLM=((DRL(L))*COSPH)+((DRM(L))*SINPH)
      RMH=R-(D(I,3)*COSTH)
      RPH=R+(D(I,3)*COSTH)
      RNMH=(R*DRN(L)*COSTH)-(D(I,3)*DRN(L))+(R*SINTH*DRLM)
      RNPH=(R*DRN(L)*COSTH)+(D(I,3)*DRN(L))-(R*SINTH*DRLM)
      A=DEL(L)/C2
      ER1X=A*((C1*(W**2)*(SINTH*DRLM+DRN(L)*COSTH)/D(I,4))+((-SINTH*DRLM
     1-DRN(L)*COSTH-((W/V)**2)*RMH*RNMH)/(D(I,4)**3))+((3.0*RMH*RNMH)/(D
     2(I,4)**5)))
      ETH1X=A*((C1*(W**2)*(COSTH*DRLM-DRN(L)*SINTH)/D(I,4))+((-COSTH*DRL
     1M+DRN(L)*SINTH-((W/V)**2)*D(I,3)*SINTH*RNMH)/(D(I,4)**3))+((3.0*D(
     2I,3)*SINTH*RNMH)/(D(I,4)**5)))
      EPH1X=A*(((-C1*(W**2)/D(I,4))+(1.0/(D(I,4)**3)))*(DRL(L)*SINPH-DRM
     1(L)*COSPH))
      ER1Y=A*(((W/V)*(-SINTH*DRLM-DRN(L)*COSTH)/(D(I,4)**2))+((W/V)*(3.0
     1*RMH*RNMH)/(D(I,4)**4)))
      ETH1Y=A*(((W/V)*(-COSTH*DRLM+DRN(L)*SINTH)/(D(I,4)**2))+((W/V)*(3.
     10*D(I,3)*SINTH*RNMH)/(D(I,4)**4)))
      EPH1Y=A*((W/V)*(DRL(L)*SINPH-DRM(L)*COSPH)/(D(I,4)**2))
      ER2X=A*((C1*(W**2)*(-SINTH*DRLM+DRN(L)*COSTH)/D(I,5))+((SINTH*DRLM
     1-DRN(L)*COSTH-((W/V)**2)*RPH*RNPH)/(D(I,5)**3))+((3.0*RPH*RNPH)/(D
     2(I,5)**5)))
      ETH2X=A*((C1*(W**2)*(-COSTH*DRLM-DRN(L)*SINTH)/D(I,5))+((COSTH*DRL
     1M+DRN(L)*SINTH+((W/V)**2)*D(I,3)*SINTH*RNPH)/(D(I,5)**3))+((-3.0*D
     2(I,3)*SINTH*RNPH)/(D(I,5)**5)))
      EPH2X=A*(((C1*(W**2)/D(I,5))-(1.0/(D(I,5)**3)))*(DRL(L)*SINPH-DRM(
     1L)*COSPH))
      ER2Y=A*(((W/V)*(SINTH*DRLM-DRN(L)*COSTH)/(D(I,5)**2))+((W/V)*(3.0*
     1RPH*RNPH)/(D(I,5)**4)))
```

TABLE II (Continued)

```
      ETH2Y=A*(((W/V)*(COSTH*DRLM+DRN(L)*SINTH)/(D(I,5)**2))+((W/V)*(-3.
     10*D(I,3)*SINTH*RNPH)/(D(I,5)**4)))
      EPH2Y=A*((W/V)*(-DRL(L)*SINPH+DRM(L)*COSPH)/(D(I,5)**2))
C
C     THE COMMON COORDINATE SYSTEM (XO,YO,ZO) IS
C
      XO=XO
      YO=YO
      ZO=0.0
      RO=SQRT((XO-XA)**2+(YO-YA)**2+(ZA)**2)
      COSTHO=(ZA)/(RO)
      SINTHO=SQRT(1.0-(COSTHO)**2)
      COSPHO=(XA-XO)/(RO*SINTHO)
      SINPHO=(YA-YO)/(RO*SINTHO)
C
C     TRANSFORMATION COEFFICIENTS
C
      TRR=(SINTH*COSPH)*SINTHO*COSPHO+(SINTH*SINPH)*SINTHO*SINPHO+(COSTH
     1)*COSTHO
      TTR=(COSTH*COSPH)*SINTHO*COSPHO+(COSTH*SINPH)*SINTHO*SINPHO-(SINTH
     1)*COSTHO
      TPR=-(SINPH)*SINTHO*COSPHO+(COSPH)*SINTHO*SINPHO
      TRT=(SINTH*COSPH)*COSTHO*COSPHO+(SINTH*SINPH)*COSTHO*SINPHO-(COSTH
     1)*SINTHO
      TTT=(COSTH*COSPH)*COSTHO*COSPHO+(COSTH*SINPH)*COSTHO*SINPHO+(SINTH
     1)*SINTHO
      TPT=-(SINPH)*COSTHO*COSPHO+(COSPH)*COSTHO*SINPHO
      TRP=-(SINTH*COSPH)*SINPHO+(SINTH*SINPH)*COSPHO
      TTP=-(COSTH*COSPH)*SINPHO+(COSTH*SINPH)*COSPHO
      TPP=(SINPH)*SINPHO+(COSPH)*COSPHO
C
C     TRANSFORMATION EQUATIONS
C
      ER1XT=(ER1X)*(TRR)+(ETH1X)*(TTR)+(EPH1X)*(TPR)
      ET1XT=(ER1X)*(TRT)+(ETH1X)*(TTT)+(EPH1X)*(TPT)
      EP1XT=(ER1X)*(TRP)+(ETH1X)*(TTP)+(EPH1X)*(TPP)
      ER1YT=(ER1Y)*(TRR)+(ETH1Y)*(TTR)+(EPH1Y)*(TPR)
      ET1YT=(ER1Y)*(TRT)+(ETH1Y)*(TTT)+(EPH1Y)*(TPT)
      EP1YT=(ER1Y)*(TRP)+(ETH1Y)*(TTP)+(EPH1Y)*(TPP)
      ER2XT=(ER2X)*(TRR)+(ETH2X)*(TTR)+(EPH2X)*(TPR)
      ET2XT=(ER2X)*(TRT)+(ETH2X)*(TTT)+(EPH2X)*(TPT)
      EP2XT=(ER2X)*(TRP)+(ETH2X)*(TTP)+(EPH2X)*(TPP)
      ER2YT=(ER2Y)*(TRR)+(ETH2Y)*(TTR)+(EPH2Y)*(TPR)
      ET2YT=(ER2Y)*(TRT)+(ETH2Y)*(TTT)+(EPH2Y)*(TPT)
      EP2YT=(ER2Y)*(TRP)+(ETH2Y)*(TTP)+(EPH2Y)*(TPP)
C
C     CALCULATION OF EH (REAL AND IMAG.) AND EV (REAL AND IMAG.)
C
      EH1X=EP1XT
      EH1Y=EP1YT
      EH2X=EP2XT
      EH2Y=EP2YT
      EV1X=(ER1XT)*(COSTHO)-(ET1XT)*(SINTHO)
      EV1Y=(ER1YT)*(COSTHO)-(ET1YT)*(SINTHO)
      EV2X=(ER2XT)*(COSTHO)-(ET2XT)*(SINTHO)
      EV2Y=(ER2YT)*(COSTHO)-(ET2YT)*(SINTHO)
C
C     CALCULATION OF FOURIER COEF. FOR INPUT TIME FUNCTIONS
C
```

TABLE II (Continued)

```
      IF (L.LE.LO) GO TO 48
      FX=0.0
      FY=0.0
      GO TO 49
   48 CONTINUE
      AL=2.00000E+04
      BE=2.00000E+05
      GA=1.00000E+03
      CURO=3.00000E+04
      CUR1=0.0
      T1=D(I,7)
      AT1=-AL*T1
      BT1=-BE*T1
      GT1=-GA*T1
      WT1=W*T1
      ST1=SIN(WT1)
      CT1=COS(WT1)
      CW=(CURO*((1.0/BE)*EXP(BT1)-(1.0/AL)*EXP(AT1))/W)-CUR1*(1.0/GA)*EX
     1P(GT1)/W
      AW=(1.0/(AL**2+W**2))
      BW=(1.0/(BE**2+W**2))
      GW=(1.0/(GA**2+W**2))
      FAX=CURO*EXP(AT1)*AW
      FBX=-CURO*EXP(BT1)*BW
      FGX=CUR1*EXP(GT1)*GW
      FAY=-(W/AL)*EXP(AT1)*AW*CURO
      FBY=(W/BE)*EXP(BT1)*BW*CURO
      FGY=-(W/GA)*EXP(GT1)*GW*CUR1
      FABX=FAX+FBX+FGX
      FABY=-CW+FAY+FBY+FGY
      FX=FABX*CT1+FABY*ST1
      FY=-FABX*ST1+FABY*CT1
   49 CONTINUE
      F1X=FX*COS(W*D(I,4)/V)+FY*SIN(W*D(I,4)/V)
      F2X=FX*COS(W*D(I,5)/V)+FY*SIN(W*D(I,5)/V)
      F1Y=-FX*SIN(W*D(I,4)/V)+FY*COS(W*D(I,4)/V)
      F2Y=-FX*SIN(W*D(I,5)/V)+FY*COS(W*D(I,5)/V)
C
      GHX=GHX+(F1X*EH1X-F1Y*EH1Y)+(F2X*EH2X-F2Y*EH2Y)
      GHY=GHY+(F1X*EH1Y+F1Y*EH1X)+(F2X*EH2Y+F2Y*EH2X)
      GVX=GVX+(F1X*EV1X-F1Y*EV1Y)+(F2X*EV2X-F2Y*EV2Y)
      GVY=GVY+(F1X*EV1Y+F1Y*EV1X)+(F2X*EV2Y+F2Y*EV2X)
      I=I+1
   50 CONTINUE
      GH=SQRT((GHX**2)+(GHY**2))
      GV=SQRT((GVX**2)+(GVY**2))
      IF (GHX) 52,51,52
   51 GHPH=1.5708
      GO TO 53
   52 GHPH=ATAN(GHY/GHX)
   53 CONTINUE
      IF (GVX) 55,54,55
   54 GVPH=1.5708
      GO TO 56
   55 GVPH=ATAN(GVY/GVX)
   56 CONTINUE
      C3=180.0/3.1416
      GHP=(C3)*(GHPH)
      GVP=(C3)*(GVPH)
```

TABLE II (Continued)

```
  66 WRITE(6,114)GH,GHP,GV,GVP,F
 999 CONTINUE
     CALL EXIT
     END
     SUBROUTINE GAUSS(IX,S,AM,V)
     A=0.0
     DO 80 I=1,12
     CALL RANDU(IX,IY,Y)
     IX=IY
  80 A=A+Y
     V=(A-6.0)*S+AM
     RETURN
     END
     SUBROUTINE RANDU(IX,IY,YFL)
     IY=IX*65539
     IF(IY)85,86,86
  85 IY=IY+2147483647+1
  86 YFL=IY
     YFL=YFL*.4656613E-9
     RETURN
     END
//GO.SYSIN DD *
//
```

APPENDIX C

z(t) PROGRAM WITH RETURN STROKE

The program used to calculate the narrow-band, half-wave linear detected field is listed in Table III. The cards between the comment card CALCULATION OF FOURIER COEF. FOR INPUT TIME FUNCTIONS and 50 CONTINUE are the cards required to compute the Fourier transform of the return stroke current indicated by Equation 4.2.7.

TABLE III

z(t) PROGRAM WITH RETURN STROKE

```
//OGM3    JOB (10174,440-38-2220,020,10),'GUY MARNEY',MSGLEVEL=1,CLASS=A
// EXEC FORTGCLG,REGION.GO=80K
//FORT.SYSIN DD *
      DIMENSION D(1000,7),N(30),DRL(30),DRM(30),DRN(30),DEL(30),DD(43,2)
      DO 600 KJ=1,43
      DD(KJ,1)=0.0
      DD(KJ,2)=0.0
  600 CONTINUE
      DO 999 III=1,12
      READ(5,101)XO,YO,ZO,LO,NB
  101 FORMAT(3E14.5,1X,I3,1X,I1)
      LONB=LO+NB
      DO 201 I=1,LONB
  201 READ(5,102)N(I),DRL(I),DRM(I),DRN(I),DEL(I)
      NN=0
      DO 1 I=1,LO
      NN=NN+N(I)
    1 CONTINUE
  102 FORMAT(I3,4E14.5)
      READ(5,103)XA,YA,ZA
  103 FORMAT(3E14.5)
      READ(5,104)VS,GS,VL,GL,VR,GR
  104 FORMAT(4E14.5/2E14.5)
      READ(5,105)TOS,TOL,TOR,IX
  105 FORMAT(3E14.5,I9)
      WRITE(6,107)
  107 FORMAT(5X,'XO',12X,'YO',12X,'ZO',9X,'LO',1X,'NB',4X,'XA',12X,'YA',
     112X,'ZA')
      WRITE(6,108)XO,YO,ZO,LO,NB,XA,YA,ZA
  108 FORMAT(3E14.5,1X,I3,1X,I1,3E14.5)
      WRITE(6,109)
  109 FORMAT(5X,'VS',12X,'GS',12X,'VL',12X,'GL',12X,'VR',12X,'GR')
      WRITE(6,110)VS,GS,VL,GL,VR,GR
  110 FORMAT(6E14.5)
      WRITE(6,111)
  111 FORMAT(5X,'TOS',12X,'TOL',12X,'TOR',12X,'IX')
      WRITE(6,105)TOS,TOL,TOR,IX
      WRITE(6,112)
  112 FORMAT(5X,'N(I)',4X,'DRL(I)',8X,'DRM(I)',8X,'DRN(I)',8X,'DEL(I)')
  115 FORMAT(3X,I3,4E14.5)
      DO 204 I=1,LONB
  204 WRITE(6,115)N(I),DRL(I),DRM(I),DRN(I),DEL(I)
      WRITE(6,113)
  113 FORMAT(1H1,5X,'GH',12X,'GHP',11X,'GV',12X,'GVP',16X,'F')
  114 FORMAT(5E14.5)
C
C     CALCULATION OF DIPOLE CENTERS
C
      I=1
      DO 10 L=1,LONB
      NK=N(L)
      DO 10 M=1,NK
      IF (L.LE.LO) GO TO 2
      GO TO 6
    2 IF (M.EQ.1) GO TO 3
      GO TO 8
    3 IF (L.EQ.1) GO TO 4
      X=D(I-1,1)+(DEL(L-1)*DRL(L-1)+DEL(L)*DRL(L))/2.0
      Y=D(I-1,2)+(DEL(L-1)*DRM(L-1)+DEL(L)*DRM(L))/2.0
```

TABLE III (Continued)

```
      Z=D(I-1,3)+(DEL(L-1)*DRN(L-1)+DEL(L)*DRN(L))/2.0
      GO TO 9
    4 X=X0+(DEL(1)*DRL(1))/2.0
      Y=Y0+(DEL(1)*DRM(1))/2.0
      Z=Z0+(DEL(1)*DRN(1))/2.0
      GO TO 9
    6 IF (M.EQ.1) GO TO 7
      GO TO 8
    7 X=D(NN,1)+(DEL(LO)*DRL(LO)+DEL(L)*DRL(L))/2.0
      Y=D(NN,2)+(DEL(LO)*DRM(LO)+DEL(L)*DRM(L))/2.0
      Z=D(NN,3)+(DEL(LO)*DRN(LO)+DEL(L)*DRN(L))/2.0
      GO TO 9
    8 X=D(I-1,1)+DEL(L)*DRL(L)
      Y=D(I-1,2)+DEL(L)*DRM(L)
      Z=D(I-1,3)+DEL(L)*DRN(L)
    9 CONTINUE
      D(I,1)=X
      D(I,2)=Y
      D(I,3)=Z
      I=I+1
   10 CONTINUE
C
C     CALCULATION OF R(DIPOLE) AND R(IMAGE)
C
      ND=0
      DO 11 I=1,LONB
      ND=ND+N(I)
   11 CONTINUE
      DO 12 I=1,ND
      D(I,4)=SQRT((D(I,1)-XA)**2+(D(I,2)-YA)**2+(D(I,3)-ZA)**2)
      D(I,5)=SQRT((D(I,1)-XA)**2+(D(I,2)-YA)**2+(D(I,3)+ZA)**2)
   12 CONTINUE
C
C
C     STREAMER TON(S)
C
      IF (NB.EQ.0) GO TO 17
      IS=1
      IF (GS.EQ.0.0) IS=2
      I=NN+1
      LO1=LO+1
      DO 16 L=LO1,LONB
      NK=N(L)
      T=TOS
      DO 16 M=1,NK
      GO TO (13,14),IS
   13 VO=VS*EXP(-GS*(T-TOS))
      DT=(1.0/GS)*ALOG(VO/(VO-GS*DEL(L)))
      GO TO 15
   14 DT=DEL(L)/VS
   15 T=T+DT
      D(I,6)=T
      I=I+1
   16 CONTINUE
C
C     STEPPED LEADER TON(S)
C
   17 CONTINUE
      DO 31 I=1,NN
```

TABLE III (Continued)

```
      D(I,6)=0.0
31 CONTINUE
      GO TO 32
      IF (VL.EQ.0.0) GO TO 22
      IL=1
      IF (GL.EQ.0.0) IL=2
      I=NN
      T=TOL
      DO 21 L=1,LO
      LL=(LO+1)-L
      NK=N(LL)
      DO 21 M=1,NK
      GO TO (18,19),IL
18 TAU=T-TOL
      VO=VL*EXP(-GL*TAU)
      DT=(1.0/GL)*ALOG(VO/(VO-GL*DEL(LL)))
      GO TO 20
19 DT=DEL(LL)/VL
20 D(I,6)=T+DT
      T=T+DT
      I=I-1
21 CONTINUE
32 CONTINUE
      NDSP=5
      DELA=0.0
      I=NN
      DO 30 KK=1,NN
      IJ=I/NDSP
      IJJ=(I-1)/NDSP
      DELAY=0.0
      IF (IJJ.LT.IJ) GO TO 28
      GO TO 29
28 S=2.30000E-05
      AM=5.00000E-05
      CALL GAUSS(IX,S,AM,DELAY)
      IF (DELAY.LT.0.0) GO TO 28
      WRITE(6,888)DELAY
888 FORMAT(E14.5)
29 CONTINUE
      DELA=DELA+DELAY
      D(I,6)=D(I,6)+DELA
      I=I-1
30 CONTINUE
C
C     RETURN STROKE TON(S)
C
22 IF (VR.EQ.0.0) GO TO 27
      I=1
      TOR=D(1,6)
      T=TOR
      IR=1
      IF (GR.EQ.0.0) IR=2
      DO 26 L=1,LO
      NK=N(L)
      DO 26 M=1,NK
      GO TO (23,24),IR
23 VO=VR*EXP(-GR*(T-TOR))
      DT=(1.0/GR)*ALOG(VO/(VO-GR*DEL(L)))
      GO TO 25
```

TABLE III (Continued)

```
   24 DT=DEL(L)/VR
   25 T=T+DT
      D(I,7)=T
      I=I+1
   26 CONTINUE
   27 CONTINUE
C
C     SET FREQUENCY FOR FIELD CALCULATIONS, W=ANGULAR FREQUENCY
C
      DO 66 J=1,43
      IF (J.GT.10) GO TO 70
      W=(6283.2)*(J)
      GO TO 72
   70 IF (J.GT.28) GO TO 71
      W=(6283.2)*(5*J-40)
      GO TO 72
   71 W=(6283.2)*(10*J-180)
   72 CONTINUE
      F=W/(6.2832)
C
C     CALCULATION OF FIELD COMPONENTS
C
      V=2.998E+08
      C1=(1.0)/((0.7958E+06)*(0.1129E+12))
      C2=(4.0)*(3.1416)*(8.854E-12)
      FX=0.0
      FY=0.0
      GHX=0.0
      GHY=0.0
      GVX=0.0
      GVY=0.0
      I=1
      DO 50 L=1,LONB
      NK=N(L)
      DO 50 M=1,NK
      R=SQRT((D(I,1)-XA)**2+(D(I,2)-YA)**2+(ZA)**2)
      COSTH=ZA/R
      SINTH=SQRT(1.0-(COSTH)**2)
      COSPH=(XA-D(I,1))/(R*SINTH)
      SINPH=(YA-D(I,2))/(R*SINTH)
      DRLM=((DRL(L))*COSPH)+((DRM(L))*SINPH)
      RMH=R-(D(I,3)*COSTH)
      RPH=R+(D(I,3)*COSTH)
      RNMH=(R*DRN(L)*COSTH)-(D(I,3)*DRN(L))+(R*SINTH*DRLM)
      RNPH=(R*DRN(L)*COSTH)+(D(I,3)*DRN(L))-(R*SINTH*DRLM)
      A=DEL(L)/C2
      ER1X=A*((C1*(W**2)*(SINTH*DRLM+DRN(L)*COSTH)/D(I,4))+((-SINTH*DRLM
     1-DRN(L)*COSTH-((W/V)**2)*RMH*RNMH)/(D(I,4)**3))+((3.0*RMH*RNMH)/(D
     2(I,4)**5)))
      ETH1X=A*((C1*(W**2)*(COSTH*DRLM-DRN(L)*SINTH)/D(I,4))+((-COSTH*DRL
     1M+DRN(L)*SINTH-((W/V)**2)*D(I,3)*SINTH*RNMH)/(D(I,4)**3))+((3.0*D(
     2I,3)*SINTH*RNMH)/(D(I,4)**5)))
      EPH1X=A*(((-C1*(W**2)/D(I,4))+(1.0/(D(I,4)**3)))*(DRL(L)*SINPH-DRM
     1(L)*COSPH))
      ER1Y=A*(((W/V)*(-SINTH*DRLM-DRN(L)*COSTH)/(D(I,4)**2))+((W/V)*(3.0
     1*RMH*RNMH)/(D(I,4)**4)))
      ETH1Y=A*(((W/V)*(-COSTH*DRLM+DRN(L)*SINTH)/(D(I,4)**2))+((W/V)*(3.
     10*D(I,3)*SINTH*RNMH)/(D(I,4)**4)))
      EPH1Y=A*((W/V)*(DRL(L)*SINPH-DRM(L)*COSPH)/(D(I,4)**2))
```

TABLE III (Continued)

```
      ER2X=A*((C1*(W**2)*(-SINTH*DRLM+DRN(L)*COSTH)/D(I,5))+((SINTH*DRLM
     1-DRN(L)*COSTH-((W/V)**2)*RPH*RNPH)/(D(I,5)**3))+((3.0*RPH*RNPH)/(D
     2(I,5)**5)))
      ETH2X=A*((C1*(W**2)*(-COSTH*DRLM-DRN(L)*SINTH)/D(I,5))+((COSTH*DRL
     1M+DRN(L)*SINTH+((W/V)**2)*D(I,3)*SINTH*RNPH)/(D(I,5)**3))+((-3.0*D
     2(I,3)*SINTH*RNPH)/(D(I,5)**5)))
      EPH2X=A*(((C1*(W**2)/D(I,5))-(1.0/(D(I,5)**3)))*(DRL(L)*SINPH-DRM(
     1L)*COSPH))
      ER2Y=A*(((W/V)*(SINTH*DRLM-DRN(L)*COSTH)/(D(I,5)**2))+((W/V)*(3.0*
     1RPH*RNPH)/(D(I,5)**4)))
      ETH2Y=A*(((W/V)*(COSTH*DRLM+DRN(L)*SINTH)/(D(I,5)**2))+((W/V)*(-3.
     10*D(I,3)*SINTH*RNPH)/(D(I,5)**4)))
      EPH2Y=A*((W/V)*(-DRL(L)*SINPH+DRM(L)*COSPH)/(D(I,5)**2))
C
C
C     THE COMMON COORDINATE SYSTEM (XO,YO,ZO) IS
C
      XO=XO
      YO=YO
      ZO=0.0
      RO=SQRT((XO-XA)**2+(YO-YA)**2+(ZA)**2)
      COSTHO=(ZA)/(RO)
      SINTHO=SQRT(1.0-(COSTHO)**2)
      COSPHO=(XA-XO)/(RO*SINTHO)
      SINPHO=(YA-YO)/(RO*SINTHO)
C
C
C     TRANSFORMATION COEFFICIENTS
C
      TRR=(SINTH*COSPH)*SINTHO*COSPHO+(SINTH*SINPH)*SINTHO*SINPHO+(COSTH
     1)*COSTHO
      TTR=(COSTH*COSPH)*SINTHO*COSPHO+(COSTH*SINPH)*SINTHO*SINPHO-(SINTH
     1)*COSTHO
      TPR=-(SINPH)*SINTHO*COSPHO+(COSPH)*SINTHO*SINPHO
      TRT=(SINTH*COSPH)*COSTHO*COSPHO+(SINTH*SINPH)*COSTHO*SINPHO-(COSTH
     1)*SINTHO
      TTT=(COSTH*COSPH)*COSTHO*COSPHO+(COSTH*SINPH)*COSTHO*SINPHO+(SINTH
     1)*SINTHO
      TPT=-(SINPH)*COSTHO*COSPHO+(COSPH)*COSTHO*SINPHO
      TRP=-(SINTH*COSPH)*SINPHO+(SINTH*SINPH)*COSPHO
      TTP=-(COSTH*COSPH)*SINPHO+(COSTH*SINPH)*COSPHO
      TPP=(SINPH)*SINPHO+(COSPH)*COSPHO
C
C
C     TRANSFORMATION EQUATIONS
C
      ER1XT=(ER1X)*(TRR)+(ETH1X)*(TTR)+(EPH1X)*(TPR)
      ET1XT=(ER1X)*(TRT)+(ETH1X)*(TTT)+(EPH1X)*(TPT)
      EP1XT=(ER1X)*(TRP)+(ETH1X)*(TTP)+(EPH1X)*(TPP)
      ER1YT=(ER1Y)*(TRR)+(ETH1Y)*(TTR)+(EPH1Y)*(TPR)
      ET1YT=(ER1Y)*(TRT)+(ETH1Y)*(TTT)+(EPH1Y)*(TPT)
      EP1YT=(ER1Y)*(TRP)+(ETH1Y)*(TTP)+(EPH1Y)*(TPP)
      ER2XT=(ER2X)*(TRR)+(ETH2X)*(TTR)+(EPH2X)*(TPR)
      ET2XT=(ER2X)*(TRT)+(ETH2X)*(TTT)+(EPH2X)*(TPT)
      EP2XT=(ER2X)*(TRP)+(ETH2X)*(TTP)+(EPH2X)*(TPP)
      ER2YT=(ER2Y)*(TRR)+(ETH2Y)*(TTR)+(EPH2Y)*(TPR)
      ET2YT=(ER2Y)*(TRT)+(ETH2Y)*(TTT)+(EPH2Y)*(TPT)
      EP2YT=(ER2Y)*(TRP)+(ETH2Y)*(TTP)+(EPH2Y)*(TPP)
C
C
C     CALCULATION OF EH (REAL AND IMAG.) AND EV (REAL AND IMAG.)
C
      EH1X=EP1XT
```

TABLE III (Continued)

```
      EH1Y=EP1YT
      EH2X=EP2XT
      EH2Y=EP2YT
      EV1X=(ER1XT)*(COSTHO)-(ET1XT)*(SINTHO)
      EV1Y=(ER1YT)*(COSTHO)-(ET1YT)*(SINTHO)
      EV2X=(ER2XT)*(COSTHO)-(ET2XT)*(SINTHO)
      EV2Y=(ER2YT)*(COSTHO)-(ET2YT)*(SINTHO)
C
C     CALCULATION OF FOURIER COEF. FOR INPUT TIME FUNCTIONS
C
      IF (L.LE.LO) GO TO 48
      FX=0.0
      FY=0.0
      GO TO 49
   48 CONTINUE
      IJ=(I+(NDSP-1))/NDSP
      IJJ=(I+(NDSP-2))/NDSP
      AL=2.00000E+04
      BE=2.00000E+05
      CURO=2.00000E+03
      AW=1.0/(AL**2+W**2)
      BW=1.0/(BE**2+W**2)
      F1=CURO*(BW-AW)
      F2=CURO*(BE*BW-AL*AW)/W
      UX=0.0
      UY=0.0
      IF (IJJ.LT.IJ) GO TO 92
      GO TO 93
   92 CONTINUE
      NWD=IJ*NDSP
      IF (NWD.GT.NN) NWD=NN
      WD=W*D(NWD,6)
      SWD=SIN(WD)
      CWD=COS(WD)
      UX=F1*CWD+F2*SWD
      UY=F2*CWD-F1*SWD
   93 CONTINUE
      FX=FX+UX
      FY=FY+UY
   49 CONTINUE
      AL=2.00000E+04
      BE=2.00000E+05
      GA=1.00000E+03
      CURO=3.00000E+04
      CUR1=0.0
      T1=D(I,7)
      AT1=AL*(D(1,7)-T1)
      BT1=BE*(D(1,7)-T1)
      GT1=GA*(D(1,7)-T1)
      WT1=W*T1
      ST1=SIN(WT1)
      CT1=COS(WT1)
      CW=(CURO*((1.0/BE)*EXP(BT1)-(1.0/AL)*EXP(AT1))/W)-CUR1*(1.0/GA)*EX
     1P(GT1)/W
      AW=(1.0/(AL**2+W**2))
      BW=(1.0/(BE**2+W**2))
      GW=(1.0/(GA**2+W**2))
      FAX=CURO*EXP(AT1)*AW
      FBX=-CURO*EXP(BT1)*BW
```

TABLE III (Continued)

```
      FGX=CUR1*EXP(GT1)*GW
      FAY=-(W/AL)*EXP(AT1)*AW*CURO
      FBY=(W/BE)*EXP(BT1)*BW*CURO
      FGY=-(W/GA)*EXP(GT1)*GW*CUR1
      FABX=FAX+FBX+FGX
      FABY=-CW+FAY+FBY+FGY
      VX=FABX*CT1+FABY*ST1
      VY=-FABX*ST1+FABY*CT1
      ZX=FX+VX
      ZY=FY+VY
      F1X=ZX*COS(W*D(I,4)/V)+ZY*SIN(W*D(I,4)/V)
      F2X=ZX*COS(W*D(I,5)/V)+ZY*SIN(W*D(I,5)/V)
      F1Y=-ZX*SIN(W*D(I,4)/V)+ZY*COS(W*D(I,4)/V)
      F2Y=-ZX*SIN(W*D(I,5)/V)+ZY*COS(W*D(I,5)/V)
C
      GHX=GHX+(F1X*EH1X-F1Y*EH1Y)+(F2X*EH2X-F2Y*EH2Y)
      GHY=GHY+(F1X*EH1Y+F1Y*EH1X)+(F2X*EH2Y+F2Y*EH2X)
      GVX=GVX+(F1X*EV1X-F1Y*EV1Y)+(F2X*EV2X-F2Y*EV2Y)
      GVY=GVY+(F1X*EV1Y+F1Y*EV1X)+(F2X*EV2Y+F2Y*EV2X)
      I=I+1
   50 CONTINUE
      GH=SQRT((GHX**2)+(GHY**2))
      GV=SQRT((GVX**2)+(GVY**2))
      IF (GHX) 52,51,52
   51 GHPH=1.5708
      GO TO 53
   52 GHPH=ATAN(GHY/GHX)
   53 CONTINUE
      IF (GVX) 55,54,55
   54 GVPH=1.5708
      GO TO 56
   55 GVPH=ATAN(GVY/GVX)
   56 CONTINUE
      C3=180.0/3.1416
      GHP=(C3)*(GHPH)
      GVP=(C3)*(GVPH)
      DD(J,1)=DD(J,1)+(GV/12.0)
      DD(J,2)=DD(J,2)+(F/12.0)
   66 WRITE(6,114)GH,GHP,GV,GVP,F
  999 CONTINUE
      DO 601 KJ=1,43
      WRITE(6,602)DD(KJ,1),DD(KJ,2)
  602 FORMAT(2E14.5)
  601 CONTINUE
      CALL EXIT
      END
      SUBROUTINE GAUSS(IX,S,AM,V)
      A=0.0
      DO 80 I=1,12
      CALL RANDU(IX,IY,Y)
      IX=IY
   80 A=A+Y
      V=(A-6.0)*S+AM
      RETURN
      END
      SUBROUTINE RANDU(IX,IY,YFL)
      IY=IX*65539
      IF(IY)85,86,86
   85 IY=IY+2147483647+1
```

TABLE III (Continued)

```
   86 YFL=IY
      YFL=YFL*.4656613E-9
      RETURN
      END
//GO.SYSIN DD *
//
```

VITA

O. Guy Marney

Candidate for the Degree of

Doctor of Philosophy

Thesis: A LIGHTNING MODEL FOR PATTERN RECOGNITION

Major Field: Electrical Engineering

Biographical:

   Personal Data: Born in Hobart, Oklahoma, September 10, 1940, the
      son of Mr. and Mrs. Guy Marney, Sr. Married with two
      children.

   Education: Graduated from Sentinel High School, Sentinel, Okla-
      homa, in June, 1958; received the Bachelor of Science and
      Master of Science degrees from Oklahoma State University in
      June, 1963, and August, 1965, respectively, with a major in
      Electrical Engineering; completed requiremenets for the
      Doctor of Philosophy degree at Oklahoma State University in
      May, 1971.

   Professional Experience: Research Assistant, School of Electrical
      Engineering, Oklahoma State University, September, 1963 to
      June, 1964; September, 1965 to September, 1966; June, 1967 to
      September, 1970; Summer Development Student, Texas Instru-
      ments, Inc., June, 1965 to September, 1965; Visiting Assistant
      Professor, The University of Oklahoma, September, 1970 to
      June, 1971.

   Professional Memberships: Member of the Institute of Electrical
      and Electronic Engineers; Phi Kappa Phi; Eta Kappa Nu;
      Sigma Tau.